VOLUME 84 DEC 7 1936 NUMBER 4

THE ASTROPHYSICAL JOURNAL

AN INTERNATIONAL REVIEW OF SPECTROSCOPY AND ASTRONOMICAL PHYSICS

Founded in 1895 by GEORGE E. HALE *and* JAMES E. KEELER

Edited by

HENRY G. GALE
Ryerson Physical Laboratory of the University of Chicago

FREDERICK H. SEARES
Mount Wilson Observatory of the Carnegie Institution of Washington

OTTO STRUVE
Yerkes Observatory of the University of Chicago

NOVEMBER 1936

PHOTOELECTRIC PHOTOMETRY AT THE SPROUL OBSERVATORY - *John S. Hall* 369

THE PHOTOGRAPHIC DETERMINATION OF STELLAR PARALLAXES WITH THE 60- AND 100-INCH REFLECTORS. FIFTEENTH SERIES - - *Adriaan van Maanen* 409

AN IMPROVED METHOD OF DETERMINING ABSOLUTE-MAGNITUDE DISTRIBUTIONS, WITH APPLICATION TO THE EARLY K STARS - - *Gustaf Strömberg* 412

INTENSITIES OF BLENDED ABSORPTION LINES - - - - - - *A. D. Thackeray* 433

THE THEORETICAL INTERPRETATION OF EQUIVALENT BREADTHS OF ABSORPTION LINES - - - - - - - - - - - - - - - - - *Donald H. Menzel* 462

NOTES

NOTE ON EQUIVALENT BREADTHS OF ABSORPTION LINES - - - - - - - *J. G. Baker* 474

CONSTANCY OF WAVE-LENGTH OF A SPECTRAL LINE *Guy C. Omer, Jr., and James L. Lawson* 477

A NEW BINARY OF LARGE PARALLAX - - - - - - - - - - *G. P. Kuiper* 478

ERRATUM - 480

THE UNIVERSITY OF CHICAGO PRESS
CHICAGO, ILLINOIS, U.S.A.

November 1936 Vol. 84, No. 4

THE ASTROPHYSICAL JOURNAL

AN INTERNATIONAL REVIEW OF SPECTROSCOPY AND ASTRONOMICAL PHYSICS

Edited by

HENRY G. GALE
Ryerson Physical Laboratory of the University of Chicago

FREDERICK H. SEARES
Mount Wilson Observatory of the Carnegie Institution of Washington

OTTO STRUVE
Yerkes Observatory of the University of Chicago

WITH THE COLLABORATION OF

WALTER S. ADAMS, Mount Wilson Observatory
JOSEPH S. AMES, Johns Hopkins University
WILLIAM W. CAMPBELL, Lick Observatory
HENRY CREW, Northwestern University
CHARLES FABRY, Université de Paris
ALFRED FOWLER, Imperial College, London
EDWIN HUBBLE, Mount Wilson Observatory
HEINRICH KAYSER, Universität Bonn
ROBERT A. MILLIKAN, Institute of Technology, Pasadena
HUGH F. NEWALL, Cambridge University
FRIEDRICH PASCHEN, Reichsanstalt, Charlottenburg
HENRY N. RUSSELL, Princeton University
FRANK SCHLESINGER, Yale Observatory
HARLOW SHAPLEY, Harvard College Observatory

Former Editors:

GEORGE E. HALE JAMES E. KEELER EDWIN B. FROST

The Astrophysical Journal is published by the University of Chicago at the University of Chicago Press, 5750 Ellis Avenue, Chicago, Illinois, during each month except February and August. ¶The subscription price is $6.00 a year; the price of single copies is 75 cents. Orders for service of less than a half-year will be charged at the single-copy rate. ¶Postage is prepaid by the publishers on all orders from the United States, Mexico, Cuba, Porto Rico, Panama Canal Zone, Republic of Panama, Dominican Republic, Canary Islands, El Salvador, Argentina, Bolivia, Brazil, Colombia, Chile, Costa Rica, Ecuador, Guatemala, Honduras, Nicaragua, Peru, Hayti, Uruguay, Paraguay, Hawaiian Islands, Philippine Islands, Guam, Samoan Islands, Balearic Islands, Spain, and Venezuela. ¶Postage is charged extra as follows: for Canada and Newfoundland, 30 cents on annual subscriptions (total $6.30); on single copies, 3 cents (total 78 cents); for all other countries in the Postal Union, 80 cents on annual subscriptions (total $6.80), on single copies, 8 cents (total 83 cents). ¶Patrons are requested to make all remittances payable to The University of Chicago Press, in postal or express money orders or bank drafts.

The following are authorized agents:

For the British Empire, except North America, India, and Australasia: The Cambridge University Press, Fetter Lane, London, E.C. 4. Prices of yearly subscriptions and of single copies may be had on application.

For Japan: The Maruzen Company, Ltd., Tokyo.

For China: The Commercial Press, Ltd., 211 Honan Road, Shanghai. Yearly subscriptions, $6.00; single copies, 75 cents, or their equivalents in Chinese money. Postage extra, on yearly subscriptions 80 cents, on single copies 8 cents.

Claims for missing numbers should be made within the month following the regular month of publication. The publishers expect to supply missing numbers free only when losses have been sustained in transit, and when the reserve stock will permit.

Business correspondence should be addressed to The University of Chicago Press, Chicago, Illinois.

Communications for the editors and manuscripts should be addressed to: Otto Struve, Editor of THE ASTROPHYSICAL JOURNAL, Yerkes Observatory, Williams Bay, Wisconsin.

The cable address is "Observatory, Williamsbay, Wisconsin."

The articles in this journal are indexed in the *International Index to Periodicals*, New York, N.Y.

Applications for permission to quote from this journal should be addressed to The University of Chicago Press, and will be freely granted.

Entered as second-class matter, January 17, 1895, at the Post-Office, Chicago, Ill., under the act of March 3, 1879.
Acceptance for mailing at special rate of postage provided for in Section 1103, Act of October 3, 1917, authorized on July 15, 1918.

PRINTED IN THE U.S.A.

THE ASTROPHYSICAL JOURNAL

AN INTERNATIONAL REVIEW OF SPECTROSCOPY AND ASTRONOMICAL PHYSICS

VOLUME 84 NOVEMBER 1936 NUMBER 4

PHOTOELECTRIC PHOTOMETRY AT THE SPROUL OBSERVATORY

JOHN S. HALL

ABSTRACT

The results of observations made mostly at the Sproul Observatory with a red-sensitive photoelectric photometer are given in this paper. Color observations numbering 1366 were made of 285 Harvard Ko stars. The effective wave-lengths are at 6800 A and 8300 A. Infra-red magnitudes of 281 stars were determined from 1089 comparisons of the effective stellar energy at 8300 A with that of a controlled incandescent lamp. The zero point of this magnitude system was determined from observations of Ao stars in accordance with the precepts of the I.A.U.

Colors from three different sources are combined with three accurate spectral classifications to form mean color excesses. The colors are from the Sproul Observatory, from Berlin-Babelsberg (Becker), and those formed by taking the difference between the infra-red and Hertzsprung's photographic magnitudes.

The color excess of giant K1 to Mo stars is definitely related to the trigonometric absolute magnitude. In the case of the G4 to Ko stars the corresponding correlation is weak. For both spectral groups color excess is related to the Victoria spectroscopic absolute magnitudes.

Photovisual, visual, and photographic magnitudes were predicted from the observed colors and magnitudes. The discussion of the predicted magnitudes indicates that the color of these stars is mostly independent of the spectral region used in measuring them.

The distribution of the effective stellar energy was directly observed (in terms of the stars) by means of an objective grating placed in front of the 24-inch lens. Spectrophotoelectric intercomparisons of Vega and β Pegasi extending over a range of 6000 A were made on several nights. These stars appear equally bright at 8250 A. The results show that if both stars are black bodies and if β Pegasi has a surface temperature of 3000° K, then that of Vega is near 11,000° K.

THE APPARATUS

During the summer of 1933 I constructed a photoelectric photometer somewhat similar to one I had previously made at the Yale Observatory.[1] This photometer was attached to the 12-inch tele-

[1] *Ap. J.*, **79**, 145, 1934.

scope of the Rutherfurd Observatory in the fall of 1933. I am grateful to the National Academy of Sciences for a grant which covered a part of its cost. Although the apparatus is under the jurisdiction of the Rutherfurd Observatory of Columbia University, Dr. Schilt kindly allowed me to bring it to Swarthmore in August, 1934.

The photoelectric cell was manufactured by the Bell Laboratories of New York. It is sensitive to light ranging in wave-length from the ultra-violet to the infra-red. Its maximum response to stellar energy is near 8000 A. This cell is used in conjunction with a Lindemann electrometer.

Dr. Bennett[2] has developed at the Yale Observatory a photometer combining an electrometer tetrode with a similar Cs-O-Ag photocell. Since his arrangement is more modern and more sensitive than mine, I shall not describe my photometer in detail.

While I was at New Haven, Dr. Bennett suggested that the apparent changes of sensitivity of the cell might be due to leakage from the cathode end of the cell to ground. This leakage would have the same effect as reducing the voltage across the cell, which, in turn, would reduce the photoelectric response to a given light source. In the present photometer dry ice is put in at the side of the cell instead of at the cathode end. As a result, the cathode lead wire is well insulated at all times, and very little trouble from leakage of any kind is experienced. The sensitivity of the photometer may decrease by as much as 10 per cent in eight hours, but I believe this is due primarily to a weakening in the voltage of the dry cells in the potentiometer circuit controlling the voltage on the electrometer.

The photometer is so mounted on the visual tailpiece of the 24-inch telescope that it can be rotated about the optical axis and clamped at any position angle. I have installed a diagonal eyepiece somewhat similar to the one designed by Professor Stebbins for the Yerkes photoelectric photometer.[3] This enables the observer to be sure that the star is accurately centered. Its crosswires are illuminated by starlight. The installation of filters offers no difficulty.

[2] *Pub. A.A.S.*, **8**, 209, 1935. [3] *Ap. J.*, **74**, 289, 1931.

A standard light source is mounted on the same rack as the color filters.

This light source is merely a small 6.2-volt incandescent lamp which throws a spot of light about 6 mm in diameter on a diffusing screen below it. By means of a pair of small diaphragms the center of this spot of light illuminates the photocell when the filter rack is turned to the proper position. For observations extending from October 28 to November 9, 1934, the current through this lamp was fixed at 0.04 ampere. This is only one-sixth of the maximum current delivered through the lamp by a 6-volt battery and it was noticed that the light intensity changed very rapidly with the current. The current through the lamp was then increased to 0.12 ampere. Another diffusing screen and several photographic filters were placed in front of it in order to cut down the light intensity to the former value. The light intensity now varies as the fifth power of the current.

I have assumed in this work that if the current through the lamp were constant, its light intensity would remain unchanged. In order to accomplish this, the current was led through an 8-ohm resistance of manganin wire. The "IR drop" across this resistance was then balanced with the voltage of a standard cell by means of a galvanometer. The voltage of the standard cell and the resistance of manganin wire have very small temperature coefficients. A galvanometer deflection of 15 mm corresponds to a 1 per cent change in light intensity.

Since magnitudes, as well as colors, were measured, it seemed of interest to know if the measured rate of electrometer deflection was proportional to the incident light intensity. On February 11 and 27, 1935, I measured the relative magnitudes of eleven bright stars in the Pleiades. There was no noticeable difference in scale between these magnitudes and those measured at Yale[4] with a different photocell. It should be mentioned that a color filter (Jena BG17) was used for the Swarthmore observations but that no filter was used at New Haven.

A laboratory test was made in the following manner: The lens

[4] Hall, *op. cit.*

was removed from a searchlight similar to an automobile headlight, and in its place was inserted an aluminum disk in which there were six holes. These were of the same diameter and were symmetrically placed on a circle around the center of the disk. A diffusing screen was fastened to the inner side of the disk. This constituted the source.

At a distance of 17 cm from the cell, in front of a 5-mm opening, there was placed another diffusing screen. Halfway between this aperture and the cell was a very small aperture. We therefore had an image of the diffusing screen on the cell. The source was placed at a distance of 4 meters from the photometer. The deflection produced by the light intensity from each of five apertures was individually determined in terms of that of the sixth aperture. The deflection produced by successively adding the light from the individual apertures was then measured.

The constancy of the current through the source was checked by means of an ammeter. One test of this kind covers a range of about 2.0 magnitudes. By changing the distance between the source and the photometer a range of 3.5 magnitudes was measured.

Measures were made over both five and ten eyepiece divisions of the microscope, and the dark current was measured in the same way as the background current in the regular observing programs. The voltage on the cell was 110 volts, as usual, corresponding to a gas amplification factor of about 7. On two different occasions complete tests of this sort were made. The scale factor on the first trial was 1.01 and on the second, 0.99. Since I did not have opportunity to make a truly elaborate test, I decided it was best to stop at this point.

DISTRIBUTION OF THE EFFECTIVE ENERGY

It has been the custom for observers in the past (myself included) to have the spectral response of photocell and the transmission of the filters determined in the laboratory. These data, combined with the spectral transmission of the atmosphere and lens, enable one to determine the distribution of the effective energy.

Professor Hertzsprung suggested by letter that I place a coarse grating in front of the objective and measure the deflection due to a

PLATE XVI

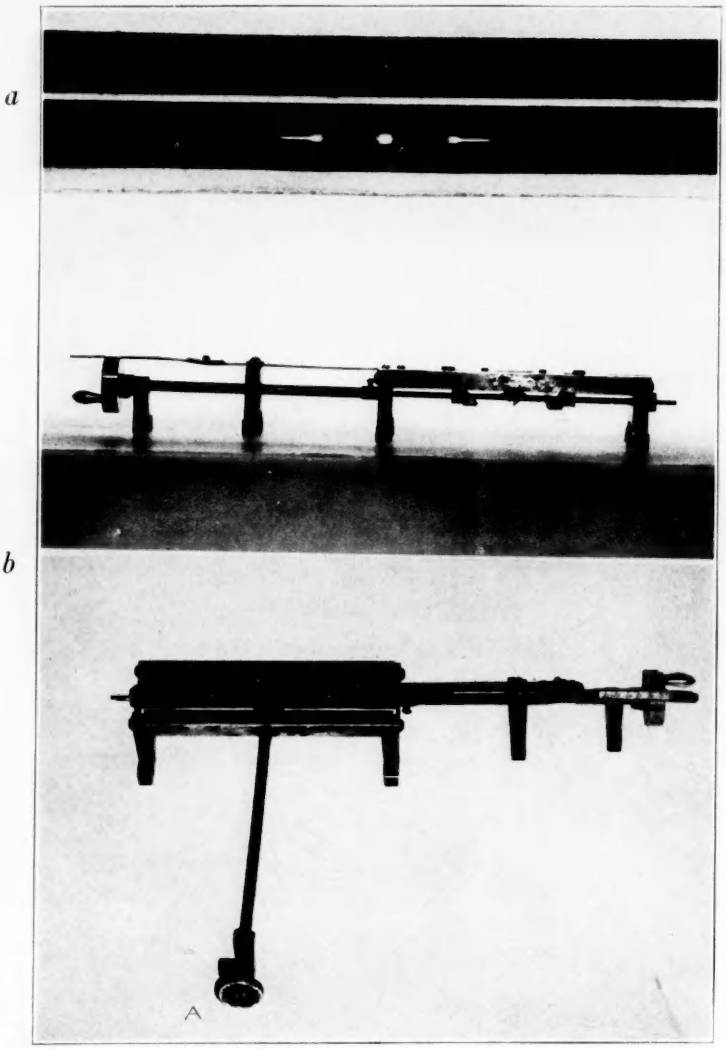

GRATING SPECTRA AND DEVICE FOR MEASURING WAVE-LENGTH

a) Two spectrograms made at the visual focus of the 24-inch with Wratten and Wainwright panchromatic plates. No attempt has been made to filter out the blue and violet light. The exposure time for Arcturus (*bottom*) was three minutes and for Nova Herculis (*top*) thirty minutes. A fifteen-minute exposure on Arcturus will show a trace of the second-order spectrum, which appears to be less than 25 per cent as intense as that of the fifth order. The intensity of the second-order spectrum is therefore less than 1 per cent of that of the first order.

b) Device for measuring the intensity of the first-order spectra. At the top the knob *A*, which would be behind the apparatus, has been removed. The two slits are visible in the lower photograph.

UNIV. OF MICH.

star of slow diurnal motion as its spectrum trails across an opening to the cell. The point of maximum deflection is then a rough measure of the effective wave-length for that particular star. I believe I misinterpreted this suggestion to some extent and constructed a grating of much higher dispersion than he had in mind.

Owing to several difficulties which I encountered, the first successful grating covers only 0.40 of the 24-inch objective. The wires are passed over threaded rods, turned out on the same lathe. The rods are kept from sagging in the middle by four other rods at right angles to them. The ends of the four rods are threaded in such a way that the tension of the copper wires can be readily adjusted. Professor Marriott very kindly made measurements on this grating with the large measuring engine. The average free space is 0.270 mm, and the average thickness of the copper wires 0.258 mm. These measures, combined with similar ones which I made, yield the value 0.5283 mm for the average distance between the centers of the slits. Since the visual focal length of the objective is 11,010 mm, the dispersion at the visual focus is 479.8 A/mm. A spectrum of Nova Herculis 1934 was observed on October 14, 1935, with this grating in front of the 24-inch objective. A contact print of this spectrum is shown in Plate XVI, together with the spectrum of Arcturus. The starlike images are blends of the nebulium lines at 5007 A and 4959 A. If the first of these lines is assigned twice the intensity of the second and a velocity of approach of 400 km/sec is assumed, the observed dispersion at the visual focus is 483 A/mm. I regard this value as a rough check on the previous one.

The first spectrophotoelectric measures with this grating were made in April, 1935. Two different methods of measuring the distance of the effective portion of the spectrum from the central image were tried. It soon became apparent that, if reliable measurements of this sort were to be made, some accurate mechanical device was necessary.

A device for measuring the intensity of both first-order spectra simultaneously is shown in Plate XVI, *b*. It was designed by Mr. Bourdelais of the engineering department of Swarthmore College and myself, and was made by his son, Chesman Bourdelais. Two prisms are mounted behind two slits of adjustable widths. One prism with its

slit is securely fastened to a right-hand screw; the other prism with its slit is fastened to a left-hand screw on the same rod. Each screw has a $\frac{1}{2}$ mm pitch. The revolving head to which the rod is attached is divided into ten divisions. One division therefore corresponds to a motion of 0.05 mm of the slits and prisms. It can, of course, be set much more accurately.

These prisms reflect the light to the central prism, which reflects it to the cell. The knob, *A*, enables one to pull the central prism out of line with the other prisms. When this is done, a 3-mm aperture allows the central image to strike the cell directly. This enables one to leave the device on the photometer at all times, even when colors and magnitudes are being measured. It also enables one to center the star accurately for grating measurements. Although this is important, such details are beyond the scope of this paper. After the necessary adjustments have been made, the observer merely uses the diagonal eyepiece to be sure the star is centered.

I do not believe that there is a systematic overlap of the two first-order spectra of more than 25 A. With the present eyepiece the accidental error of centering is about 50 A. However, there is a very distinct consolation in losing so much light in the central image. The diagonal eyepiece is so set that the central image may be used for the guiding of long exposures (of the order of a minute). For short exposures this is unnecessary.

Professor Wright, of the physics department of Swarthmore College, evaporated an excellent coat of aluminum on the prisms several months ago. They show no signs of deterioration. By comparing the response due to a star whose energy strikes the cell directly and then by way of one of the slits, it appears that, by using both first-order spectra instead of one, about 0.5 mag. is gained in light intensity. There is another important advantage aside from the two already mentioned. If the star is not accurately centered, the effective wavelength of the energy striking the cell is not radically changed, since the two spectra tend to counterbalance one another. Considerable time was spent in calibrating the spectrometer on the same measuring engine as that used for the grating calibration.

Four series of infra-red plates were used to determine the color-curve of the 24-inch telescope in the deep red. It was found that,

beginning at 6000 A, the focal length increased almost linearly with the wave-length. At 9000 A the best focus is about 30 mm behind the visual focus. The focal length changes very rapidly from the visual region toward the violet end of the spectrum. Since the photometer was on the visual tailpiece, the focal length could be changed at will.

Vega and β Pegasi.—In order to test rigorously the efficacy of the apparatus just described, the difference in magnitude between Vega and β Pegasi as a function of the wave-length was determined on several different nights in October, 1935. The slit widths were set at 1.00 mm, which corresponds to 480 A at the visual focus. Beginning at the shorter wave-lengths, the slits were moved in 1-mm steps away from the central image until the point was reached where the cell is insensitive. Two readings were taken at each position, and the focus was changed in about 6-mm steps whenever the observed color-curve of the 24-inch demanded it. Then, with the slits displaced $\frac{1}{2}$ mm from the former settings, similar readings were taken as the slits were moved together toward the shorter wave-lengths. The deflection due to background, leakage, and motion of the telescope was measured at frequent intervals over the same number of eyepiece divisions, as was the deflection due to the addition of starlight. This was tedious but, I believe, necessary, since the range of intensity was so large. The laboratory tests already described to determine the scale of the photometer were made under very similar conditions at about the same time. I neglected at the time, however, to carry these tests as far as the small deflections indicated by β Pegasi for wave-lengths shorter than 0.525 μ.

Several readings were taken on the standard light source during the observation of each star. In this way corrections were made for small changes in the sensitivity of the photometer dependent on changes of tilt and time.

Although the two stars under consideration were observed at nearly the same zenith distance, Abbot's[5] values for the atmospheric extinction as a function of wave-length were used. The largest correction for differential extinction was 0.04 mag.

The results of five of these comparisons are given in Table I. The

[5] *Ap. J.*, **34**, 208, 1911.

mean magnitude differences were first determined with the observations of October 16 omitted. On this night the first half of the measures of Vega were 0.07 mag. brighter than the second half. It seems

TABLE I

Wave-Length (μ)	Observed Magnitude Differences (β Pegasi *minus* Vega)					
	October, 1935					Mean
	15	16	17	19	21	
0.454	.....	$+3^{M}48$	$+3^{M}60$	$+3^{M}52$	$+3^{M}51$	$+3^{M}53$
0.478	.....	(3.34)	3.07	2.96	.....	3.02
0.501	.....	2.80	2.88	2.84	2.90	2.85
0.525	($2^{M}18$)	2.47	2.49	2.55	.....	2.50
0.549	+2.32	2.18	2.34	2.21	2.37	2.28
0.573	2.09	2.03	2.17	2.02	.....	2.08
0.597	1.93	1.84	1.89	1.87	1.91	1.89
0.621	1.64	1.69	1.67	1.62	.....	1.65
0.645	1.43	1.35	1.41	1.40	1.38	1.39
0.669	1.17	1.27	1.05	1.25	.....	1.18
0.693	1.00	1.01	1.00	1.11	1.12	1.05
0.717	0.73	0.80	0.82	0.75	.....	0.78
0.741	0.45	0.43	0.45	0.48	0.42	0.45
0.765	0.28	0.35	0.28	0.32	.....	0.31
0.789	0.22	0.10	0.16	0.22	0.22	0.18
0.813	+0.04	+0.07	+0.05	+0.08	.....	+0.06
0.838	−0.04	−0.08	−0.05	−0.05	−0.06	−0.06
0.862	0.11	0.15	0.17	0.11	.....	0.14
0.886	0.22	0.13	0.16	0.17	0.17	0.17
0.910	0.21	0.30	0.28	0.25	.....	0.26
0.934	0.34	0.25	0.27	0.30	.....	0.29
0.958	0.43	0.28	0.40	0.41	.....	0.38
0.983	.....	0.37	0.50	0.44	.....	0.44
1.007	(0.90)	0.39	0.61	0.48	.....	−0.49
Sky	good	fair	good	good	fair to clouds	.....
Constant	$0^{M}00$	$+0^{M}21$	$+0^{M}02$	$-0^{M}02$	$-0^{M}02$	.....

probable that Vega was observed through thin cirrus clouds. The foregoing constant was applied to the second half of these measures. The constant applied to the magnitude differences of the respective nights in order to make their sum equal to the preliminary mean

differences is given at the bottom of each column. The eye estimates of the transparency for each night are also given. The focal length was kept constant on October 15, but on the other nights it was adjusted as the color-curve of the objective demanded. Values given in parentheses were not used in forming the means.

Vega was always observed first. On October 17, I reobserved Vega and found that, after making due allowance for change of apparent sensitivity of the photometer and for differential extinction, these

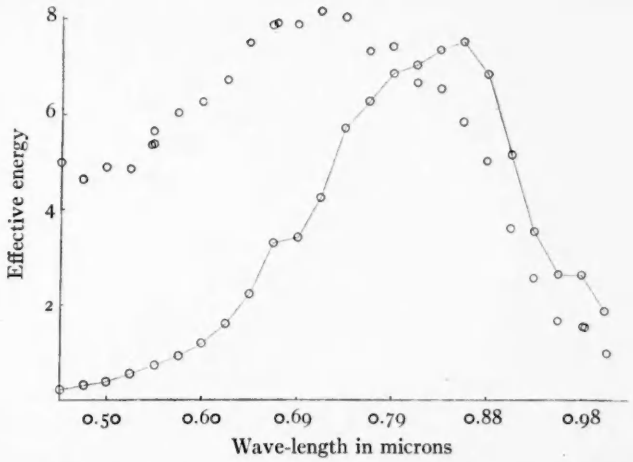

FIG. 1.—The distribution of the effective energy of Vega and β Pegasi observed on October 17, 1935. The average secant of the zenith distance is 1.09 in each case. The observations of β Pegasi are connected by straight lines.

measures agreed well with those made two hours before. There is plenty of evidence that the color-curve of the cell does not change after it is once cooled. In fact, cold winter weather will keep the color-curve very nearly constant.

The electrometer deflection as a function of the wave-length for observations taken October 17 is given in Figure 1. The dip in the deep red is due to a water-vapor band in this region of the spectrum. The graph also shows that the two stars are of equal brightness at 8250 A.

In Figure 2 the mean magnitude differences given in Table I are plotted against wave-length. The three points at the left end of the diagram should be given less weight than the others because of the

uncertainty in the scale. The large circles in Figure 1 represent photographic and visual differences in magnitude.

Abbot found a temperature of 2850° K for β Pegasi from his radiometer measures at Mount Wilson.[6] Nicholson and Pettit[7] derived

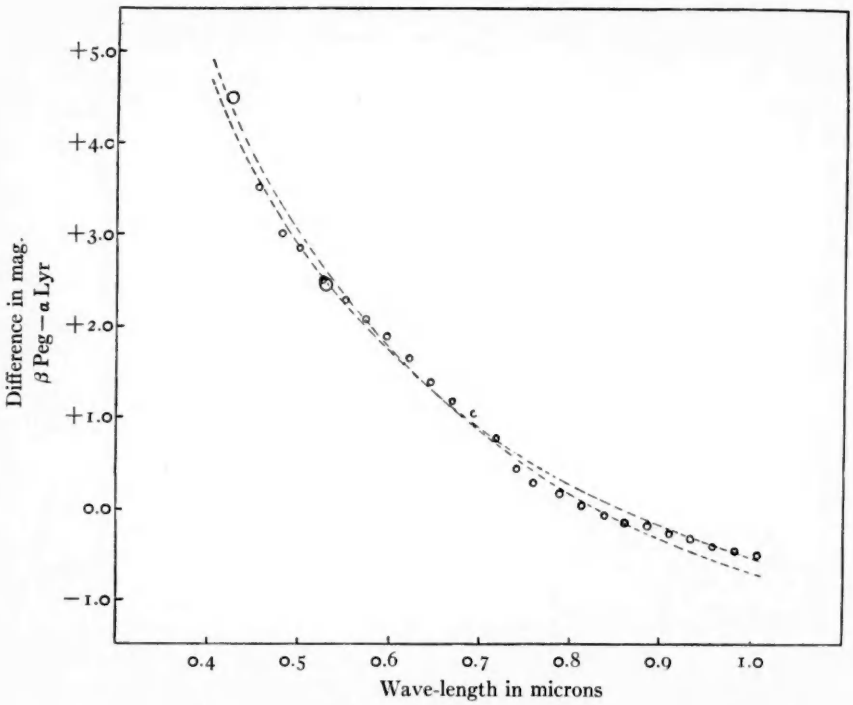

FIG. 2.—The ordinates are the mean magnitude differences given in Table I. The large circle at 0.422 μ represents the mean photographic magnitude difference from the data given by Hertzsprung and King. The other large circle at 0.529 μ is the visual difference taken from the HR, its effective wave-length being that determined by Brill. The corresponding effective wave-length found by Nicholson and Pettit at Mount Wilson is 0.555 μ. The steeper of the two curves represents the magnitude differences of two black bodies at 3,000° K and 13,000° K. The corresponding temperatures for the other curve are 3,000° K and 10,000° K. The zero point of these magnitude differences for each of these curves is arbitrary.

the value 2710° K from measures made with a thermopile at Mount Wilson. Spectrophotometric investigations made in the visual region of the spectrum yield temperatures slightly higher than 3000° K.[8] The results of these latter investigations should not be affected by

[6] *Ibid.*, **60**, 87, 1924.

[7] *Ibid.*, **68**, 279, 1928.

[8] Brill, *Handbuch der Astrophysik*, **5**, Part I, 150, 1932.

lines and bands. If we assume that β Pegasi is a black or gray body and has a color temperature of 3000° K, it appears that Vega best resembles a perfect radiator with a color temperature of 10,000°–13,000°, depending on the spectral region given the most weight. If β Pegasi is hotter than 3000° K, Vega is cooler than the foregoing figures would indicate.

The results of this investigation seem encouraging. It is my intention gradually to abandon measures with color filters in favor of observations of the kind just given.

Cell with filters.—Several curves showing the spectral response of the cell to stars of different color are given in Figure 3. The distribution of the effective energy shown by these curves has not been corrected for possible changes in reflectivity with wave-length of the aluminized surfaces. The two curves beneath the upper one for each star show the response when the color filters are in the light path. Except for the case of Pollux, these filter-curves were computed from the observed response-curve, using the transmission data given by the manufacturer for the particular melt from which my filters were made. I have checked these data by observations of other stars and have found them very reliable. Pollux was observed with and without filter RG9.

The effective wave-length or the wave-length dividing the total effective energy with these filters in place is given in Table II. The last column shows the mean secant of the zenith distance at the time of observation. No extinction corrections have been applied in deriving the values shown in columns 2 and 3. It is to be regretted that only one of these stars was observed when most of the observations contained in the following sections were being made. That star is Arcturus, and its effective wave-lengths are imperfectly known because I had only a crude method of determining the wave-length at the time. In the case of Vega the effective wave-length for BG17 is based somewhat on the measurement of color. The observed color, combined with the grating data, indicates that about 10 per cent of the effective energy through this filter is of shorter wave-length than 0.45 μ. With the exception of Arcturus, which was observed directly without any reflections, these wave-lengths have not been corrected for possible changes due to the two reflections from the prisms.

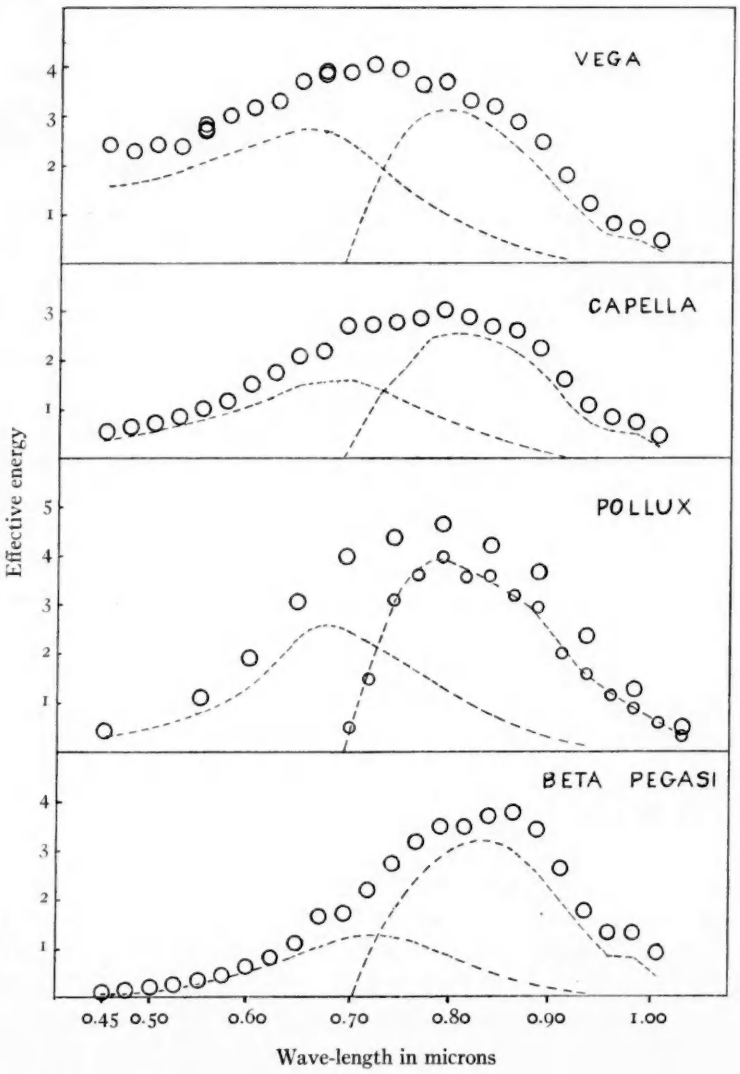

FIG. 3.—The observations represented in this diagram by circles form the basis of the data given in Table II. The dotted curve at the left applies to BG17 and the other to RG9. These are Jena colored optical glasses. The thicknesses of BG17 and RG9 are 3 and 2 mm, respectively. The water-vapor absorption at 0.95μ is evident on two of the three nights represented.

THE OBSERVATIONS

The color observations made at the Sproul Observatory were begun October 7, 1934, and finished December 4, 1935. The first observations of magnitude were made October 28, 1934, contemporaneously with the color observations. The artificial light source already described was used as the comparison star. These observations include only stars designated as Ko in the *Henry Draper Catalogue*. From the Equator to $+75^\circ$ the visual magnitude limit was 5.5, and below the Equator to -20° this limit was 5.0. All Ko stars north of the Equator brighter than 4.4 visual magnitude were observed at Yale. The relative colors of 64 of the Yale stars were ob-

TABLE II

Star	Effective Wave-Length (μ)		HD Spec.	Date of Obs.	Sec. z
	BG17	RG9			
Vega	0.611	0.800	Ao	Oct. 17, 1935	1.09
Capella	.671	.823	Go	Oct. 19, 1935	1.19
Pollux	.678	.828	Ko	Mar. 22, 1936	1.07
Arcturus	.69	.81	Ko	July 17, 1935	1.44
β Pegasi	0.716	0.840	Mb	Oct. 17, 1935	1.09

served at Swarthmore at least once to increase their weight and to establish a relationship between the two scales of color. A few very bright Ko stars were not reobserved at Swarthmore.

The observations of color at the Rutherfurd Observatory were made in the same way as "colors 89" at the Yale Observatory. These observations represent 4 per cent of the weight of the Swarthmore observations. The Rutherfurd Observatory is located on top of a fourteen-story building, within a few blocks of the Hudson River. When the wind is from the west or northwest the transparency is good. The scattered light from incadescent lamps was quite noticeable but did not preclude observations of fifth-magnitude stars. Fainter stars could be observed after midnight.

The Sproul Observatory, on the other hand, is seven miles southwest of the city limits of Philadelphia. The sky is relatively dark,

and the city is in such a direction as not to interfere with photometric work. The observatory is about 70 meters above sea-level.

The spectral transmission of the two color filters used at Sproul has already been shown in Figure 3. The readings were taken in the following order: two with BG17, two with RG9, four with the standard lamp, two with RG9, and two with BG17. The photocurrent due to the sky and leakage was measured at frequent intervals.

The current passing through the standard lamp was usually checked once for each setting of the telescope. The light from the standard lamp always passed through RG9 before striking the cell.

This paper contains the results of 1366 observations of the colors of 285 stars and 1089 semi-independent magnitude observations of 281 stars. The color program was started before the standard lamp was working properly. At the end of the program, special observations of magnitude were made to complete this part of the data. In general, except for special observations for the determination of the extinction correction, each star was observed but once on a single night.

The light intensity of about 30 bright stars was cut down by means of a filter made from a developed photographic plate. Since this filter is not neutral in color, a special series of measurements was made to correct both the colors and the magnitudes of these stars. Several other bright stars were observed with the cell at reduced voltage.

The color of Arcturus was measured twice at Sproul by different methods. It was found to differ radically from the Yale color reduced to the same scale. My notes show that this star, Altair, and α Hercules were observed through a small circular diaphragm at the center of the objective of the Loomis Telescope. The Yale observations of Arcturus are not used in the discussion of the colors. Since it was well observed by Becker, his mean color on the Sproul scale is given double weight in the subsequent discussion.

THE EXTINCTION CORRECTION

The atmospheric extinction for each effective wave-length was found from 29 determinations on eleven different nights. The transparency on these nights was better than average. Since I was careful

to avoid observing at large zenith distances on nights of fair or poor transparency, this procedure seems justified. I believe that it is impossible to determine the extinction with any satisfactory degree of accuracy on nights of fair or poor transparency.

The mean extinction coefficient for filter RG9 is 0.13 ± 0.01 mag. (probable error). Its differential value for RG9 and BG17 averages $0.050 \pm .004$ mag., making the extinction coefficient for BG17 0.18 ± 0.01 mag.

The reduction to the zenith was made in the usual manner, assuming the air mass to be proportional to the secant of the zenith distance.

THE REDUCTION OF THE COLORS

The colors were reduced in the same general way as were those at Yale. The reduction differs in one respect: Instead of choosing a standard night, and reducing all colors observed on any other night to this standard night, a color system resulting from averaging the colors observed on several nights was used. The problem then was to find the two constants which would best reduce the original colors of each night to this average system of colors. Four complete reductions were made in this way. The last reduction changed the mean colors very little from the results of the third reduction.

The Yale colors 89 and 87 were averaged according to Harvard spectral type. When these mean colors are plotted against one another, a smooth curve fits the points very closely. This curve was used to reduce colors 89 to 87. The mean color on scale 87 was then derived.

A comparison of the internal agreement of the Sproul and Yale colors indicated that the latter should be given a weight of 0.6 after reduction to the Sproul scale of colors.

A graph showing the relationship of the Sproul and the Yale colors observed in common, including a few early- and late-type stars, indicates that the relationship is linear over almost the entire range of color. It was assumed, therefore, that a linear relationship exists for the G- and K-type stars. Assigning the weight 0.6 to the Yale colors, I derived from a least squares solution the relationship:

$$S = 0.862\ Y + 0.715 \text{ mag.}$$

The colors observed at the Rutherfurd Observatory were first reduced to Yale 87 and thence to the Sproul scale. As these extended over about half the sky, it was gratifying to find that the systematic differences as a function of the right ascension were small. As a result of a comparison of the internal agreement of the Sproul and the Columbia colors, the latter were given half-weight.

The probable error of a single observation of color made at the Sproul Observatory (BG17 minus RG9) is $\pm$0.016 mag.

At the end of the observing program, the observed colors were 0.2 mag. redder than those found for the same stars nearly a year before. It is quite possible that the cell was not as blue-sensitive then as it was previously. Since the range of wave-lengths is much more limited by the filter and by the atmosphere for RG9 than for BG17, a change of this sort would shift the effective wave-length of BG17 much more than it would that of RG9.

The reductions of color are based on observations made during the early part of the program. Therefore, the data given in Table II are applicable to the colors given in Table VII, if 0.2 mag. is added to the colors.

THE REDUCTION OF MAGNITUDES

A comparison of the readings made with filter RG9 and the standard light source enables one to determine the relative magnitudes of the stars in the infra-red. The magnitude differences were first reduced to the zenith in the usual manner.

Since nearly all stars on the program fainter than 4.4 visual magnitude were each observed on four different nights, and since I did not know which stars were variable and which were not, every star previously observed was used as a standard.

I have assumed throughout the magnitude reductions that the incident light intensity is proportional to the observed rate of electrometer deflection. The problem then was to find the lone constant which would make the sum of the differences in magnitude between a group of stars observed on a particular night and the standard lamp equal to the sum of the magnitude differences found for the same stars observed on a previous night The zero point was at first arbitrary.

Actually on 15 of the 54 nights two such constants were used in place of one. Several factors might produce this change in the observed magnitude differences—among them changes in transparency, hydroscopic effects, radical changes in the seeing, and possible changes in the intensity of the standard light source. On 33 of the 54 nights the transparency was rated as either good or excellent, and on only three of these nights was it called poor.

I was materially aided in this reduction by Mr. Thomas Spencer. We made four complete reductions before we were satisfied that we had found the constants which would eliminate real systematic errors. When the final constants were decided upon, the residuals were checked by adding these constants to the original magnitude differences and comparing the result with the reduced mean difference for each star.

The residuals resulting from this final comparison are given in Table III, which contains only those stars observed three or more times. The unit is 0.01 mag., and a positive residual means that the observed brightness is greater than the mean brightness. Each night was given the same weight in forming the mean magnitude differences. The six residuals given in the table which are larger than 0.11 mag. were assigned zero weight in the final reduction. Since stars were usually observed in order of right ascension, I have indicated by a heavy horizontal rule in Table III the point at which the constant was changed for 14 of the 15 nights on which two constants were used. On the other night (April 25) I have not indicated this point because the stars were not observed in order of right ascension. In the case of January 1, 1935, the same constant was used for the first and last portion of the program. With a single exception, these observations were made within the interval of October 28, 1934, to October 4, 1935. The exception, December 4, 1935, is designated by an asterisk.

Twenty-seven observations were reduced and rejected. Twenty-two of these were rejected in seven groups of 2–4 stars each and constitute observations made either at the very beginning or end of a nocturnal sequence. Five of these seven groups represent observations made just previous to the formation of haze or clouds which precluded further photometric work. I have borne in mind the fact

TABLE III

Star BS	X 28	X 29	XI 2	XI 9	XI 24	XII 25	XII 5	XII 14	XII 15	XII 16	I 24	I 27	I 29	VII 4	VII 5	IX 25	IX 26	IX 28	IX 4
3	+2	-	-	+1	-	-	-1	-	-1	-	-	-	-	-	-	-	-2	-	-
74	+4	-	-	-6	-	-	+5	-	-	-	-	-	-	-	-	-	-2	-	-
194	0	-4	-	-	-	-	-	-	-	-	-	-	-	-	-	-	0	+5	-
248	+4	-3	-	-	-	-	-	-	-	-	-	-	-	-	-	-	-2	+1	-
253	-	-	-	-	+3	-	-	-	-	-	-	-	+4	-	-	-	-1	-5	-
265	-	-	-	-3	-	-	-	-	-	-	-	-	+7	-	-	-	-1	-1	-
294	-	-	-	-1	-6	-	-	-	-	-	-	-	+3	-	-	-	+1	-	-
351	+1	+2	-3	+3	-	-	-	XII	-	-	-	-	-1	0	0	0	+1	-	-3
352	-	-	+2	-	+7	-3	-	4	-3	-	-	-	-	+6	-	-5	-5	-	-
360	-	-	-	-1	-1	-	-	+1	-	-	-	-	-	-	-	-	-	-	-
390	-	-	-	+3	-1	-3	-	-1	-	-	-	-	-1	-	-	-	-	-	-
399	-	-	-	XII	-2	+2	-1	-	-	-	-	-	-	-	-	-	-	-	-
402	-	-	-	8	-2	-2	-	-	+2	-	-	-	-	-	-	0	0	-	-
442	-	-	-	+4	-2	+4	-3	-	-	-	-	-	0	-	-	-	-	-	-
456	-	-	-	+2	-2	-1	+2	-	-	-	-	-	-	-	-	-	-	-	-
489	-	-	+2	-	-	+1	-	-	-	-	-	-	-	-	-	-1	-1	-	-
515	0	-	-	-	-	+3	-	-	-	-	-	-	-	-	-	+3	-4	-	-
539	-	-	-	-	-	-3	-	-3	-	-	-	-	-	-	-	0	+5	-	-
549	-	-	+2	-	-1	-	-4	-	-	-	-	-	-	-	-	-	-	-	-
643	-	-	-	-	+2	-1	-	-	-	-	-	-	-	-	-	-2	-1	-	-
645	-	-	-	+8	-4	-	-1	-5	-	-	-	-	-	-	-	-	-	-	-
736	-	-	+4	-	+1	-	-	-	-	-	-	-	-4	-	-	-	+1	-	-
737	-	-	-	-	0	+1	-	+1	-	-	-	-	-	-	-	+3	-5	-	-
741	-	-	-	-2	-3	+4	+1	-	-	-	-	-	-	-	-	-	-	-	-
874	-	-	-	+2	XII	-1	-	-	-	-	-	-	-	-	-	+1	+3	0	-
882	+2	0	-4	-	17	-	-	-	-	-	-	+3	-	+1	-	+2	-1	-4	-
948	-	-	-1	-6	+4	-	-	-	-	-	-	-	-	-	-	-	-	+2	-
947	-1	+3	10	-	-	+5	-5	-	-	-	-	-2	-	-	-	-6	-	+1	-
951	+1	-2	-	-	-	-	+7	-	-	-	-	-6	-	-	-	-	-	-	-
989	-	-	-	+1	+6	-11	-	-	-	-	-	-	-	-	-	-	-	+6	-
991	XII	-4	-	-	-	-	-	-	-	-	-	-	-	+1	-	-	+6	-4	-
1015	27	+5	-	-	-	-	-	-	-	-	-2	-1	-	-	-	-3	-	-	-
1052	+6	-	-4	9	-2	-	-	-	-	-	-	-	-	-	-	-	-	-1	-
1084	-	-	-	-	-	-	+4	-	-	-	-	-	-	-	-	-1	-2	-	-
1136	-	-	XII	-	-	+2	-	I	I	-	-	-	-	-	-	0	+3	-	-
1254	-	-	10	-	-5	-	-	-2	14	-	+2	+6	-2	-	-	-6	-	+1	-
1348	+2	-	0	-2	-	-	-	-3	+5	-	0	0	-	-	-	-	-	0	-
1390	-	-	-	+3	-	-	-	-	-	-	-	-4	-	-	-	0	0	-	-
1396	-	+1	-	-	+2	-	-	-	-	-2	-	-	-	-	-	-3	-	-	-
1437	-	-2	-	+5	-	-3	-	-	-	-	-2	-1	-	-	-	-3	-	-	-
1467	-5	-	-3	+5	+3	-3	-	-	-	-	-	-	-	-	-	-	-	-2	-
1481	-	+1	-	0	-	-	0	-	-	-	-	-	-	-	-	-1	0	-	-
1601	-	+3	-	+1	-	-	0	-	-	-3	-	-	-	-	-	0	-3	-	-
1684	-	-	-	-2	+2	-5	-	-	-	-	-	-3	-	-	-	-	-	+5	-
1698	-	+1	-	-1	-	+4	-	-	-2	-	-	-	-	-	-	-	-	0	-
1726	-	-	-	+2	+1	+3	-	-	-	-	-	-	-	-	-	-	-	-1	-
1739	-5	-	-	-5	+5	0	-6	-2	-	-	-	-	-	-	-	-	-	-	-
1784	-	-4	-	-	-	-	+3	0	-	-	-	-	-	-	-	-	-	-	-
1805	-	-	-	-3	+2	-	-	-	-	-	-	+1	-	-	-	-2	+1	-1	-
1895	-	-2	+3	-	-	-	-	-	-	-	-	-	-1	-	-	-	-	-	-
2037	-3	+4	+2	-	-	+5	-	+1	+4	-	+1	-	II	II	-	III	-	-	-
2113	-2	0	+4	-	-	+9	-	+1	-	-	-2	-	17	20	17	-	-	-	-
2152	-	-	-	-	0	-	-	-	-	-	-	-	+4	-5	-1	-	-	+1	-
2165	-	-	-	-7	-	-	-	-	-	-	-	-	-3	0	+3	-	-	-	-
2259	+4	-	-	+1	-	-	-	-	-	-	-2	-2	-1	-	-	-	-	-	-
2327	+5	0	-8	-	-	+4	-	-	-	-	-	-	-	-	-	-	-	-	-
2334	-5	0	+2	-	-	+5	-	-	-	-	-	-	-	-	-	-	-	-	-
2429	+3	9	0	-	-	-2	-	-	-	-	-	-	-	-	-	-	-	-	-
2443	-4	+5	-	-	-	+7	-	-	-2	-	-	-	-	-	-	-	-	-	-
2450	+2	+5	+4	-	-	-9	-	-	+1	+6	-	-	-	-	-	-	-	-	-
2478	0	-	0	-	+5	-	-	-3	-	-	-	-	-	-	-	-	-	-	-
2480	+2	-	-	-1	-	-	-	-2	-	+2	0	-2	-	-	-	+2	0	I	-
2487	-	-	-	-8	-	-	-	-	-	-	-	-	-4	+3	+1	-	-	4	II
2503	-3	-	-	-	-	+3	-	-	-	-	-	+4	-	-	-	-	-	-3	11
2506	0	-	-	-	-	+2	-	-	-	-	-	-	-	-	-	-	-	-1	0
2516	+5	-	-	+1	-	-	-	-	-	-	-	-	-	-3	-3	-	-	-	-
2630	+5	-	-	+2	-	-	-	-	-	-2	-2	-2	-	-	-	+5	-	+4	-
2697	0	-	-	+2	-	-	-	-	-	-	+1	-	-	-	-	-	-	-3	-
2701	-	-	-	-	-	+1	-	-	-4	-	-	-	-	-	-	-	-	+1	-1
2715	-	-	-	-	-	-	-	-	-	-	-	-	-	0	+1	0	-	-	-
2793	-	-	-	-	-	-	-	+2	+1	-	-	-	-	0	-3	-	-	-	-
2805	-	-	-	-	-	I	-	+2	0	-	-	-	-1	-2	-	-	-	-	-
2854	-	-3	-	-	-	31	+3	0	-	-	+4	-	-	-	-	-	-	-4	-
2881	+5	-	-	-	-	-6	-	+2	-	-	-2	-	-	-	-	-	-	-	-
2884	-	+6	I	+4	-6	-	-	-	0	-	-	-	-	-	-	-	-	+4	-
2898	-	-	3	-5	+2	-	-	+2	-	-	+2	-	-	-	-	-	-	-4	-
2970	-	-	-	+1	-	-	-	+1	-5	-	-	-	-	-	-	-	IV	-	+1
3110	-	-	-	-4	-	-	-2	+2	-	+5	-	-	-	-	-	25	-	-	-
3141	I	-	-	-	-	-	+2	-4	-	-	-	-	-	-	-	0	-	-	-
3145	1	-	-	-1	-	-	-2	+2	-	-	-	-	-	-	-	-	-	-	-
3149	+6	-	-	-	-	-	-3	-3	-	-1	+3	-1	-	-	-	-	-	-	-
3211	-2	XII	+7	-	-	-	-	-	-	-	-	-	-2	-	-	-	-	-	-4
3306	-4	3	+4	-	+3	-	-	-	I	-	-4	-	-	-	-	-	-	-1	-
3366	-	-4	+5	-3	-3	-3	0	-6	-	-	-	-	-	-	-	-1	+1	-	-
3403	-	-	-	-	-	-	-	-	+4	-	-	0	0	-3	-	-	-	-	-
3418	-5	-	+3	-	-1	-	-	-	IV	-	-	-	-	-	-	-1	-	+3	-
3441	-8	-	+4	-	+4	-	-	-	18	-	-	-	-	-	-	-	IV	-	-1
3583	-1	-	-2	-	-	-	0	-	-	+2	-	-	-	-	-	0	26	-	-
3731	-	+3	+1	-10	-	8	+6	-	-	-	-	-	-	-	-	-1	-	-	-
3779	-2	-	0	0	-	-	-	-	-	-	+1	-	-	-	-	-	-	-	-
3809	-	-1	-3	+4	+1	-	-	+1	-	-	-	-	-	-	-	-	-	+2	-
3815	-	-	-1	+3	-	-	-3	-	-	-	-	-	-	-	-	-	-	-	-
3827	0	-	+1	-	-	+1	-	-3	-	-	-	-1	-	-	-	-	-	-	-
3834	+2	-	-1	-	-	+1	-	+5	-	-5	-	-4	-	-	-	-	-	-	-
3939	-	-	-	-	-	-	-	-1	-	-	-	-	-5	-	-	-	-	+1	+4
3945	0	-	+1	-	-	0	-	-1	-	-	-	-	-	-	-	-	-	-	-
3951	-	-	-2	+1	-	+2	-	-	-	-	-	-	-	-	-	-	-	-2	-
3983	-2	-	-1	-3	-	-	-	-	-	-	+5	-	-	-	-	-	-	-	-
3994	-3	-	+1	+7	-	-	-	-6	-	-	-	-	-	W	-	-	-	-	-
4100	-	-5	-2	-	+2	+4	0	-	-	-	+3	15	+3	-	-	-	-	-	+4
4146	-	+2	-	-	-	-2	-	0	-	-	-	0	-	-	-	-2	-	-	-
4178	-	-	-	-	-	-	+3	-	-	-	-	-	-	-	-	-	-	-20	0
4181	-	-	-	-	-	+3	-	-	-	+3	-	-	-	-	-	-	-	-6	-1
4246	-	-	-	-	-	+1	-	-	-	+1	-	-	-	-	-	-	-	-1	0
4258	-	0	-	-	-	-3	-	0	-	-	-	-	-	-	-	-	-	+3	-
4287	+2	-	-12	+1	I	-	-	-2	-	-	-	-	-	-	-	-	-	-	-
4291	0	0	-	-	27	-2	-	-1	-	-	-	-5	-	-	-	-	-	-	-
4365	-	-	-	-	+3	+1	-	-	-3	+2	-	-	-	-	-	-1	0	-	-
4382	+1	-	-1	+5	-1	-	-	-	-4	-	-	-	-	-	-	-	-	-	-
4418	-	-	-	-	+2	-1	-	-	-3	-	-	0	-	-	-	-	-	-	-
4471	-	-	-	-	+2	-2	-	-	+1	-	+1	-	-	-	-	-	-	-	-
4667	-	-	-	-3	-	0	+2	-	-	-	-	-	-	+2	-	-	-	-	-
4668	0	-	-	-6	-	+1	-	-	-	+7	-	0	-	-	-	-	-	-	-
4695	-	-	-	+3	-	-	-	0	-	+2	-	-	-	-	-	0	-5	-	-
4697	-	-	-1	-	-	-	+3	-2	-	-	-	-	-	+1	-	-	-	-	-
4728	+5	-	-	0	-	-6	-	0	-	-	-	-	-	-	-	-	-	-	-
4737	-	-	-	-	-	+1	-1	-1	-	-	-	-	-	-	-	-	-	-2	-
4783	-	-	-1	-	-	+3	-	-	-	+1	-	-	-	-	-	-	-	-2	-

Star BS	I 1	I 3	I 4	I 27	I 31	II 6	II 20	II 27	II 17	III 4	III 28	IV 14	IV 18	IV 25	IV 26	V 30	V 8	V 15	V 23	V 24	VII 29	VII 5	IX 15	IX 23	IX 6	IX 25	IX 20	IX 16
4792	-	-	-	-3	-	-	-	-	-	-	-	-	-	+2	-2	+3	-	-	-	-	-	-	-	-	-	-	-	-
4795	-	-	+6	-	-	-	-	-	-	-	-	-	-5	0	+1	-	-	-	-	-	-	-	-	-	-	-	-	-
4813	-	+2	-	-	-	+2	-5	-	0	-	-	-	-	-	-	-	-	-	-	-	-	-	-	-	-	-	-	-
4815	-	0	-2	-	-	-	+3	-	0	-	-	-	-	-	-	0	-	-	-	-	-	-	-	-	-	-	-	-
4894	-	-1	0	-	-	-	-1	-	+1	-	-	-	-	-	-	0	-	-	-	-	-	-	-	-	-	-	-	-
4924	+4	+2	-7	-	-	+1	-	-	-	-	-	-	-	-	-	-	-	-	-	-	-	-	-	-	-	-	-	-
4928	-	-	+5	-	-	-	-	-	-	-	-	-	-3	-3	-1	-	-	-	-	-	-	-	-	-	-	-	-	-
4997	+3	-1	-	-	-	-2	-1	-	-	-	-	-	-	-	-	-	-	-	-	-	-	-	-	-	-	-	-	-
5203	-	-	+2	0	0	+2	+2	-	-	-	-	-	-	-	-	-	-	-	-	-	0	-	-	-	-	-	-	-
5247	-	III	-	-2	+1	+1	-	+2	-	-	-	-	-	-	-	-	-	-	-	-	0	-	-	-	-	-	-	-
5345	-	10	-	-3	+7	-5	-5	+2	-	-	-	-	-	-	-	-	-	-	-	-	-	-	-4	-	-	-	-	-
5361	-	-6	-	-	-	-	-	-	-	-	-	-	-	0	-	-	-	-	-	-	-	-	+3	-	-	-	-	-
5370	-	-6	-	-	-	+3	-	-	-1	-	-	-	-	+1	-	-	-	-	-	-	+3	-	-	-	-	-	-	-
5502	-	0	-	+6	+3	-	-	-4	-	-	-	-	-	-	-	-	-	-	-	-	-1	-	-	-	-	-	-	-
5535	-	-	-	-	+2	-6	-	-	-	-	-	-	-	-	-	-	-	-	-	-	-	-	+2	+1	-	-	-	-
5541	-	-1	-3	-	-	-	-	-	-	-	-	-	+6	-2	-	-	-	-	-	-	-	-	-	-	-	-	-	-
5601	-	-	-	-	+1	+3	-	-	-	-	-	-	-	-	-	-	-	-	-	-	-	-	+1	-6	-	-	-	-
5616	-	-3	-6	-2	+3	-	-	-	-	-	-	0	-	-	-	-	-	-	-	-	-	-	-	-	+6	-	+4	-
5675	-	-3	-	+2	-	+4	-	-	-	-	-	-	-	-	+3	-	-	-	-	-	-	-	-1	-	-	-	-	-
5710	-	-	-	-	-	+1	-	-	-	-	-2	-1	-	-2	-1	-	-	-	-	-	-	-	-	-	-	-	-	-
5714	-	+1	-	-	-	-	-	-	-	-	-	-	-2	-	-	+3	-1	-	-	-	-	-	-	-	-	-	-	-
5777	-	-	-	-	-	-	-	-	-	-	-3	-	+2	0	+2	-	-	-	-	-	-	-	-	-	-	-	-	-
5787	-	-	-	-	-	-	-	-	-	-	-2	-	+1	+2	+6	-	-	-	-	-	-	-	-	-	-	-	-	-
5802	-	-	-1	+1	-	+3	-	-	-4	-	-	-	-	-	-	-	-	-	-	-	-	-	-	-	-	-	-	-
5988	-	-	-	-	-	-1	+4	-1	-	-	+3	-	-	-	-	-	-	-	-	-	-	-	-	-	-	-	-	-
5901	-	-1	0	-2	-	-	-	-	-	-	-	-	-	-	-	-	-	-	-	-	-	-	+2	-	-	-	-	-
5908	-	-	-	-	-	-	-	-	-	-	-2	III	+1	+2	0	-	-	-	-	-	-	-	-	-	-	-	-	-
6018	-	-	-1	-	-	-	-	-	-	-	-	11	+4	-	-	-3	-	-2	-	-	-	-	-	-	-	-	-	-
6075	-	-	-	-	+4	-	-	-	-	+3	-2	-	-	-	-5	-	-	-	-	-	-	-	-	-	-	-	-	-
6103	-	-	0	+4	-	-2	-	-	III	-	+2	-	-	-	-1	-	0	-1	-	-	-	-	-	-	-2	-	+2	-
6104	-	-	-	-	-	-	-	-	26	+1	-1	-	+7	-	-6	-	-	-	-	-	-	-	-	-	-	-	-	-
6126	-	+3	-	-	-	-	-	-	0	-	-	-	-4	-	+1	-	-	-	-	-	-	-	-	-	-	-	-	-
6147	-	-	-	-	-	-	-	-	-	-	-	-3	+3	-3	+1	-	-	-	-	-	-	-	-	-	-	-	-	-
6196	-	-	-	-	-	-	-	-	-	-	-	-4	-	-	-	-5	+17	+2	-	-	-	-	-	-	+6	-	-	-
6223	-	+6	-2	-	-	-	-	-	+1	-	-	-	-2	-	-	-2	-	-	-	-	-	-	-	-	-	-	-	-
6270	-	+1	-13	-1	-	+3	-1	-	-	-	-	-	-	-	-	-	0	-	-	-	-	-	-	-	-1	+6	0	-
6287	-	-3	-	+3	-	0	-2	-	-	-	-	-	-	-	-	-	-	-	-	-	-	-	-	-	-	-	-	-
6318	-	-	-	-	-	-	+5	-	-	-	-	-	-	-2	+1	+3	-	-	-	-	-	-	-	-	-	-	-	-
6388	-	-	-	-	-	+1	-	-	-3	+19	-	-	+3	-	-	-	-	-	-	-	-	-	VII	-	-	-	-	-
6415	-	-	-	-	-	-2	-	-	-	-	-2	-	-	+2	-	-	-	-	-	-	-	-	24	-	-	-	-	-
6498	-	-	-	-	-	-4	-	+2	-	-	+3	-	-	-	-	-	-	-	-	-	-	-	-2	-1	-	-	-	-
6526	-	-	-	-	IX	+1	-2	-	-	-	-	-	0	-	-	-	-1	-	-	-	-	-	-	-	-	-	-	-
6566	-	-	-	-	17	-	-	0	+1	-	-	-2	-	-	-2	0	-	-	-	-	-	-	-	-	-	-	-	-
6644	-	-	-	-	-2	0	-	-	-	-	-	-	-2	-	-	-	-1	-	-	-	-	-	-	-	-1	+6	0	-
6677	-	-	-	-	+4	-2	-3	+1	-	-	-	-	-	-	-	-	-	-	-	-	-	-	-	-	-	-	-	-
6698	-	-	-	-	-	-	-	-	-	-	-5	-	-	-	-1	+2	-	-	-	-	-	-	+3	-	-	-	-	-
6713	-	-	-	-	-1	-1	-	-	-	-	-	-1	-	-	+4	-	-	-	-	-	-	-	-	-	-	-	-	-
6866	-	-	-	-	-	-	-	-	-	+4	+3	-	-	-	-	-	-	-6	-	-	-	-	-	-	-	-	-	-
6885	-	-	-	-	-	-	-	-	-	+9	-2	-	-	-2	+2	-6	0	-	-	-	-	-	-	-	-	-	-	-
6945	-	-	-	-	-	-	-	-	-1	+2	-	0	+1	-	-	-	-	-	-	-	-	-	-	-	-	-	-	-
6979	-	-	-	-	-	-	-	-	-	+4	-10	-	-	-	-	-	-	+8	-	-	-	-	-	-	-	-	-	-
6983	-	-	-	-	-	-	-	-	-1	-1	-	-1	+3	-	-	-	-	-	-	-	-	-	-	-	-	-	-	-
7054	-	-	-	-	-	-	-	-	-5	-	+2	-1	-	+6	+3	-	-	0	-	-	-	-	-5	-	-	-	-	-
7125	-	-	-	-	-	-	-	-	-1	-	-	+3	+1	-	-2	-	-	-	-	-	-	-	-	-	-	-	-	-
7180	-	-	-	-	-	-	-	-	-	-2	-	+3	-	+3	-3	-	-	-	-	-	-	-	-	-	-	-	-	-
7181	-	-	-	-	-	-1	-	-	-	0	+1	-	-	+4	-2	-	-	-1	-	-	-	-	-4	+3	-	-	-	-
7193	-	-	-	-	-	-	-	-	-	+2	0	-	-6	+3	-	-	-	-	-	-	-	-	-	-	-	-	-	-
7295	-	-	-	-	-	0	-	-	-	-	-	0	-	+3	-1	-	-	-	-	-	-	-	-1	-	-	-	-	-
7309	-	-	-	-	-	+1	-	-	-	-	-	-	-	+1	-2	-	-	-	-	-	-	-	+1	-	-	-	-	-
7314	-	-	-	-	-	-	-	-	-	+3	-	-	-	0	-	-3	-1	-	-	-	-	-	-	-	-	-	-	-
7315	-	-	-	-	-	-	-	-	-	-	-	0	+2	+4	-	-	-	-5	-	-	-	-	-	-	-	-	-	-
7352	-	XI	XI	-	-	-	-	-	-	-1	-	-	-	-	+3	+3	+1	-	-	-	-	-	-	-	-	-	-	-
7385	-	2	3	-	-	-	-	-	-	-	-1	+11	-	+1	-	-	-	-1	-	-	-	-	-	-	-3	-	-	-
7429	+	+6	+1	-	-	-	-	-	-	-	-	-	+1	-	-	-	-	-	-	-	-	-	-6	-	-	-	-	-
7462	-	-	-	-	-	-	-	-	-	+3	-	-	-	-	+2	-6	0	-	-	-	-	-	-	-	-	-	-	-
7478	-	-	+1	-	-	-1	-	-	-	-	-	-	-	-2	-	-	-	-	-	-	-	-	+5	-5	-	+2	+2	-5
7480	-	-	+3	-	-	-	-	-	-	-	-	-	-	+5	-	-	-	-6	-	-	-	-	+1	-2	-	-	-	-1
7537	-	-	-	-	-	-	-	-	-	-	+2	-2	-	0	-	-	0	-	-	-	-	-	-	-	-	-	-	-
7595	-	+3	-	-	-	-	-	-	-	XI	-	-	-	-	-	-	-	-	-	-	-	-	-2	+2	-	-	-1	-
7660	-	-	-	-	-	-	-	-	-	0	-	-	-	-	+1	-2	+1	-	-	-	-	-	-	-	-	-	-	-
7679	-	+1	-	-	-	-	-	+2	-	0	-	-	-	-	-	-	-	-	-	-	-	-	-	-	-	-	-	-
7753	I	-	-	-	-	-	-	+2	-	-2	-	-	-	-1	+4	0	-2	-	-	-	-	-	-	-	-	-	-	II
7794	+4	-2	-	-	-	-	-	+2	-	-	-	-	-	-	-	-	+1	-	-	-	-	-	-5	-	-	-	-	+2
7854	-	-	-	-	-	-	-	-	-	-	-	-	-	+6	-	-	-	-	-	-	+2	-4	+1	X	-	-	-	-3
7897	-3	-9	-	-	-	-	-	-	-	-	-	-	-	-	-	-	-	-	-	-	+9	0	4	-	-	-	-	+5
7956	-	-	-	XI	-	+1	-	-	-	-	-	+3	-	-	-	-	0	+3	+1	-	-1	-2	-2	-1	-2	-1	-3	-
8011	-	-	25	-	-	-	-	-	-	-	+4	-1	-	-	-	-	-	-	+2	-	-4	-	-	-	-	-	-	-
8093	-	-	-	-	-	+5	-	-	-	-	-	-	-	-	-	-	-	-	-	-	-2	0	-	-	-	-	-	-
8167	-	-1	0	-	-	-	-	-	-	-	-	-	-	-	-	-	-	-	-	-	-8	+7	-	-	-	-	-	-
8228	-	-3	-	-	-	-	-	-	-	-	-	-	-1	-	-	+1	+1	-	-	-	+3	-	-	-	-	-	-	-
8255	-	0	XI	-	-	-	-	-	-	-	-	-	-	+2	-	-5	+2	-	-	-	-5	-	-	-	-	-	-	-
8277	-9	-	24	-	-	-	-	-	-	-	-	-	-	-	-	-	-	-	-	-	+3	+7	-	-	-	-	-	-
8317	-	-1	-	-	-	-	-	-	-	-4	-	-	-	-	+6	-1	-	-	-	-	-	-	-	-	-	-	-	-
8321	-5	-	-	-	-	-	-	-	-	-1	-	-	-	-	-	-	-	-	-	-	+2	-2	-	-	+5	-	-	-
8324	-	-3	-	-	-	-	-	-	-	+4	-	-	-	-	-1	-	-2	-	-	-	-4	-	-	-	+3	+1	-2	+1
8475	-	+1	-	-	-	+5	-	-	-	+1	-	-	-6	-	-	-	-	-	-	-	+4	-1	-4	+3	+1	-2	+1	-
8499	-1	+4	-	-	-	III	XII	-	-	-	-	-	-	-	-	-	-	-	-	-	-	-	-	-	-	-	-	-3
8551	-2	+2	-	-	-	2	4	-	-	-	-	-	-	-	-	-	-	-	-	-	+2	-1	-	-	-	-	-	-
8632	-	-	+4	-1	+1	0	-	-	-	-	-	-	-	-6	-	-	-	-	-	-	-	-	-	-	-	-	-	-
8692	-	-	+3	+1	+1	+1	-	-	-	-	-	-	-3	-	-	-	-	-	-	-	-	-	-	-	-	-	-	-
8726	-	-	+2	+2	+1	+1	-	-	-	-	-	-	-	-	-	-	-	-	-	-	-	-	-	-	+1	-2	-	-
8779	-	-	-1	-1	+1	+4	-	-	-	II	-	-	-	-	-	-	-	-	-	-	-	-	-	-	0	-4	-	-
8780	-	-	0	+1	+3	+7	-	-	-	4	-	-	-	-	-	-	-	-	-	-	+1	-	-	-	-4	+3	-	-
8798	-	-	-3	+2	-	-	-	-	-	+4	-	-	-	-	-	-	-	-	-	-	-	-	-6	0	+5	0	-4	-	-
8841	+4	-	+1	-	-	-	-	-	-	-	-	-	-	-	-	-	-	-	-	-	-	-	0	-3	-	-	-	-
8874	-	-	-	-	-	-	-6	+1	-	-	-	-	-	-	-	-	-	-	-	+1	+2	-	-	-	-	-	-	-
8878	-2	+4	-	-	-	-	-	-	-	-	-	-	-	-	-	-	-	-	-	-	-	-	0	-7	-	-	-	-
8892	-5	-	+9	-	-	-	-	-	-	-	-	-	-	-	-	-	-	-	-	-	-	-	+1	-3	-	-	-	-
8893	-2	-4	-	-	-	-	-	-	-	-	-	-	-	-	-	-	-	-	-	-	-	-	+6	0	-	0	0	-
8923	-14	+1	-	-	-	-	-	-	-	+7	-	-	-	-	-	-	-	-	-	-	-	-	+1	-	-4	-3	-	-
8930	-	-5	-2	-	-	-	-	-	-	-	-	-	-	-	-	-	-	-	-	-	+4	+2	-	-	-	+1	-1	-
8981	-	-1	-	-	-	-	-	-	-	-	-	-	-	-	-	-	-	-	-	-	+3	-2	-	-	-	+1	+1	-
9008	-	-	+1	0	-1	+4	-	-	-	-	-	-	-	-	-	-	-	-	-	-	-4	+1	-	-	-	-	-	-

TABLE III. With a single exception, these observations were made within the interval of October 26, 1934, to October 4, 1935. The exception, December 4, 1935, is designated by an asterisk. The months are denoted by Roman numerals. The day of the month is given directly below the numerals. If the star was observed after midnight, the residual is listed under the preceding day.

that any star may be a variable and that large discordances may result from this alone.

The probable error of a single observation derived from every residual given in Table III is ±0.027 mag. An average of 4.6 observations was made of every star in this table. The average probable error of the mean magnitude derived from these observations is therefore ±0.013 mag.

It seems probable that this accuracy can be substantially increased by checking the transparency at frequent intervals. Dr. Bennett and I have agreed upon a list of 20 stars which should be favorable for this purpose. They are designated by an asterisk in Table VII.

I have already mentioned the fact that the effective wave-length in the case of BG17 which I found for a group of bright stars in October probably does not apply to the colors given in this paper without first correcting these colors. The data shown in Figure 3 indicate that the color-curve of the cell was substantially the same in March, 1936, as in October, 1935. This is not surprising, since the cell is kept in the dome during the winter months. On November 18, 1935, and December 6, 1935, I reobserved a total of 16 stars of widely different color which had been observed many times during the regular program. Although the reobserved colors are redder, there is no apparent dependence of the magnitude residuals on color. In view of these observations, the evidence is strong that effective wavelengths derived for RG9 apply to all magnitudes given in this paper.

THE ZERO POINTS OF THE MAGNITUDES

The infra-red magnitudes were first reduced to an arbitrary zero point. It is desirable to express this arbitrary zero point in terms of the international system of magnitudes. Through the suggestion of Dr. Shapley, Mrs. Gaposchkin kindly sent me a list of photovisual magnitudes of Ao stars, within the limits 5.5 and 6.5 mag. As they all culminated within less than 30° of the zenith at Swarthmore, I I used the same extinction coefficient as that derived from observations of the K stars. Twenty of these stars were observed between April 4, 1935, and September 9, 1935.

The observed magnitudes of these Ao stars were reduced to the

arbitrary magnitude system by means of the same constants derived for the Ko stars. The sum of these reduced magnitudes was made equal to the sum of their photovisual magnitudes. The magnitude of the arbitrary zero point was found in this way to be 3.74 ± 0.02 mag. If the HR magnitudes had been used, this value would be 3.77 mag.

SYSTEMATIC ERRORS

Throughout this discussion, unless otherwise specified, all known spectroscopic binaries and a few close visual binaries are omitted.

The combined colors of the stars observed at Columbia and Swarthmore were divided into seven nearly equal groups according to the right ascension of the stars. The average color and spectral type (Mount Wilson classification) was found for each of these groups. After allowance is made for the fact that the mean spectral types differed slightly from one another, the lowest mean color for any one group is +0.063 mag. and the highest is +0.084 mag. The mean color of 51 southern stars is +0.067 mag.

The magnitudes were investigated for systematic errors by an indirect method not independent of small systematic errors in the colors. Mrs. Gaposchkin very kindly sent me photovisual magnitudes of all stars on my observing program. These magnitudes are derived from the *Potsdam Durchmusterung* and from the *Harvard Annals*. Her corrections to the photovisual scale are on the basis of the mean color index of bright Ko stars.

Let M_r be the observed infra-red magnitude and C the reduced mean color, including observations made at Yale, Columbia, and Swarthmore. Then the photovisual magnitude

$$M_{pv} = M_r + 3.00C + 0^{M}.95 .$$

There is better agreement if a scale factor is introduced, giving

$$M_{pv} = 0.955\, M_r + 3.00C + 1^{M}.09 .$$

Photovisual magnitudes were computed by means of the latter relationship and subtracted from the Harvard photovisual magnitudes. These differences, averaged over four-hour intervals of right ascension, are given in Table IV. N is the number of stars in each group.

The average residual for 38 southern stars is +0.013 mag. Table IV also shows similar comparisons using photographic and visual in place of the photovisual magnitudes.

Professor Hertzsprung's data[9] have been used as a basis for the photographic magnitudes The photographic magnitudes of stars between the Equator and +20° declination given in the *Göttingen Actinometry B*[10] were reduced to the Hertzsprung system by means

TABLE IV

R.A.	Photovisual		Photographic		Visual (HR)	
	O−C	*N*	O−C	*N*	O−C	*N*
0h− 4h.....	+0M023	34	+0M003	20	+0M011	35
4 − 8.....	+ .003	43	+ .019	19	+ .004	43
8 −12.....	+ .030	34	+ .001	18	+ .040	33
12 −16.....	+ .019	30	+ .074	13	+ .012	29
16 −20.....	− .019	45	− .047	22	− .010	45
20 −24.....	−0.029	40	−0.014	24	−0.034	39

of the relationship he has found Whenever a star had both magnitudes, the mean was used.

The differences between the photographic and infra-red magnitudes were plotted against the observed colors. The two co-ordinates were assigned equal weight on the same scale. A least-squares solution gave the relationship:

$$M_{pg}=M_r+6.59C+2^{M}08 .$$

The observed visual magnitudes are those of the HR. Since they are not entirely independent of the photovisual data, we would expect to find similar systematic differences.

The relationship used to derive the computed visual magnitudes is:

$$M_v=M_r+3.02C+1^{M}20 .$$

I believe the comparison with the photovisual magnitudes affords the best evidence by which to judge the extent of the systematic

[9] *B.A.N.*, **1**, No. 35, 1923.

[10] *Göttingen Actinometry B. Abhandlungen der Gesellschaft der Wissenschaften zu Göttingen*, Math-phys. Klasse, **8**, No. 4, 1912.

errors in my own data. The results appear to be satisfactory. If we assume that there are no systematic differences in the two systems of magnitudes, the systematic errors in the colors must be of the order of 0.01 mag. or less. On the other hand, if we assume that the colors are systematically correct, the systematic differences in the magnitudes compare favorably with differences between other systems of magnitudes.

THE PREDICTED ACCURACY OF OTHER MAGNITUDES

The average difference between the observed and the computed magnitude was found for each of the three systems mentioned above and, when multiplied by 0.845, gave the probable difference shown in Table V.

TABLE V

	Photovisual	Photographic	Visual
Probable diff. (O−C)	$\pm 0^{M}052$	$\pm 0^{M}082$	$\pm 0^{M}061$
P.E. of prediction	.034	.062	.034
P.E. of magnitude	± 0.039	± 0.054	± 0.051

By means of the relationships already given, the errors of the computed magnitudes can be easily deduced. I have assumed that the average probable error of the colors is ± 0.009 mag. and that of the magnitudes is ± 0.020 mag. This last value was chosen in view of the fact that the magnitudes of many of the brighter stars were measured but once.

As an example, we have for the visual magnitudes:

$$\text{P.E. of predicted } M_v = \sqrt{[3.02(0.009)]^2 + 0.020^2}$$
$$= \pm 0.034 \text{ mag.}$$

Since we now have a measure of the accuracy of the computed magnitudes and have found the actual differences between the computed and the observed magnitudes, the probable error of each observed magnitude system can be found. This figure is given for each system in the bottom line of Table V. These values are, of course, to be regarded as upper limits, since it is natural to expect that my data are not free from systematic errors and that the stars do not exactly conform to the same law of radiation.

Since the probable difference between Hertzsprung's magnitudes and those reduced to his system from the *Göttingen Actinometry* for 31 Ko stars in common is ±0.07 mag., the agreement between the predicted and the observed photographic magnitudes seems remarkably good. It must also be remembered that most of the observations embodied in the three magnitude systems were made many years ago and that some of the stars may be variables.

It is evident that this discussion is partly arbitrary. It is, however, difficult to escape the conclusion that the relative colors of these stars must to a large extent be independent of the spectral region in which they are measured. The average difference between the predicted and the observed photographic magnitudes for 7 c-stars is +0.06 mag. I have not been able to find any relationship between absolute magnitude and these residuals.

Up to this point the spectroscopic binaries have been entirely omitted from the discussion. Using the same formulae derived when spectroscopic binaries were excluded, photographic magnitudes were computed for 26, and photovisual magnitudes for 43, known spectroscopic binaries. The sum of the differences between the computed and the observed magnitudes averages substantially zero in both cases, although the average probable differences are slightly larger than those given in Table V. This may be taken to mean that the fainter star, on the average, is of the same color as the primary star or is much fainter than the primary star. For 40 of the 45 spectroscopic binaries, the Mount Wilson observers derived the spectroscopic parallaxes given in *Mount Wilson Contribution* No. 511, after first subtracting 0.3 mag. from the apparent visual magnitude. The evidence seems to be that the secondary is usually similar in color to the primary.

Measures with the diffraction grating similar to those made on Vega and β Pegasi may, in cases where the colors of the two components are widely different, show both the color and magnitude of the secondary.

COLOR EXCESS AND ABSOLUTE MAGNITUDE

It is a well-known fact that in the case of late-type stars the giants are redder than the dwarfs for any given spectral type. Several observers (myself included) have attempted to combine measures of

color with spectral type and to correlate the resulting combination with absolute magnitude. Recently, W. Becker[11] has shown that a rough relationship exists between color excess and absolute magnitude, from a discussion of observations made in the blue and violet. He concluded that, although colors may be used to determine definite physical characteristics of the stars, they cannot be used to predict the absolute magnitudes with any satisfactory degree of accuracy, owing to the influence of other parameters. His discussion for the giant stars is based largely on mean spectroscopic absolute magnitudes. In a recent paper[12] I gave a preliminary discussion showing a relationship between color excess, derived from a combination of the Sproul colors with accurate spectral types, and trigonometric absolute magnitude.

Since colors observed in various regions of the spectrum seem to be intimately related to one another, I have also used two other systems of color having similar accuracy. One of these is Becker's, which I shall denote as system *B*. The other is the difference between Hertzsprung's magnitudes (together with *Actinometry B*) and the infra-red magnitudes RG9, H_m. The weighted mean of the Yale, Columbia, and Sproul colors on the scale of the last will be denoted by H_c.

Color excess.—The reader will recall that the color excess of a star is the difference between its observed color and the average color of its particular spectral type. In other words, it is the difference between the spectral and color classifications. The color of a star depends mostly on the distribution of spectral energy at levels below those at which the spectral lines are produced. The color excess may therefore be a function of the temperature gradient in the stellar atmosphere. It is conceivable that it should be related to the absolute magnitude (roughly the size) of the star. This is probably an incomplete picture; other parameters undoubtedly should be taken into consideration.

The average color of each spectral type for each of the three systems of color was found. Since there are only a few dwarfs among these bright stars, the colors of all stars whose trigonometric *M* is

[11] *Veröff. Steinwarte Berlin Babelsberg*, **10**, No. 6, 1935.

[12] *Pub. A.A.S.*, **8**, 212, 1935.

greater than 4.0 were excluded in this procedure. Becker evidently mixed giants and dwarfs in forming mean colors. Three systems of accurate spectral classifications were used: Mount Wilson,[13] Victoria,[14] and Harvard.[15]

The mean color for each spectral type for the different scales of color and the different classifications is shown in Table VI. If there were less than six values of color for a given type, the mean color was not derived. The spectral classifications of Mount Wilson and

TABLE VI

Type	Mount Wilson			Victoria			Harvard		
	B	*Hc*	*Hm*	*B*	*Hc*	*Hm*	*B*	*Hc*	*Hm*
G4	$0^{M}303$	$0^{M}014$	.....	$0^{M}303$	$0^{M}014$	.....	.....	.....	.....
G5	.382	.016	.....	.382	.016	.....	.....	.....	.....
G6	.347	.018	$2^{M}25$	.347	.018	$2^{M}19$	.....	.....	.....
G7	.385	.025	2.29	.385	.025	.....	$0^{M}340$	$0^{M}008$	$2^{M}08$
G8	.397	.041	2.32	.397	.041	2.30	.407	.038	2.40
G9	.....	.048	.....	.....	.048	2.37	.....	.044	.....
K0	.491	.060	2.48	.491	.060	2.48	.464	.058	2.49
K1	.490	.075	2.56	.490	.075	2.44	.528	.077	2.59
K2	.511	.100	2.74	.511	.100	2.69	.....	.092	.....
K3	.602	.121	2.85	.602	.121	2.89	.....	.158	.....
K4	.675	.175	3.17	.675	.175	3.07	0.716	0.182	.....
K5	0.714	.181	.....	0.714	.213	.....	.....	.....	.....
M0	.....	0.293	.....	.....	.....	.....	.....	.....	.....

Victoria are very similar; consequently, whenever feasible, the mean colors have been made the same for the sake of convenience. The mean colors under *B* are derived only from those giant stars which Becker and I have observed in common.

A color excess for each star was then computed for every color and every spectral type available for that star. Therefore, if all three sets of color and all three classifications were available for a particular star, nine color excesses were formed. In order to reduce these to the same scale, excesses *B* were divided by 1.9 and H_m by 6.6.

[13] *Mount Wilson Contr.*, No. 511, 1935. [14] *Pub. Dom. Ap. Obs.*, **3**, 48, 1927.

[15] I am very grateful to Dr. Shapley and to Miss Hoffleit for these unpublished Harvard data. They have generously given me permission to publish them in this paper.

The mean color excess was then derived by assigning the same weight to each of the three components.

A comparison of the Mount Wilson and Victoria spectral classifications indicated that the probable error of a single determination of spectral class corresponds to ±0.011 mag. in color on the scale of H_c.

A similar comparison of the mean color excesses B and H_c indicated that the probable error of a single determination of color is about ±0.014 mag. on the scale of H_c. This is larger than would be expected from the internal agreement of the two scales of color. However, it includes the influence of systematic errors and errors in the zero points of the color excess as well as possible differences arising from local peculiarities in the stellar energy curves.

The probable error of a single color excess derived from one measure of color and one measure of spectrum is about ±0.018 mag. It is larger than this for late K stars, where the color varies rapidly with spectral class. If there are three measures of spectrum and color, the probable error of the mean color excess is ±0.010 mag. In Table VII the mean color excesses having a colon after them have a probable error of ±0.013 mag. or less.

Absolute magnitude.—I have endeavored to use only trigonometric parallaxes as the basis of absolute magnitude. Since my observations have been confined almost entirely to giant stars, the observed parallaxes are usually small and the errors in the absolute magnitudes are therefore large.

The trigonometric parallaxes have been adjusted by the method developed by Professor Eddington and Sir Frank Dyson.[16] This method assumes that the errors are distributed in a normal curve whose modulus corresponds to a definite probable error. If the probable error of the parallax given in Dr. Schlesinger's *General Catalogue of Stellar Parallaxes* exceeds 0".010, the star was not used to determine the systematic corrections. The average probable error of the remaining stars, ±0".0066, was used as the modulus. The effect of this systematic adjustment is to decrease parallaxes larger than 0".015 and to increase parallaxes smaller than this value, all negative paral-

[16] *M.N.*, **86**, 686, 1926.

laxes being made positive in the process. Since it was evident in the case of the small and the negative parallaxes that the absolute magnitudes derived in this fashion are extremely sensitive to these systematic corrections, I have used in the discussion only the absolute magnitudes of those stars whose given parallax is greater than 0".011.

The trigonometric data indicate that stars whose mean spectral type is later than Ko are, on the average, 0.4 mag. brighter than the G-type stars. The two groups will be discussed separately.

Both spectral groups were used in deriving the systematic corrections to the observed parallaxes. This is not quite correct, since the median parallax of the K group is 0".015, and that of the G group 0".018, and the two distributions of the observed parallaxes are not exactly the same. Since there are, roughly, a hundred stars in each group, I combined the data in the hope that the resulting corrections would be more reliable than if they were determined separately for each group. Separate corrections were, however, derived for the K1 to Mo stars.

Since the same systematic corrections have been used for all stars, it is of equal importance to show that these corrections are the same for stars of different color excess. The frequency distribution of the trigonometric parallaxes of stars with positive color excess is similar to that of stars with negative color excess. Here again the data are not sufficiently numerous to derive the corrections separately for each group. In either case the most frequent parallax is near 0".015, although stars with positive color excess have fewer parallaxes in excess of 0".025.

K1 to Mo stars.—In Figure 4 the mean color excess given in Table VII is plotted against trigonometric absolute magnitude. On the left side of the diagram the trigonometric parallaxes have been adjusted by the method of Eddington and Dyson. On the right side, the trigonometric data have not been changed in the derivation of absolute magnitudes. All stars with trigonometric parallaxes larger than 0".011 have been included.

The three components of the mean color excess (B, H_c, and H_m) are separately plotted against adjusted absolute magnitudes in Figure 5. Each of the three components indicates the same trend; and

if one takes account of the size of the errors in absolute magnitude for the particular stars contained in each diagram, it seems that H_m will yield the most reliable results.

The straight line has been arbitrarily drawn and represents the relationship I have used to derive the absolute magnitude from the mean color excess. It is

$$M_c = -3\text{o C.E.} + \text{o.6 mag.}$$

For the data on the left side of Figure 4, the coefficient of correlation is o.6o. According to the probable errors given in Dr. Schle-

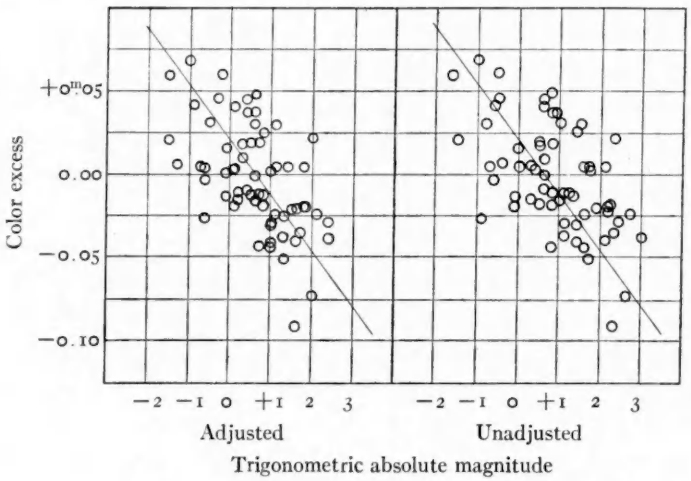

FIG. 4.—Aside from indicating a definite relationship between the co-ordinates, this diagram shows how the array is changed when the parallaxes are adjusted for systematic errors.

singer's *Catalogue*, the average probable error in the abscissa is ±o.6 mag. The probable difference between the adjusted trigonometric absolute magnitudes and the absolute magnitude derived from the mean color excess is ±o.6o mag. These figures are partly arbitrary, but they indicate that the color excess is related to the absolute magnitude of these stars.

I have excluded from this discussion known spectroscopic binaries, close visual binaries, and the dwarf BS1084. I have assumed that the average color for each spectral type corresponds to the same absolute magnitude for all stars whose mean spectral type is between

K1 and Mo, inclusive. This is probably only approximately true, but the data are not sufficient to indicate possible differences.

If the systematic corrections to the trigonometric parallaxes which were derived from the K1 to Mo stars alone were used to determine the abscissae in Figure 4, the effect is to increase slightly the slope of the given line.

The mean color excess of the K stars is plotted against the Mount Wilson and the Victoria spectroscopic absolute magnitudes in Figure 6. The same straight line as that drawn in Figure 4 is shown.

G4 to Ko stars.—The mean color excess of stars whose average spectral types fall within the limits G4 and Ko, inclusive, is plotted against absolute magnitude in Figure 7. In the left half of the diagram the abscissae have been adjusted for systematic error, and the diameters of the circles represent the weights of the respective stars. These weights have been derived according to a definite system depending upon the weight of the mean color excess and the probable error of the parallax as given in Dr. Schlesinger's *Catalogue*.

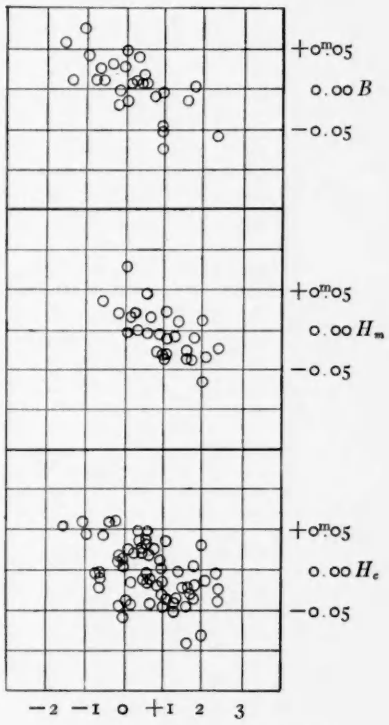

FIG. 5.—K1 to Mo stars. No star with a mean trigonometric parallax of less than 0".012 has been included.

The straight line has the same slope as that shown in the previous graphs. It is based primarily on the Victoria absolute magnitudes, and its zero point has been changed by 0.4 mag. The very discordant star at $M_t = 3.5$ is BS6196. Its spectroscopic M (Mount Wilson) is +0.2.

For stars whose trigonometric absolute magnitude is less than +3.0, the correlation is weak at best. Were it not for the fact that the Victoria absolute magnitudes are related to color excess for this

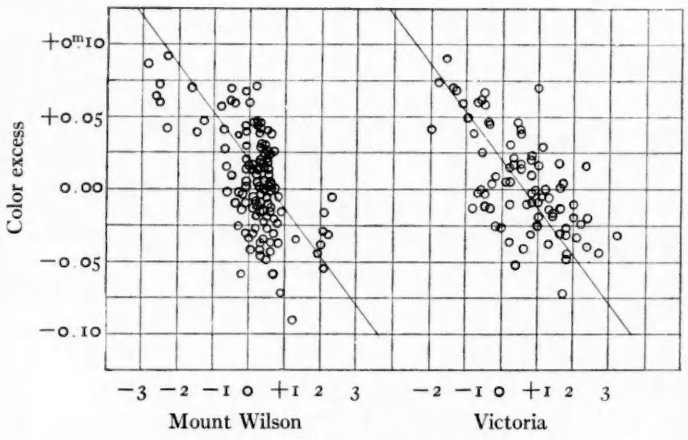

FIG. 6.—The agreement with the Victoria data is satisfactory. A comparison between Figure 6 and Figure 4 suggests that the Mount Wilson results do not give the same frequency distribution of absolute magnitudes as that indicated by the trigonometric data for giant HD Ko stars.

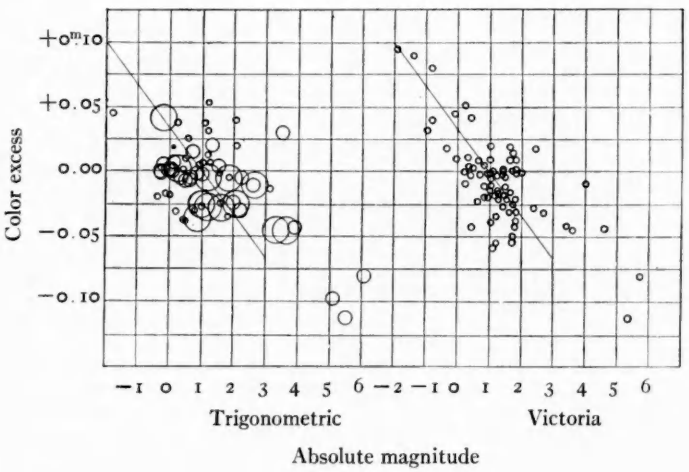

FIG. 7.—Although the evidence of correlation in the left figure is weak, this may be partly due to the fact that there are few supergiants in this group having reliable parallaxes. This graph includes all stars whose mean parallax is at least twice its probable error.

group—the correlation coefficient is 0.67—I would not attempt at this time to derive absolute magnitudes from these data. The probable difference $M_v - M_c$ is ± 0.48 mag. The fact that there are so few highly luminous stars within these spectral limits makes it difficult to judge the significance of these figures.

It is tempting to draw a single curve through the giants and dwarfs, but the data are not sufficiently numerous to show whether there is a gradual change of color as we pass from giants to dwarfs of the same spectral class. A similar color program embracing 200 G-type stars is now about half completed at the Sproul Observatory.

The various columns in Table VII contain the following data: (1) the number of the star in the *Bright Star Catalogue* (same as HR); (2) the number of the star in the *Preliminary General Catalogue* by Boss; (3) the photographic magnitude on Hertzsprung's scale of either Hertzsprung's value, that of *Actinometry B*, or the mean of both values; (4) the *Revised Harvard Photometry* visual magnitude; (5) the infra-red magnitude on the international scale with RG9 in position; (6) the number of magnitude observations; (7) the observed mean color from observations made at Columbia and Swarthmore only (Jena glass filters $[M_{BG17} - M_{RG9}]$ for Swarthmore, 96 per cent of weight; no filter minus Wratten 89 for Columbia, 4 per cent of weight); (8) the weight in units of one observation of color at Swarthmore; (9–11) the spectral type from Victoria, Mount Wilson, and Harvard, respectively (the letter *A* denotes a visual double star, and a plus sign after the spectrum denotes a spectroscopic binary); (12) the mean color excess derived from as many of its three components as exist; (13) the parallax computed from the data in columns 4 and 12 in units of 0".001 (a colon means that the probable error of the mean color excess is ± 0.013 mag. or less; in such cases it always contains measures of color from more than one observatory); (14–15) the Victoria spectroscopic and the mean trigonometric parallaxes, respectively; and (16) the absolute visual magnitude derived from the color excess.

Corresponding data for stars whose colors I have previously observed at the Yale Observatory are shown in Table VIII. If the figures in the eighth column are followed by a colon, the star was also observed by Becker. The good agreement between π_c and π may be attributed to more accurate trigonometric parallaxes and

TABLE VII

CATALOGUE OF SWARTHMORE OBSERVATIONS

STAR		MAGNITUDES				COLOR	WT.	SPECTRUM			MEAN C.E.	PARALLAX			VIS. M_c
BS	PGC	Ptg.	Vis.	Infr.	N			V	W	H		π_c	π_v	π_t	
3	1	....	4.68	3.47	4	+0^{M}047	6	Ko	Ko+	.....	−0^{M}013	...	25	+ 11	.....
74	53	....	3.75	2.33	4	+ .094	5	K3	AK3	K1	− .012	28	12	+ 9	+1.0
168	135	3.71	(2.5)	....	..	+ .09	2	G7	AG7	.....	+ .045	26:	31	+ 11	−0.4
188	147	....	2.24	0.93	2	+ .043	2.5	....	G6	G8	+ .015	45	...	+ 57	+0.5
194	151	....	4.93	3.65	4	+ .058	5	....	G6	.....	+ .040	10	...	+ 19	−0.2
215	164	5.40	4.30	2.85	2	+ .06	3	G6	G8+	.....	+ .037	...	23	+ 34	.....
248	191	....	4.92	2.92	4	+ .293	5	K7	Mo	.....	.000	14	8	− 7	+0.6
253	193	6.32	4.95	3.52	4	+ .112	5	....	AK2	.....	+ .012	11	.....	.....	+0.2
265	200	5.84	4.83	3.54	4	+ .072	4	G5	G4	.....	+ .040	10	13	+ 39	−0.2
294	226	5.34	4.45	3.15	4	+ .032	4	G6	G5	G8	− .006	23:	16	+ 29	+1.2
334	255	....	3.60	2.26	1	+ .065	4	....	K1	K1	− .011	29	...	+ 32	+0.9
351*	270	5.89	4.89	3.54	9	+ .025	11	....	G9	.....	− .025	24	...	+ 14	+1.8
352	271	5.81	4.70	3.33	7	+ .073	9	K2	K1+	.....	− .018	...	18	+ 37	.....
360	281	5.92	4.64	3.55	3	+ .01	2	K1	AG7+	G9	− .007	...	18	− 7	.....
390	304	6.09	4.99	3.73	4	+ .046	5	K1	G9	.....	− .014	19	19	+ 33	+1.4
399	310	6.03	4.96	3.62	3	+ .050	4	....	AG8	.....	+ .013	13:	...	+ 9	+0.6
402	313	....	3.83	2.39	4	+ .055	4	Ko	AKo	K2	− .016	29	32	+ 28	+1.1
442	338	5.92	4.88	3.61	5	+ .016	6	G6	G6	.....	+ .006	15:	13	+ 19	+0.8
456	349	....	5.50	4.27	4	+ .025	4	....	AG5	.....	.000	13	.....	.....	+1.0
464	357	5.14	3.77	2.18	1	+ .09	1	K3	K2	K4	− .013	28:	34	+ 17	+1.0
489	378	6.00	4.68	2.89	4	+ .159	6	K5	K4	.....	− .018	19:	12	+ 32	+1.1
509	391	....	3.65	2.56	2	− .060	2	G7	G4	.....	− .080	...	295	301	.....
510	393	5.30	4.50	3.19	4	+ .003	6	G6	G6	G9	− .011	23:	19	+ 16	+1.3
539	416	....	3.92	2.49	4	+ .085	5	....	Ko+	.....	+ .025	...	.....	+ 43	.....
549	426	5.64	4.84	3.52	3	+ .024	5	G7	G7+	.....	− .029	...	26	− 20	.....
643	499	....	5.08	3.21	4	+ .210	4	K5	.....	.....	− .003	13	8	.....	+0.7
645	500	....	5.40	4.33	4	+ .019	4	G7	AG6+	.....	− .002	...	13	+ 7	.....
736	571	....	5.35	3.42	4	+ .253	6	.....	.....	.....	.....	...	.....	.....	.....
737	572	6.68	5.44	3.85	4	+ .126	5	....	K3	.....	+ .001	11	...	.....	+0.6
743	577	....	5.34	4.21	4	− .012	4	....	G6	.....	− .026	20	...	+ 11	+1.8
824	634	5.81	4.62	3.36	2	+ .030	2	Ko	K1	.....	− .024	22:	22	+ 23	+1.3
834	639	5.81	3.93	1.99	1	+ .25	1	K4	AcK4	.....	+ .081	7:	7	+ 1	−1.8
874	665	....	4.05	2.67	8	+ .049	7	....	K2	K1	− .012	25	...	+ 27	+1.0
882*	670	6.40	4.97	3.61	8	+ .104	11	K4	K2	.....	− .027	19:	10	.....	+1.4
918	697	....	5.08	3.71	4	+ .037	5	G6	.....	.....	+ .019	12	28	.....	+0.4
941	713	4.92	4.00	2.74	2	+ .00	2	G8	AG8+	Ko	− .038	...	40	+ 28	.....
947	717	5.96	4.82	3.39	4	+ .054	7	....	G9	.....	+ .006	16	...	+ 22	+0.8
951	718	5.62	4.53	3.18	4	+ .044	7	....	K2	K1	− .041	29:	...	+ 24	+1.8
969	729	....	5.29	3.85	3	+ .084	5	....	cG2	.....	.....	...	.....	.....	.....
991	746	6.69	4.92	3.28	4	+ .192	8	K2	K4	.....	+ .063	6	7	+ 10	−1.3

TABLE VII—*Continued*

Star		Magnitudes				Color	Wt.	Spectrum			Mean C.E.	Parallax			Vis. M_c
BS	PGC	Ptg.	Vis.	Infr.	N			V	W	H		π_c	π_v	π_t	
1015*	770	....	5.25	3.73	4	+0M110	7	K3	K5	.....	−0M042	22	12	+ 7	+1.9
1052	795	6.05	4.55	2.84	4	+ .180	5	K4	K4	K3	+ .001	16:	10	− 1	+ .6
1066	804	5.48	4.28	3.06	1	+ .04	1	G9	G7+	Ko	+ .017	...	27	.....	.....
1084	814	....	3.81	2.57	3	+ .015	6	K1	K2	Ko	− .063	...	302	+305	.....
1136	848	....	3.72	2.45	3	+ .019	6	G9	Ko	K1	− .043	...	151	+114	.....
1256*	936	5.74	4.50	3.22	6	+ .035	8	Ko	Ko	K1	− .015	24:	24	+ 11	+1.4
1346	1000	4.91	3.86	2.67	1	+ .04	1	G6	Ko+	G9	− .018	...	31	+ 26	.....
1348	1002	....	5.06	3.62	8	+ .098	8	...	AK1	.....	+ .023	9	...	.....	−0.1
1373	1017	5.02	3.93	2.73	1	+ .01	1	G8	G8	G7	+ .005	25:	39	+ 16	+0.9
1390	1030	....	5.33	4.17	4	+ .033	6	....	G6	.....	+ .015	12	...	.....	+0.6
1396	1036	5.90	4.94	3.52	4	+ .050	7	....	G6	.....	+ .026	12	...	+ 13	+0.2
1409	1044	4.81	3.63	2.47	1	+ .07	1	G8	G7	Ko	.000	30:	48	+ 22	+1.0
1437	1063	....	4.97	3.48	4	+ .117	6	....	K4	.....	− .058	29	...	− 15	+2.3
1467	1082	....	5.31	3.88	6	+ .048	6	....	AG6+	.....	+ .030	...	...	.....	.....
1481	1091	....	3.98	2.61	5	+ .090	6	....	K3+	Ko	.000	...	...	+ 33	.....
1580	1169	5.54	4.28	2.85	1	+ .09	2	K2	AK2	.....	− .008	20:	19	+ 18	+0.8
1601	1181	6.10	4.73	2.94	4	+ .158	5	....	cK3	.....	+ .042	8	...	.....	−0.7
1684	1234	7.03	5.36	3.37	5	+ .221	7	....	K5	.....	+ .040	6	...	.....	−0.6
1698	1240	5.88	4.64	3.16	5	+ .092	6	K2	AK3+	.....	− .017	...	22	− 16	.....
1726	1258	6.04	4.81	3.06	4	+ .168	6	....	AK3+	.....	+ .034	...	...	+ 11	.....
1739	1266	....	5.14	3.85	6	+ .009	7	....	G5	.....	− .006	17	...	.....	+1.2
1784	1299	....	4.21	2.97	3	+ .030	6	....	G9	G8	− .012	28	...	+ 7	+1.4
1805*	1311	....	5.26	3.56	6	+ .156	8	....	K5	.....	− .025	17	...	.....	+1.4
1907	1373	5.22	4.39	2.92	1	+ .08	2	G7	G6	Ko	+ .002	20:	30	+ 24	+0.9
1995	1429	5.48	4.64	3.42	4	+ .027	7	G5	AG5	Ko	− .018	24	18	+ 3	+1.5
2002	1434	....	5.02	3.67	1	+ .042	6	Ko	K3	.....	− .048	25	18	+ 5	+2.0
2012	1442	5.33	4.18	2.70	2	+ .083	6	Ko	AK1	Ko	+ .006	21	27	+ 16	+0.8
2037	1458	6.34	5.01	3.27	6	+ .158	7	....	cK2	.....	+ .039	8	...	+ 2	−0.6
2077	1472	4.94	3.88	2.61	1	+ .03	1	G6	G6	Ko	+ .001	26:	37	+ 18	+1.0
2113	1494	....	4.68	3.09	6	+ .125	6	....	K2	.....	+ .025	11	...	+ 22	−0.2
2152	1520	....	5.42	4.12	5	+ .078	5	....	G8	.....	+ .037	8	...	.....	−0.1
2165	1530	....	5.39	3.94	4	+ .151	4	K1	K2	.....	+ .039	6:	10	.....	−0.6
2219	1565	5.47	4.45	3.10	5	+ .043	6.5	G9	G6	.....	+ .010	18:	16	+ 18	+0.7
2227	1570	....	4.09	2.50	4	+ .132	4	....	AK2	G9	+ .060	9	...	+ 12	−1.2
2334	1626	6.55	5.29	3.96	4	+ .042	4	Ko	cKo	.....	.000	14:	10	+ 2	+1.0
2429	1695	....	4.14	2.77	4	+ .049	4	....	K1	G9	− .010	27	...	+ 55	+1.3
2443	1698	....	4.65	3.15	4	+ .080	4	....	K1	.....	+ .005	14	...	+ 8	+0.4
2450	1703	....	4.97	3.19	6	+ .208	5	....	K5	.....	+ .027	9	...	− 12	−0.2
2478	1721	5.92	4.65	3.22	4	+ .084	4	....	AK2	.....	− .011	28	...	− 15	+0.9
2480*	1722	....	5.54	3.79	8	+ .191	9	K5	K3	.....	+ .024	7	6	.....	−0.1
2487	1728	....	5.28	4.06	4	+ .045	4	Ko	Ko	.....	− .015	17	13	.....	+1.4
2503	1737	6.50	5.00	3.18	4	+ .146	4	....	K5	.....	− .035	21	...	+ 8	+1.6
2506	1740	5.80	4.70	3.22	4	+ .035	4	....	Ko+	.....	− .013	...	...	+ 13	.....
2516	1748	....	5.04	3.62	4	+ .099	4.5	....	K3	.....	−0.020	17	...	− 5	+1.2
2630	1806	....	5.21	4.08	6	+0.009	7	....	cG2	.....	.....	...	...	+ 13	.....

TABLE VII—*Continued*

Star		Magnitudes				Color	Wt.	Spectrum			Mean C.E.	Parallax			Vis. M_c
BS	PGC	Ptg.	Vis.	Infr.	N			V	W	H		π_c	π_v	π_t	
2697	1840	5.94	4.48	3.00	4	+0^{M}119	4	K3	AK3	Ko	+0^{M}030	11:	21	+ 4	−0.3
2701	1844	....	5.02	3.70	4	+ .042	4	...	K1	.....	− .033	21	..	.....	+1.6
2715	1854	....	5.33	4.04	3	+ .042	3	Ko	K2	.....	− .038	19	27	+ 34	+1.7
2793	1912	....	5.21	3.86	4	+ .079	4.5	....	AG9	.....	+ .031	9	...	+ 22	+0.1
2805	1919	....	5.28	3.92	4	+ .092	5.5	Ko	Ko	.....	+ .032	9	6	+ 5	0.0
2821	1931	4.95	3.89	2.62	1	− .01	1	....	G7	G8	− .004	28:	...	+ 26	+1.1
2854	1953	6.01	4.60	2.63	4	+ .225	5	K5	AK4+	K2	+ .057	...	9	+ 15	.....
2861	1959	....	5.09	3.81	3	+ .042	4	....	AK1+	.....	− .033	...	...	+ 16	.....
2864	1962	6.04	4.85	3.15	5	+ .106	5	K4	K3	.....	− .025	20:	10	+ 27	+1.4
2896	1981	....	5.34	4.24	4	+ .011	4.5	Ko	AKo+	.....	− .049	...	16	.....	.....
2970	2021	....	4.07	2.77	5	+ .028	6	....	Ko	Ko	− .031	37	...	+ 19	+1.9
2973	2023	5.42	4.26	2.88	1	+ .02	1	Ko	K1p+	G7	+ .004	...	34	+ 18	.....
3110	2104	6.36	5.40	4.20	4	+ .020	4	....	G6	.....	− .005	15	...	+ 25	+1.2
3141	2126	....	4.88	2.96	4	+ .225	4	....	K5	.....	+ .044	8	...	+ 8	−0.7
3145	2130	5.86	4.52	2.89	3	+ .14	4	K2	K3	Ko	+ .047	9:	15	+ 18	−0.8
3149	2131	....	5.04	3.70	6	+ .071	7	....	K2+	.....	− .018	...	...	+ 14	.....
3211	2170	....	4.68	3.60	4	− .010	4	....	AG7	.....	− .035	29	...	+ 33	+2.0
3306	2234	6.18	5.23	4.08	5	− .005	5	G5	AG6	.....	− .022	20	12	+ 6	+1.7
3366*	2271	....	5.52	3.96	7	+ .090	7	K2	K5	.....	− .053	22:	10	.....	+2.2
3403	2290	5.99	4.76	3.27	3	+ .100	4	Ko	K2	.....	+ .019	11:	22	+ 14	0.0
3418	2302	5.86	4.54	3.11	5	+ .102	5.5	K3	K3	K1	− .001	16:	19	+ 17	+0.6
3441	2321	....	4.98	3.65	4	+ .040	4	....	AG8	.....	− .001	16	...	+ 23	+1.0
3461	2336	5.18	4.17	2.69	1	+ .03	2	K1	AKo	K1	− .018	24:	23	+ 14	+1.1
3547	2393	4.35	3.30	2.08	1	− .03	1	G7	G5	G8	.000	35:	26	+ 28	+1.0
3613	2439	6.39	5.41	3.83	5	+ .081	4	K3	K2	.....	− .034	17:	9	.....	+1.6
3731*	2524	5.94	4.61	3.10	5	+ .090	6.5	K2	AK2	Ko	+ .024	11:	17	− 4	−0.1
3779	2556	6.60	5.28	3.51	4	+ .155	4.5	K4	AK4	.....	− .012	14:	7	.....	+1.0
3809	2570	6.05	4.99	3.65	5	+ .020	6	....	G8	.....	− .004	17	...	.....	+1.1
3815	2573	....	5.48	4.47	3	− .059	3.5	G9	AKo	.....	− .113	...	120	+ 95	.....
3827	2582	6.18	5.14	3.82	5	+ .031	5.5	....	G9+	.....	− .017	...	...	.....	.....
3834	2589	6.19	4.78	3.15	6	+ .179	5.5	K1	K3	.....	+ .071	6:	18	.....	−1.5
3839	2592	....	5.39	4.03	4	+ .015	4	....	G7	.....	− .010	15	...	.....	+1.3
3845	2595	....	4.10	2.39	4	+ .139	5	....	K3	K2	+ .032	13	...	+ 24	−0.4
3851	2601	....	5.50	4.58	4	− .005	5.5	....	G6	.....	− .023	17	...	+ 19	+1.7
3903	2645	....	4.29	2.95	4	− .025	4	....	G6	G7	− .038	36	...	+ 18	+2.1
3905	2648	5.39	4.10	2.51	1	+ .06	1	K2	K3	K3	− .011	23:	38	+ 22	+0.9
3994	2706	....	3.83	2.43	4	+ .018	4	....	AG9+	Ko	− .035	...	...	+ 14	.....
4100	2776	5.21	4.41	3.12	8	− .002	9	G6	AG8	Ko	− .036	35:	30	+ 15	+2.1
4146	2816	6.10	5.17	3.98	5	+ .042	5	....	G6	.....	+ .002	14	...	.....	+0.9
4178	2841	....	5.12	3.83	4	+ .084	4	....	K4	.....	− .091	43	...	+ 27	+3.3
4181	2844	....	5.23	3.45	4	+ .162	4	....	K4	.....	− .030	18	...	+ 4	+1.5
4246	2898	....	5.36	3.64	4	+ .138	4	....	K2	.....	+ .038	7	...	.....	−0.5
4247	2899	4.97	3.92	2.58	1	+ .06	3	K1	K2	K1	− .032	34:	39	+ 32	+1.6
4258*	2910	....	5.23	3.78	4	+ .085	6	K1	K1	.....	+ .010	10	13	.....	+0.3
4287	2925	....	4.20	2.83	3	+ .055	4	....	K1	K1	− .021	25	...	+ 39	+1.2

TABLE VII—*Continued*

Star		Magnitudes				Color	Wt.	Spectrum			Mean C.E.	Parallax			Vis. M_c
BS	PGC	Ptg.	Vis.	Infr.	N			V	W	H		π_c	π_v	π_t	
4291	2927	6.14	5.05	3.57	5	+0^{M}071	5.5	....	K3	.....	−0^{M}046	25	...	.....	+2.0
4335	2958	4.33	3.15	1.91	1	+ .11	1	Ko	K1	G8	+ .012	31:	49	.....	+0.6
4365	2978	6.68	5.48	3.93	6	+ .102	6.5	K1	K 3+	.....	+ .020	...	10	.....	.....
4377	2985	5.19	3.71	1.89	1	+ .16	1	....	AK3	K1	+ .070	9:	...	+ 7	−1.5
4382	2989	....	3.82	2.22	5	+ .088	5	....	Ko	G8	+ .039	16	...	+ 25	−0.2
4418	3021	6.05	5.18	3.82	4	+ .024	5	....	AG7	.....	− .005	16	...	+ 32	+1.2
4471	3058	....	4.47	3.12	4	+ .028	5	K1	G8	G7	− .023	28:	25	+ 16	+1.7
4518	3090	5.06	3.85	2.28	1	+ .12	1	Ko	K1	K1	+ .031	15:	19	+ 12	−0.3
4667*	3194	....	5.06	3.83	4	+ .009	5.5	....	G8	.....	− .032	24	...	+ 6	+2.0
4668	3195	....	5.08	3.69	5	+ .064	5.5	....	Ko+	.....	+ .004	...	...	.....	.....
4695	3213	6.24	5.10	3.61	3	+ .082	6	Ko	K1	.....	+ .016	10:	12	− 3	+0.1
4697	3216	5.82	4.91	3.54	4	+ .040	5.5	G8	AG6	.....	+ .008	15:	25	.....	+0.8
4728	3235	....	5.22	3.93	4	− .002	5	G8	G4	.....	− .022	20:	21	+ 29	+1.7
4737	3242	5.63	4.56	3.11	4	+ .041	6.5	K1	K3	G8	− .015	20:	22	+ 2	+1.1
4783	3278	....	5.43	4.28	4	+ .030	5	G8	G7	.....	− .003	14	12	.....	+1.1
4792	3285	5.99	5.18	3.72	4	+ .035	4	....	AG9	.....	− .013	...	...	.....	.....
4795	3287	....	5.18	3.44	4	+ .185	4	....	K2+	.....	+ .085	...	...	.....	.....
4813	3298	....	4.78	3.31	4	+ .078	4	....	K3	.....	− .043	26	...	+ 16	+1.9
4815	3299	....	5.51	4.36	5	+ .028	6	....	G8+	.....	− .013	...	...	.....	.....
4894	3355	....	5.10	3.86	5	− .010	7	....	AG6+	.....	− .028	...	...	.....	.....
4924*	3379	....	5.08	3.63	4	+ .084	5	....	AG9	.....	+ .036	9	...	+ 16	−0.1
4928	3380	....	5.50	3.96	4	+ .146	4	Ko	G9	.....	+ .092	3	4	+ 7	−1.8
4932	3383	3.97	2.95	1.77	1	− .04	1	G6	G6	K1	− .027	59:	48	.....	+1.8
4997	3432	....	5.05	3.78	4	+ .039	5.5	....	.....	.....	.....	...	...	− 4	.....
5201	3573	....	5.06	3.32	5	+ .178	5	....	K5	.....	− .003	13	...	.....	+0.7
5247	3601	....	5.18	3.42	5	+ .183	5	K5	K5	.....	− .014	14	7	.....	+1.0
5315	3642	....	4.31	2.64	4	+ .165	4	....	K2	K3	+ .036	11	...	+ 20	−0.5
5340	3662	1.30	0.24	.....	..	+ .134	2.0	Ko	Ko	K1	+ .042	78:	100	+ 85	−0.3
5361	3673	6.04	4.83	3.62	4	+ .033	4.5	Ko	K1+	.....	− .020	...	16	.....	.....
5370	3681	6.23	4.97	3.54	5	+ .086	4.5	K6	K3	.....	− .030	20	20	.....	+1.5
5429	3717	5.02	3.78	2.10	2	+ .13	3	K3	AK3	K1	+ .017	18:	20	+ 25	+0.1
5502	3770	5.61	4.69	3.53	5	− .014	6.5	....	G6	.....	− .029	28	...	+ 44	+1.9
5535	3790	....	5.05	3.81	4	+ .028	6	....	G6	.....	+ .010	14	...	.....	+0.7
5541	3795	....	5.50	4.31	4	+ .056	5	G9	Ko	.....	+ .002	12	15	.....	+0.9
5601	3835	5.62	4.62	3.21	4	+ .042	7	....	Ko	G8	− .006	21:	...	+ 20	+1.2
5616*	3842	5.93	4.67	3.12	7	+ .102	7	....	K2	.....	+ .003	14	...	.....	+0.5
5675	3882	6.67	5.44	4.06	4	+ .051	4.5	....	Ko	.....	+ .006	12:	...	+ 19	+0.6
5681	3887	4.45	3.54	.....	..	+ .04	1	G5	AG4	G7	+ .001	31:	34	+ 26	+1.0
5710	3907	6.80	5.48	4.02	5	+ .075	4.5	K2	AK4	.....	− .042	19	13	+ 5	+1.9
5714	3912	....	5.14	3.59	4	+ .158	4	....	K4	.....	− .017	16	...	+ 12	+1.1
5777	3952	....	4.83	3.47	4	+ .023	4	....	K1	.....	− .052	30	...	+ 24	+2.2
5787	3959	....	4.02	2.78	4	+ .025	4	....	AG6	G6	+ .007	23	...	+ 36	+0.8
5802	3968	6.44	5.40	4.18	4	− .006	5	....	G7+	.....	− .018	...	...	+ 29	.....
5854	4001	3.96	2.75	1.43	1	+ .05	1	K3	AK2	K1	− .029	56:	64	+ 45	+1.5
5888	4023	6.47	5.33	4.02	4	+ .025	4.5	....	G6	.....	+ .018	11	...	+ 31	+0.5

TABLE VII—*Continued*

Star		Magnitudes				Color	Wt.	Spectrum			Mean C.E.	Parallax			Vis. M_c
BS	PGC	Ptg.	Vis.	Infr.	N			V	W	H		π_c	π_v	π_t	
5901	4032	5.95	4.77	3.69	4	+0^{M}030	4.5	K1	K1	.....	−0^{M}040	25:	38	+ 29	+1.8
5908	4039	....	4.34	2.96	4	+ .032	4	....	G8	G9	− .010	25	...	.....	+1.3
6018	4108	5.85	4.94	3.58	4	+ .037	4	K0	AK1	.....	− .034	22:	28	+ 30	+1.6
6075	4147	....	3.34	2.10	4	+ .006	5	....	G7	G5	− .008	37	...	+ 37	+1.2
6103*	4169	5.93	4.72	3.78	9	+ .003	10	K0	K0	.....	− .053	38:	25	+ 12	+2.6
6104	4170	....	4.59	3.40	4	+ .005	4	....	G9	G9	− .042	35	...	− 7	+2.3
6126	4186	....	5.44	4.08	4	+ .062	4	K0	K1	.....	− .005	12	14	+ 9	+0.8
6147	4202	....	4.40	3.27	4	− .022	4	....	AG5	G7	− .034	33	...	.....	+2.0
6148	4204	3.81	2.81	1.67	1	+ .03	1	G4	G5+	G7	+ .008	...	41	+ 15	.....
6196	4239	....	5.04	3.68	3	+ .070	5	....	G8	.....	+ .029	10	...	+ 57	+0.1
6220	4255	4.49	3.61	2.40	1	.00	1	G6	AG4	G7	− .005	33:	31	+ 53	+1.2
6223	4259	6.22	5.00	3.54	5	+ .102	5	....	K2	.....	+ .004	12	...	+ 21	+0.5
6270*	4294	....	5.20	3.77	8	+ .091	8.5	....	K1	.....	+ .016	10	...	+ 10	+0.1
6287	4307	....	5.48	4.28	4	+ .017	4	G7	G7	.....	− .008	14	9	− 3	+1.2
6299	4315	4.52	(3.4)	2.00	1	+ .05	1	K3	K2	K0	− .021	36:	57	+ 51	+1.2
6318	4323	....	5.00	3.17	4	+ .178	4	....	K4	.....	+ .003	13	...	+ 28	+0.5
6388	4364	....	5.12	3.66	3	+ .115	4	K2	K3+	.....	+ .004	...	14	+ 18	.....
6415	4379	....	4.82	3.47	3	+ .058	5	....	AK4+	.....	− .117	.....	...	+ 9	.....
6498	4425	6.04	4.44	2.73	5	+ .170	5	....	K1	G8	+ .120	4:	...	+ 4	−2.6
6526	4438	5.91	4.48	2.83	4	+ .162	4.5	K5	K4+	K2	− .002	...	24	+ 12	....
6566	4464	....	5.21	3.92	4	+ .066	5	....	G9+	.....	+ .018	.....	...	− 8	.....
6603	4487	....	2.94	1.55	1	+ .07	1	K2	K1	K0	+ .003	33:	58	+ 26	+0.5
6644*	4508	....	5.34	3.84	8	+ .065	8.5	....	K1	.....	− .010	13	...	.....	+0.9
6677	4522	....	5.12	3.83	4	+ .091	4.5	K3	AK1	.....	− .007	14	15	.....	+0.8
6688	4531	5.14	3.90	2.47	2	+ .09	2	K3	K3	K2	− .044	40:	39	+ 34	+1.9
6695	4535	5.23	3.99	2.49	1	+ .11	1	K1	cK1	K0	+ .049	11:	10	− 1	−0.9
6698	4536	....	3.50	2.21	4	+ .035	6	....	G9	K0	− .018	40	...	+ 21	+1.5
6703	4538	4.65	3.82	2.67	1	+ .01	2	G7	G7	G7	− .015	33:	33	+ 17	+1.4
6713	4547	6.02	4.71	3.38	4	+ .073	4.5	K2	G8	.....	+ .011	16:	11	+ 7	+0.7
6752	4571	4.99	4.07	2.96	1	.00	1	AK	AK	K2	.....	...	162	+196	.....
6869	4638	....	3.42	2.06	3	+ .032	4	....	AG8	K0	− .027	47:	...	+ 53	+1.8
6872	4639	5.61	4.34	3.11	1	+ .07	1	K2	K1	K1	− .015	22:	41	+ 8	+1.0
6885	4651	6.68	5.48	3.88	6	+ .131	6.5	K2	K2	.....	+ .022	8:	12	+ 23	−0.1
6895	4656	5.15	3.92	2.55	1	+ .08	1	K1	K2	K2	+ .005	20:	35	+ 17	+0.4
6945	4686	6.23	4.99	3.51	4	+ .110	4	....	K1	.....	+ .030	9	...	+ 20	−0.3
6973	4705	....	4.06	2.37	4	+ .122	4	....	K5	K0	+ .003	19	...	+ 16	+0.5
6983	4711	....	5.42	4.18	4	+ .052	4	....	ABG5	.....	+ .036	8	...	+ 3	−0.1
7064	4758	6.16	4.92	3.53	6	+ .073	6.5	....	K1	.....	+ .004	13	...	+ 23	+0.5
7125	4790	6.06	4.78	3.32	4	+ .118	4	G8	AG5+	.....	+ .068	...	14	+ 2	.....
7176	4823	5.21	4.21	2.84	1	+ .07	1	....	K0+	K1	− .020	.....	...	+ 25	.....
7180	4825	6.09	4.91	3.61	4	+ .068	4	....	K0+	.....	+ .006	.....	...	− 18	.....
7181*	4826	....	5.28	3.86	9	+ .126	7.5	....	K2	.....	+ .026	8	...	− 2	−0.2
7193	4834	....	4.15	2.74	4	+ .068	4	....	K1	K2	− .015	23	...	+ 17	+1.0
7295	4894	....	5.24	4.05	5	+ .017	5	....	G7	.....	− .008	16	...	+ 10	+1.2
7309	4907	....	5.26	3.75	4	+0.082	4	K2	K2	.....	−0.018	15	22	+ 24	+1.1

TABLE VII—*Continued*

Star		Magnitudes				Color	Wt.	Spectrum			Mean C.E.	Parallax			Vis. M_c
BS	PGC	Ptg.	Vis.	Infr.	N			V	W	H		π_c	π_v	π_t	
7310	4909	4.16	3.24	1.98	1	+0^{M}09	1	G8	G8	G8	−0^{M}002	37:	36	+ 27	+1.1
7314	4912	5.72	4.46	3.00	4	+ .075	4	....	AG9	G9	+ .029	13	...	− 5	+0.1
7319	4916	6.49	5.32	3.86	4	+ .055	4	....	AKo	.....	+ .009	12	...	+ 4	+0.7
7328	4923	....	3.98	2.76	2	+ .03	2	G5	G8+	G8	− .026	...	41	+ 22	.....
7352	4940	....	4.63	3.16	4	+ .105	4	....	K4+	K3	− .063	...	...	+ 13	.....
7385	4960	6.31	5.31	4.03	4	+ .008	5	....	AG7	.....	− .017	17	...	− 3	+1.5
7429	4995	5.88	4.65	3.19	4	+ .094	6	K4	AK4	.....	− .073	43:	26	+ 39	+2.8
7462	5009	....	4.78	3.76	4	+ .044	4	G9	G8	.....	− .081	...	151	+181	.....
7478*	5021	5.71	4.79	3.61	8	+ .026	9	Ko	Ko+	.....	− .047	...	12	+ 7	.....
7488	5027	5.52	4.40	3.32	5	+ .033	6	G7	G7	Ko	− .011	24:	19	+ 12	+1.3
7517	5045	....	5.02	3.84	4	− .002	4	G6	G8	.....	− .022	22:	15	+ 18	+1.7
7582	5079	4.96	3.99	2.84	1	+ .02	1	....	.....	.....	.....	...	...	+ 1	.....
7595	5089	5.90	4.86	3.57	3	+ .056	8	G8	Ko	.....	− .002	18:	17	+ 22	+1.1
7602	5093	4.61	3.90	2.74	1	− .01	1	G7	AG8	G7	− .045	...	80	+ 77	.....
7615	5103	4.87	4.03	2.80	1	+ .06	1	G9	AKo	Ko	− .035	39:	56	+ 10	+2.0
7660	5137	....	5.28	3.89	4	+ .048	4	Ko	AG9	.....	− .006	15	12	+ 14	+1.2
7679	5151	6.39	5.26	3.98	4	+ .074	5	K2	K1	.....	− .024	16:	24	+ 31	+1.3
7685	5153	6.14	4.66	3.13	4	+ .124	4	....	K2	.....	+ .032	10	...	− 10	−0.4
7753	5201	....	5.45	4.30	4	+ .033	6	G7	G7	.....	+ .008	12	11	− 4	+0.8
7794	5226	6.59	5.41	4.24	5	+ .030	7	G9	G7	.....	− .001	13	16	− 4	+1.0
7884	5294	....	4.51	3.30	5	− .006	5	G8	AG5+	G8	− .038	...	17	+ 6	.....
7897	5305	....	5.39	4.10	5	+ .048	6	....	AG9	.....	.000	13	...	+ 7	+1.0
7942	5331	5.47	4.34	3.03	1	+ .06	1	G9	AG7	Ko	− .016	27:	30	+ 12	+1.5
7949	5336	3.72	2.64	1.31	1	− .01	1	G7	AKo+	Ko	− .018	...	58	+ 39	.....
7956*	5345	....	5.20	3.55	11	+ .135	10	....	AK3	.....	+ .014	10	...	+ 4	+0.2
7957	5346	4.60	3.59	2.32	1	.00	1	G6	AG7	G8	− .011	35:	123	+ 69	+1.3
8011	5358	6.55	5.39	4.02	4	+ .078	5	G9	Ko	.....	+ .020	10:	13	.....	+0.4
8093	5441	....	4.52	3.47	4	+ .002	5	....	G8	G6	− .039	34	...	+ 15	+2.2
8115	5452	4.47	3.40	2.22	1	.00	1	G5	G4+	.....	− .019	...	18	+ 21	.....
8167	5484	....	4.30	3.27	4	− .012	4	....	G6	G6	− .030	33	...	+ 27	+1.9
8173	5489	5.40	4.24	2.93	1	+ .02	1	Ko	AKo	K1	− .026	33:	38	+ 12	+1.8
8228	5523	....	5.34	4.17	5	+ .028	5	G8	Ko	.....	− .025	20:	18	+ 31	+1.8
8252	5543	5.01	4.22	2.91	1	− .02	1	G4	G5	G8	− .042	41	33	+ 4	+2.3
8255	5546	6.22	4.98	3.73	3	+ .044	5	G9	G7	.....	+ .015	13:	21	+ 7	+0.6
8277	5560	6.30	5.33	4.04	4	+ .056	5	G8	Ko	.....	− .006	15:	13	+ 10	+1.2
8308	5584	4.27	2.54	.....	..	+ .11	1	K2	AcKo	K1	+ .092	12:	15	− 1	−2.2
8317	5594	5.89	4.85	3.39	4	+ .042	4	....	K1	.....	− .015	17	...	+ 6	+1.0
8321	5599	....	5.45	3.89	5	+ .157	7	....	cK1	.....	+ .082	3	...	+ 5	−1.9
8324	5603	....	5.40	4.03	4	+ .038	4	....	K1	.....	− .037	18	...	+ 14	+1.7
8405	5714	5.26	3.62	1.85	1	+ .18	1	K3	cK5	K2	+ .042	14:	7	+ 25	−0.7
8475*	5724	....	5.42	4.15	11	+ .086	11	K1	K2	.....	− .001	11	17	+ 4	+0.6
8498	5746	5.84	4.22	2.67	1	+ .19	1	K4	K4	K3	− .003	20:	11	0	+0.7
8499	5744	....	4.32	3.13	3	+ .033	6	....	G6	G9	+ .002	21	...	+ 19	+0.9
8551	5790	6.02	4.93	3.59	4	+ .080	8	K1	Ko	.....	+ .002	13:	19	+ 21	+0.5
8632	5852	6.02	4.64	3.07	5	+0.178	5	K3	K2	K3	+0.040	9:	16	+ 8	−0.6

TABLE VII—*Continued*

Star		Magnitudes				Color	Wt.	Spectrum			Mean C.E.	Parallax			Vis. M_c
BS	PGC	Ptg.	Vis.	Infr.	N			V	W	H		π_c	π_v	π_t	
8656	5869	....	5.24	4.09	6	+0^M.007	6	....	AG7	.....	−0^M.002	15	...	+ 7	+1.1
8667	5875	5.21	4.14	2.47	1	+ .02	1	G6	G6	.....	+ .038	14:	20	+ 35	−0.1
8684	5885	4.58	3.67	2.43	1	+ .06	1	G6	G6	G7	− .006	32:	35	+ 30	+1.2
8694	5891	4.72	3.68	2.37	1	+ .03	1	G9	K1	G9	− .025	42:	39	+ 38	+1.8
8726	5914	....	5.10	2.96	8	+ .356	10	....	cK3	.....	+ .191	1	...	0	−4.7
8779	5943	....	5.50	3.95	6	+ .107	8	....	K3	.....	− .014	12	...	− 4	+1.0
8780	5942	5.92	4.91	3.50	7	+ .059	9	G8	G8	.....	+ .019	12:	21	− 6	+0.4
8796*	5954	6.36	4.98	3.33	7	+ .162	8	K2	cK0	.....	+ .070	5:	5	+ 2	−1.5
8841	5981	....	4.48	3.07	4	+ .093	6	....	AK0	.....	+ .033	...	...	+ 52	.....
8852	5988	4.67	3.85	2.60	1	+ .05	1	G4	G4	G7	+ .001	27:	26	+ 26	+1.0
8874	6001	....	5.42	4.33	4	+ .022	4	K0	K0	.....	− .038	22	13	.....	+2.1
8878	6004	6.36	5.18	3.67	5	+ .149	8	....	AK0	.....	+ .060	6	...	+ 11	−0.8
8892	6012	....	4.20	2.71	4	+ .113	6	....	AK0	K0	+ .054	11	...	+ 33	−0.6
8893	6015	6.57	5.28	3.71	6	+ .151	11	K4	ABK4	.....	− .031	18:	13	− 2	+1.5
8923	6040	5.57	4.67	3.50	5	+ .004	11	K0	G9	.....	− .057	40:	19	− 8	+2.7
8930	6049	....	5.34	4.08	6	+ .061	8	G9	G8	.....	+ .008	12	13	+ 14	+0.8
8961	6071	4.91	4.00	2.52	1	+ .12	2	G6	G7+	.....	+ .023	...	48	+ 37	.....
8974	6078	4.54	3.42	2.16	1	+ .06	2	K1	K1	K1	− .029	41:	93	+ 67	+1.5
8997	6094	6.01	4.98	3.89	5	+ .030	7	G9	AG7+	.....	− .025	...	17	+ 18	.....
9008	6106	....	5.09	3.73	6	+0.066	6	....	G9	.....	+0.018	12	...	.....	+0.5

to the fact that these brighter stars may have been classified more thoroughly. These stars have been included in the former discussion.

GENERAL DISCUSSION

The method of deriving absolute magnitudes from color excess is similar in some respects to the spectroscopic method. The arbitrary part of the color excess is the spectral classification. According to the Victoria observers, measures of any pair of lines for the determination of spectral type need to be corrected for changes in absolute magnitude. It is conceivable that the results given in this paper could be noticeably improved if the spectroscopist would consider the color when he determines the spectral type. In this connection it is interesting to note that Mount Wilson has classified two HD K0 stars as G2. Both are c stars.

The stars in Dr. Schlesinger's *Catalogue* which I have observed and whose mean trigonometric parallax is negative have not been

observed as often by the photographic method as have other stars of the same apparent magnitude. Perhaps they have unsatisfactory comparison stars, or perhaps some of them have not been reobserved

TABLE VIII

STARS OBSERVED AT YALE

STAR		VIS. MAG.	SPECTRUM			MEAN C.E.	PARALLAX			VIS. M_c
BS	PGC		V	W	H		π_c	π_v	π_t	
224	173	4.55	K5	K5	K4	+0^{M}045	9:	10	16	−0.8
337	259	2.37	Mo	AMo	K6	+ .009	38	34	44	+0.3
617	477	2.23	K2	K1	K1	+ .002	45:	63	44	+0.5
843	646	4.67	K4	Mo	.....	+ .058	7	7	3	−1.1
1457	1077	1.06	K8	AK5	K5	+ .063	34	76	46	−1.3
1577	1167	2.90	K4	K3	K1	+ .068	14:	21	18	−1.4
2473	1717	3.18	G9	AcG8	.....	+ .095	10:	10	8	−1.8
2905	1987	4.22	K7	Mo	K6	+ .016	15:	18	13	+0.1
2985	2029	3.68	G7	G7	G5	− .015	35:	32	12	+1.4
2990	2031	1.21	G9	AG8	K1	− .028	132:	174	100	+1.8
3249	2195	3.76	K4	K4	.....	+ .046	12:	15	14	−0.8
3705	2507	3.30	K8	Mo	K5	− .003	30	32	17	+0.7
3275	2208	4.43	K6	K5	K4	+ .017	14:	14	17	+0.1
4434	3031	4.06	K5	Mo	.....	+ .036	12	10	23	−0.5
4608	3155	4.24	G6	G5	G7	+ .018	18:	12	33	+0.5
5430	3718	4.37	.....	AK4	K3	+ .007	16	.....	10	+0.4
5563	3809	2.24	K4	K5	K4	+ .007	43:	33	27	+0.4
5602	3836	3.63	G4	G5	G5	+ .005	27:	27	24	+0.8
5744	3936	3.47	K1	K3	.....	− .012	32:	42	36	+1.0
5947	4063	4.22	K1	AK2	K0	+ .019	15:	23	.....	0.0
6132	4192	2.89	G5	AG6	G8	− .034	66:	59	40	+2.0
6418	4381	3.36	K3	K5	K4	+ .005	25:	23	15	+0.4
6705	4541	2.42	K5	K5	K5	+ .021	33:	38	17	0.0
7525	5047	2.80	K3	K4	K4	+ .059	16:	22	13	−1.2
7635	5118	3.71	K8	Mo	K5	− .027	35	25	12	+1.4
7735	5187	3.95	G9	cK1	.....	+ .041	15:	11	− 6	−0.2
7866	5279	4.85	.....	cK4	.....	+0.063	6	.....	1	−1.3

because a previous determination gave a negative parallax. The average parallax of this group of stars derived from color excess is 0″.015. The mean Victoria spectroscopic value is the same. On the other hand, the average parallax of 12 c-stars computed on the basis of color excess is 0″.009.

I have found no evidence of interstellar scattering from a dis-

cussion of the colors given in this paper. There is also no relation between apparent magnitude and color excess.

It was, of course, possible to use the apparent infra-red magnitudes as a basis for the computation of parallax. Although I believe these magnitudes are more accurate than those of the HR, the latter are sufficiently accurate for our purpose.

It has been stated in a previous section that the absolute magnitude of a K-type star is apparently not related to the difference between the observed photographic magnitude and that computed on the basis of its infra-red magnitude and color. This implies, but does not prove, that its absolute magnitude cannot be found in terms of its spectral energy distribution alone. I hope to investigate this possibility by making accurate spectrophotoelectric intercomparisons of some of the brightest stars.

For the giant K stars it is evident that the color excess yields more reliable absolute magnitudes than does the assumption that the absolute magnitudes of each subtype are constant. Since the spectroscopist can readily separate giants from dwarfs, the condition that this method may apply only to giants offers no serious difficulty. It is simpler than the spectroscopic method, but whether or not it is more accurate only the future will disclose.

ACKNOWLEDGMENTS

Aside from the acknowledgments made in the text, I am grateful to Dr. Miller, Dr. Schlesinger, Dr. Schilt, and Dr. Bennett for valuable suggestions and encouragement and also for reading this manuscript. The general co-operation of the staff of the Sproul Observatory is also appreciated. This is particularly true of Mr. Delaplaine, who voluntarily rendered valuable assistance by recording observations and by checking many of the reductions. I am also grateful to Miss Emma Di Lauro, to Mr. Thomas Spencer, and to Mr. Stewart Baker for assistance in checking the reductions. Grants from the American Philosophical Society and the Joanna Wharton Lippincott Fund of Swarthmore College made possible the execution of the program which constitutes the foundation of this paper.

SPROUL OBSERVATORY, SWARTHMORE COLLEGE
SWARTHMORE, PENNSYLVANIA,
June 1936

THE PHOTOGRAPHIC DETERMINATION OF STELLAR PARALLAXES WITH THE 60- AND 100-INCH REFLECTORS. FIFTEENTH SERIES*

ADRIAAN VAN MAANEN

ABSTRACT

Trigonometric parallaxes determined with the 60- and 100-inch reflectors.—Results are given for 25 fields including 26 stars, 10 of which have photographic absolute magnitudes of +10 or fainter; 2 are fainter even than +15. One white dwarf is included, Ross 627, for which the spectrum, according to Humason, is Ao, while the absolute magnitude is +13.8. Also included are 3 stars of peculiar spectrum (put on the program at the request of Merrill), 2 planetaries, and 1 nova, Nova Geminorum 1912.

The present paper gives the results for twenty-six stars in twenty-five fields, which have recently been measured for parallax. The work has been carried out in the same way as for the previously published series.[1]

Table I gives the results of the measures. Some of the stars require special comment. Sixteen of them (Table II) have proper motions exceeding 0".5 annually; seven of these have been observed elsewhere, and in these cases (marked by an asterisk) the absolute parallaxes given in Table II are based on the mean result for all observers.

Ten of the 26 stars have photographic absolute magnitudes of +10 or fainter; Ross 64 and Ross 92 are as faint even as +15.0 and +15.6, respectively.

For Ross 627, Humason has found a spectrum Ao. The star is therefore a white dwarf, the faintest at present known, with the exception of van Maanen's F-type star and Wolf 219, which have photographic absolute magnitudes of +14.8 and +14.6, respectively.

Three of the stars—HD 35155, 207757, and Z Andromedae—were

* *Contributions from the Mount Wilson Observatory, Carnegie Institution of Washington*, No. 553.

[1] *Mt. Wilson Contr.*, Nos. 111, 1916; 136, 1917; 158, 1918; 182, 1920; 204, 1921; 237, 1922; 270, 1923; 290, 1925; 321, 1926; 356, 1928; 391, 1929; 435, 1931; 468, 1933; 506, 1935.

TABLE I

Object	α 1900	δ 1900	Vis. Mag. Harvard	Mt. Wilson Spectrum	Relative Parallax	μ_α rel	P.E.	No. of Exp.	Instrument
Wolf 124	$2^h\ 7^m22^s$	+ 3 9′	11.0*	M4	+0″.021	−1″.767	14 3	16	100
A.G. Berlin A 767	2 45 2	+15 18	9.19	K6	+ .017	+0.331	14 3	16	100
Wolf 1323	2 45 51	+34 0	10.9*	Mo	+ .081	+ .997	8 3	18	60
Σ 422 br	3 31 39	+ 0 16	6.12	G9	.000	− .020	13 5	18	60
Σ 422 f	3 31 39	+ 0 16	8.2	K5	+ .012	− .024	12 5	18	60
δ Eridani	3 38 27	−10 6	3.72	Ko	+ .083	− .098	15 3	16	100
Ross 25	3 53 36	+51 7	14.9*	.....	+ .037	+ .369	5 2	20	60
HD 35155	5 17 36	− 8 45	7.02	S	+ .019	+ .036	8 5	18	100
NGC I 418	5 22 48	−12 46	13.0†	Pl. neb.	− .026	+ .001	6 1	20	100
Ross 49	5 39 32	+ 9 13	12.3*	.....	.000	+ .091	3 2	18	60
Ross 64	6 18 34	+23 30	14.5*	.....	+ .119	+ .552	4 1	20	100
Nova Gem. No. 2	6 48 25	+32 16	14.5‡	.....	+ .006	− .001	4 1	20	60
Ross 54	6 59 34	−10 21	12.8*	.....	+ .079	− .129	7 3	18	100
Ross 90	9 32 42	+22 28	14.8*	.....	+ .028	− .706	4 1	20	100
Ross 92	9 35 24	+22 29	15.7*	.....	+ .088	+ .458	4 1	20	100
Wolf 365	11 5 54	+ 6 59	11.6*	.....	− .001	−0.553	8 2	18	100
Ross 627	11 19 3	+21 54	14.1*	Ao	+ .080	−1.041	8 2	16	100
Ross 129	11 50 3	+ 1 32	13.3*	.....	+ .036	−0.724	9 3	18	100
Lal. 24774	13 16 6	+43 38	8.2	K2	+ .027	− .410	7 1	18	60
29 Herc.	16 27 55	+11 42	4.92	Mo	− .006	− .174	6 1	18	60
26 Drac. C	17 34 30	+61 45	11.1*	.....	+ .066	+ .248	7 1	18	60
Ross 133	17 27 24	−18 28	13.5*	.....	+ .037	− .144	8 3	20	100
NGC 6842	19 50 54	+29 1	16.0†	Pl. neb.	− .007	+ .001	3 1	18	100
HD 207757	21 46 12	+12 9	7.6	Bep	− .014	− .039	10 3	18	60
Z Andr.	23 28 48	+48 16	Var.	Pec.	− .020	− .006	8 2	20	60
85 Pegasi	23 56 57	+26 33	5.85	G1	+0.127	+0.827	19 5	20	60

* Photographic magnitude by H. C. Willis.

† Photographic magnitude derived from star counts based on *Pub. Astr. Lab. Groningen*, **27**, Table IV, 1917.

‡ Magnitude estimated by Steavenson, *M.N.*, **94**, 767, 1934.

TABLE II

Name	Pg *m*	Sp	μ	πabs	Pg *M*
Wolf 124*	11.0	M4	2″.60	+0″.049	+ 9.4
A.G. Bal. A 767*	10.4	K6	0.51	+ .038	8.3
Wolf 1323*	10.9	Mo	1.39	+ .066	10.0
δ Eridani*	4.7	Ko	0.75	+ .120	5.1
Ross 25	14.9	.....	0.72	+ .031	12.4
Ross 49	12.3	.....	0.60	− .003	.....
Ross 64	14.5	.....	0.49	+ .126	15.0
Ross 54	12.8	.....	0.82	+ .072	12.1
Ross 90	14.8	.....	0.84	+ .036	12.6
Ross 92	15.7	.....	0.72	+ .095	15.6
Wolf 365*	11.6	.....	0.82	+ .020	8.1
Ross 627	14.1	Ao	1.23	+ .089	13.8
Ross 129	13.3	.....	0.71	+ .045	11.6
26 Drac. C*	11.1	.....	0.57	+ .072	10.4
Ross 133	13.5	.....	0.56	+ .044	11.7
85 Pegasi*	6.4	G1	1.29	+0.088	+ 6.1

put on the program at the request of Merrill, as they have peculiar spectra. For the last two, as well as for the three stars HD 45910, BD $+14^{\circ}3887$, and HD 190073, for which the results were published in *Mt. Wilson Contr.*, No. 506, the parallaxes found are zero or negative. This type of star must therefore have rather high luminosity.

The absolute parallax for the S-type star HD 35155 is $+0''.027 \pm 0''.008$. This result would give a visual absolute magnitude of $+4.2$, but it is felt that the value of the parallax is too uncertain to permit any definite conclusion.

CARNEGIE INSTITUTION OF WASHINGTON
MOUNT WILSON OBSERVATORY
June 1936

AN IMPROVED METHOD OF DETERMINING ABSOLUTE-MAGNITUDE DISTRIBUTIONS, WITH APPLICATION TO THE EARLY K STARS*

GUSTAF STRÖMBERG

ABSTRACT

A method of determining the distribution of absolute magnitudes for a group of stars of known radial velocities, proper motions, and apparent magnitudes has been developed. The radial velocities and proper motions are projected on several fixed axes, each of which defines two "polar" areas and a corresponding "equatorial" zone. The radial velocities of the stars in the two polar areas give the distribution of the linear velocities projected on the axis; the proper-motion components in the equatorial zone give the corresponding distribution of angular velocities, which have been reduced to a common apparent magnitude. The unknown distribution of absolute magnitudes is determined from a solution of an integral equation involving the unknown and the two known distributions. The method can be applied to any fixed axis, and several solutions can thus be obtained.

The method has been applied to the stars of spectral types G8 to K2, brighter than apparent magnitude 5.8, and of a certain range in absolute magnitude as derived from spectroscopic criteria. Three independent determinations of the luminosity distribution, corresponding to velocity components along three mutually perpendicular axes, agree fairly well and show that most of these stars have absolute magnitudes around +0.6, with a very small dispersion. A group of subgiants of mean absolute magnitude +2.3, separated from the normal giants by a frequency minimum, appears in all three solutions. The supergiants are found to be somewhat brighter than the spectroscopically determined values.

Some years ago the writer[1] described a method of determining the absolute-magnitude distribution for a group of stars from the distributions of the logarithms of the reduced parallactic and peculiar proper motions and of the radial velocities. This method was applied to stars brighter than apparent magnitude 6.0 and of spectral types B to M. The unknown distribution of absolute magnitudes was determined by the numerical solution of an integral equation containing the two distributions mentioned above. The distribution was derived in a more detailed form than had previously been attempted, but the resolving power of the method was questioned in a paper by Öpik, Olmstead, Maulbetsch, and Barnes.[2] These au-

* *Contributions from the Mount Wilson Observatory, Carnegie Institution of Washington*, No. 554.

[1] *Mt. W. Contr.*, No. 395, 396, 410, 411, 418, 430, 440, 442; *Ap. J.*, **71**, 163, 175; **72**, 111, 117, 1930; **73**, 40; **74**, 110, 342, 1931; **75**, 115, 1932.

[2] *H.C.*, No. 381, 1933.

thors also claimed that the use of the logarithms of the total proper motion was preferable to that of its components since the effect of the so-called "cosmical errors" would then be smaller. Gratton,[3] using the writer's method, found that it was preferable to use the actual reduced proper-motion components instead of their logarithms, since the sign of the parallactic motion could then be utilized. Notes were published in this connection by the writer,[4] who at the time did not know about the work by Öpik *et al.* and by Gratton.[5]

There is no doubt that the original method can be improved. In particular, the use of the numerical values of the proper motions and radial velocities has certain advantages over that of their logarithms, which were introduced on account of their simple relationship to the absolute magnitudes. On the other hand, the advantage of using total proper motions is not obvious, except in certain cases. Naturally, the percentage uncertainties are smaller when we use μ (the total proper motion) than when we use v and τ (the parallactic and the peculiar proper motions), but what we gain by combining velocity components belonging to the same star may well be lost by the neglect of that quality of motion we call "direction." In particular is this the case when we are dealing with non-spherical velocity distributions of stars which are not uniformly distributed over the sky. Further, there is a certain satisfaction in obtaining two or more independent determinations of the unknown distribution, since the agreement may tell something about the accuracy of the results.

THEORY

All methods of determining absolute magnitudes in which proper-motion data are compared with radial-velocity data presuppose a velocity distribution which is constant for all the stars in the group studied. If the distribution is not constant, corrections must be applied, as, for instance, for differential galactic rotation. The ideal case would be one in which we combined the radial-velocity distributions for two small opposite areas (poles) in the sky and compared the result with the distribution of proper motions, reduced to a com-

[3] *B.A.N.*, **7**, 85 (No. 248), 1933.

[4] *M.N.*, **94**, 68, 1933.

[5] *Ibid.*, **94**, 467, 1934.

mon apparent magnitude, in an equatorial narrow zone, 90° from the two poles, and projected on an axis through these poles. The procedure would be repeated for a large number of axes joining any two poles, and from all these observed distributions the unknown luminosity distribution could then be determined. We never have enough stars for such a detailed subdivision, and in this form the method would also be too elaborate. But we can relax the conditions somewhat by using larger areas around the poles and a correspondingly greater width for the equatorial zones. Disregarding the effect of the finite width of the polar areas and the equatorial zones, we can then study a class of stars with any kind of distribution over the surface of the sky, provided, of course, that there are enough stars in the areas under consideration. The study can be repeated for other axes of projection, and several entirely independent determinations of the absolute-magnitude distribution can thus be obtained for the same class of objects. The disadvantage of the method is that we are dealing with quantities numerically smaller than μ, and that in general we have more stars in the equatorial zones than in the polar regions. But the assumptions made are more likely to be fulfilled than are those on which other methods are based.

For each star in the spectral class studied we assume that the six following data have all been determined: the right ascension, α, and the declination, δ; the radial velocity, V; the proper motions in right ascension and declination; and the apparent magnitude, m. The spectroscopically determined absolute magnitude, M_{sp}, can also be used in order to limit the range in M and to reduce the effect of an eventual correlation between velocity and absolute magnitude.

Denoting the unknown distance to the star by R, its co-ordinates in the equatorial system are expressed by the equations

$$X = R \cos \alpha \cos \delta , \qquad Y = R \sin \alpha \cos \delta , \qquad Z = R \sin \delta . \tag{1}$$

Differentiating with regard to time, we find expressions for the velocity components of the form

$$x = V\gamma_{11} + kR(\mu_1\gamma_{12} + \mu_2\gamma_{13}) . \tag{2}$$

In this equation, μ_1 and μ_2 are the components of the proper motion in the equatorial system, and $k=4.738$ km year/sec, if R is expressed in parsecs, V in km/sec, and μ_1 and μ_2 in seconds of arc per year. The expressions for the direction cosines γ are immediately given by the differentiation and by the direction cosines of the axes of projection.

The distance R can be expressed as a function of the absolute and the apparent magnitudes. Using the ordinary units for M, we have

$$R=\frac{1}{\pi}=10^{0.2(m-M)+1}\,. \tag{3}$$

If, further, we write

$$A=10^{-0.2M}\,, \tag{4}$$

the x-component of a star's velocity relative to the sun takes the form

$$\left.\begin{aligned} x &= x_1+Ax_2\,,\\ x_1 &= V\gamma_{11}\,,\\ x_2 &= k10^{0.2m+1}(\mu_1\gamma_{12}+\mu_2\gamma_{13})\,, \end{aligned}\right\} \tag{5}$$

x_1 and x_2 being quantities known for each individual star.

Obviously, we can project the radial velocities and the proper motions on any axis fixed in direction. We may even use a great number of axes; but for practical purposes it is convenient to use a set of three mutually perpendicular axes, since the observational data are then independent and lead to three independent solutions. In the following we shall use equations (5), with the understanding that the x-axis represents any axis fixed in direction.

The principal assumption we have to make is that the distribution of the velocity components x is the same everywhere within the volume of space around the sun in which the stars studied are moving.

For small areas around the two poles of the x-axis, γ_{12} and γ_{13}, and hence x_2, are all zero. For a narrow belt 90° from the two poles, on the other hand, γ_{11} is zero. In the first case we have $x=x_1$; in the second, $x=Ax_2$. We can therefore determine the distribution of x from the radial velocities in the two polar regions. Hence we know

the distribution of Ax_2 for the equatorial zone; and, knowing the distribution of the "reduced" proper-motion components x_2, we can determine the distribution of A, and hence of M. It is clear that the distribution functions of x_1 and x_2 vary but little when the axes of projection are slightly changed or when the width of the areas is increased. For practical reasons I have given the polar regions a radius of 30° and the equatorial zones a width of 60°. The disturbing effects of the finite width and radius are in general not serious, and corrections can easily be applied for them.

The observed distributions are those of x_1 from the six polar regions and of x_2 for the three equatorial zones. There is obviously a very pronounced correlation between A and x_2, but between x_1 and A there can be no correlation other than that arising from a possible dependence of motion upon absolute magnitude. To reduce the eventual effect of such a dependence, the spectroscopic absolute magnitudes were used, and groups which could be assumed to be homogeneous with regard to motion were thus formed. When this precaution is taken, there can be no doubt that x_1 and A (or M) are independent variables. Since the dependence of motion on absolute magnitude is not very pronounced, except in certain cases, the method can be applied even if a preliminary grouping according to absolute magnitude cannot be made, although the distribution of M for the intrinsically brightest stars is then difficult to determine.

We denote the unknown distribution of A by $\psi(A)dA$ and the corresponding distribution of M by $\varphi(M)dM$. The distribution of x_1 is denoted by $F_p(x_1)dx_1$, and that of x_2 by $F_e(x_2)dx_2$, the subscripts indicating that the first function is derived from stars in the polar areas and the latter from stars in the corresponding equatorial zone. All distributions are reduced to the same total number, N. On account of the assumed equivalence of the distributions of x_1 and of Ax_2 in the two regions, we have also an equivalence of the distributions of x_1/A and of x_2. Multiplying the independent probabilities of x_1 and of A and adding, we find:

$$F_e(x_2)dx_2 = \frac{1}{N}\int F_p(x_1)\psi(A)dx_1dA \ . \qquad (6)$$

Putting $x_1 = Ax_2$, we obtain

$$F_e(x_2)dx_2 = \frac{dx_2}{N}\int_0^{\infty} AF_p(Ax_2)\psi(A)dA\ , \tag{7}$$

or, expressed in M,

$$F_e(x_2)dx_2 = \frac{dx_2}{N}\int_{-\infty}^{+\infty} AF_p(Ax_2)\varphi(M)dM\ . \tag{8}$$

The problem is now to solve the integral equation (8) for the unknown distribution function $\varphi(M)dM$. Analytically this can be done by expressing the three functions in terms of Fourier integrals and deriving the relations between the coefficients, a method which has been given an elegant form by Schwarzschild.[6] This method is impractical, however. Different types of Fourier series were tried, and also Hermite's and Laguerre's polynomials and the method of moments; but a numerical solution was, in the end, found to be simpler than the analytical method, especially since a system of weighting must be introduced.

Before describing the numerical method used, attention must be called to a few points. It is clear that it is impossible to determine the absolute-magnitude distribution beyond a certain upper limit in brightness. To stabilize the solution it is hence necessary to fix arbitrarily an upper limit in brightness for the stars in the group studied. Further, there is obviously a limit to the "resolving power" of the method; and if we go beyond this limit, the function sought becomes indeterminate and begins to oscillate violently with a "wave-length" twice that of the separation between the individual points on the distribution-curve we are trying to determine.

The method used for solving the integral equation (8) is similar to that described in *Mount Wilson Contribution* No. 395. The functions $F_p(x_1)dx_1$ and $F_e(x_2)dx_2$ are changed into continuous functions by a graphical method, and hence may be regarded as smooth, tabulated numerical functions with relatively small class widths. We can always find a first approximation to $\varphi(M)dM$, denoted by $\varphi_1(M)dM$, from the spectroscopic data, or by assuming that all

[6] *A.N.*, **185**, 80, 1910.

three functions involved are normal error-curves. The computed value of $F_c(x_2)dx_2$ is denoted by n_c, the observed value by n_o.

We have then from (8)

$$n_c = \frac{dx_2}{dx_1 N}\int_{-\infty}^{+\infty} AF_p(Ax_2)dx_1\varphi_1(M)dM \ . \tag{9}$$

We divide the range in M into several intervals M_2-M_1, M_3-M_2, etc., covering the assumed total range in absolute magnitude. These intervals need not be constant, and their size should correspond more or less to the resolving power attainable. A practical advantage is gained by introducing the function $\varphi_2(M)=A\varphi_1(M)$ and deriving the corrections to this function by a least-squares solution.

We have then for a constant value of x_2

$$n_c = \frac{dx_2}{dx_1 N}\left[\int_{M_1}^{M_2} F_p(Ax_2)dx_1\varphi_2(M)dM + \int_{M_2}^{M_3} F_p(Ax_2)dx_1\varphi_2(M)dM + \cdots\right],$$

and, approximately,

$$n_o - n_c = \frac{dM\,dx_2}{dx_1 N}\left[\Delta\varphi_2(M_{12})\sum_{M_1}^{M_2} F_p(Ax_2)dx_1 + \Delta\varphi_2(M_{23})\sum_{M_2}^{M_3} F_p(Ax_2)dx_1 + \cdots\right]. \tag{10}$$

The number of equations of condition (10) is equal to the number of finite intervals in x_2.

If we make the intervals M_2-M_1, etc., too small, the solution becomes indeterminate, as already mentioned; for large errors in $\Delta\varphi_2(M)$ corresponding to a particular value of M would cause large errors of opposite signs at the two adjacent points of the frequency-curve for which $\Delta\varphi_2$ is to be determined, and the curve representing the corrections to the assumed distribution would then show large fluctuations. This means that arbitrary "waves" of large amplitude can be superimposed on the absolute-magnitude distribution without affecting the computed distribution of x_2. This effect can be mini-

mized by making the interval in M sufficiently large, and also by arranging the least-squares solution in such a way that the corrections to φ_2 for which φ_2 itself is small are the first to be determined. These corrections can then be so adjusted that the corrected $\varphi_2(M)$ does not become negative; the corrections at other points of the distribution functions are then, in general, automatically improved, and the amplitude of the "wave of uncertainty" is thus greatly reduced.

APPLICATION

The method thus outlined has been applied to the early K stars, which form a numerous and homogeneous group. Specifically, the group used includes all stars within the spectral interval G8 to K2 as determined by Mount Wilson slit spectrograms, brighter than or

TABLE I

CO-ORDINATES OF PROJECTION AXES

Axes	α	δ	l	b
x	266°	−25°	332°	0°
y	310	+57	61	+ 9
z	185	+20	241	+81

equal to apparent magnitude 5.8 on the Harvard scale, and having spectroscopic absolute magnitudes between the limits −0.5 and +2.5. In order to make the distributions of spectroscopic and computed absolute magnitudes fully comparable, Mount Wilson absolute magnitudes, from the list of Adams, Joy, Humason, and Miss Brayton,[7] alone were used. It should be noted that, since this list includes no stars in the chosen spectral interval which have absolute magnitudes between +2.5 and +4.0, we have reason to believe that the group contains only a negligible number of stars whose true absolute magnitudes are brighter than −2.0 or fainter than +4.0. From the standpoint of spectral criteria in general, the group studied is extraordinarily homogeneous, in spite of the complex character of the spectra. The group consists of 313 stars, all with well-determined radial velocities.

The proper-motion components were taken from the *Preliminary*

[7] *Mt. W. Contr.*, No. 511; *Ap. J.*, **81**, 187, 1935.

General Catalogue, and Raymond's systematic corrections were applied to the values in declination. The distributions were corrected for the effect of accidental error, although this effect is very small.

The axes on which the radial velocities and the proper motions are projected may be chosen arbitrarily, but it was regarded as of interest to choose those having a certain fundamental character. The

TABLE II

FREQUENCIES OF RADIAL-VELOCITY COMPONENTS IN THE POLAR AREAS

x y z	$F_p(x_1)dx_1$	$F_p(y_1)dy_1$	$F_p(z_1)dz_1$
km/sec			
−90	24	0	0
−80	8	0	0
−70	0	26	0
−60	16	0	0
−50	81	26	0
−40	97	132	50
−30	169	158	163
−20	178	118	200
−10	145	316	200
0	137	132	212
+10	65	13	50
+20	48	53	75
+30	16	26	50
+40	16	0	0
+50			
No. of stars	62	38	40

ones used were those derived in *Mount Wilson Contribution* No. 293,[8] the y-axis being the axis of asymmetry in stellar motions, the x-axis lying in the galactic plane and representing approximately the axis of preferential motion. The z-axis coincides nearly with the axis of the galaxy. Since the distribution-curves change very slowly with the direction of the axes of projection, the exact values of the three directions, the equatorial and galactic co-ordinates of which are given in Table I, are not of very great importance.

The boundaries of the polar and equatorial areas, radius 30° and width 60°, respectively, were plotted on a map, and the stars grouped

[8] *Ap. J.*, **61**, 363, 1925.

according to the area in which they were situated. Naturally, most of the stars belong to a polar area for one axis and to an equatorial area for another axis of projection. Since the two polar areas combined have an area of only 27 per cent of that of the corresponding equatorial zone, there are in general many more stars in an equatorial zone than in the corresponding polar areas. The distribution-

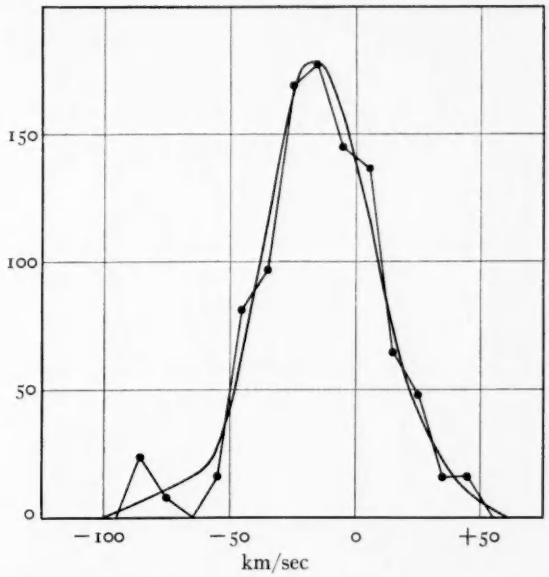

FIG. 1.—Distribution of radial velocities for stars in the polar areas of the x-axis. Points indicate observed frequencies; continuous curves represent smoothed values of the distribution. Spectral types G8 to K2; spectroscopic absolute magnitudes -0.5 to $+3.8$. Apparent magnitudes ≤ 0.5.

curves for the former area are therefore better determined than those for the latter, a peculiarity that is inherent in the method and cannot be avoided.

Table II shows the distribution of the radial velocities projected on the three axes for stars in the polar areas. The corresponding curves are shown in Figures 1–3. Table III gives the observed and computed values of the three distributions of reduced proper motions, the data being shown graphically in Figures 4–6. In the computation the final luminosity distribution derived from the combined data has been used for the three axes. Table IV shows separately the

computed absolute-magnitude distributions derived for each of the three axes and from a simultaneous solution using all the differences between observed and computed distributions of proper-motion

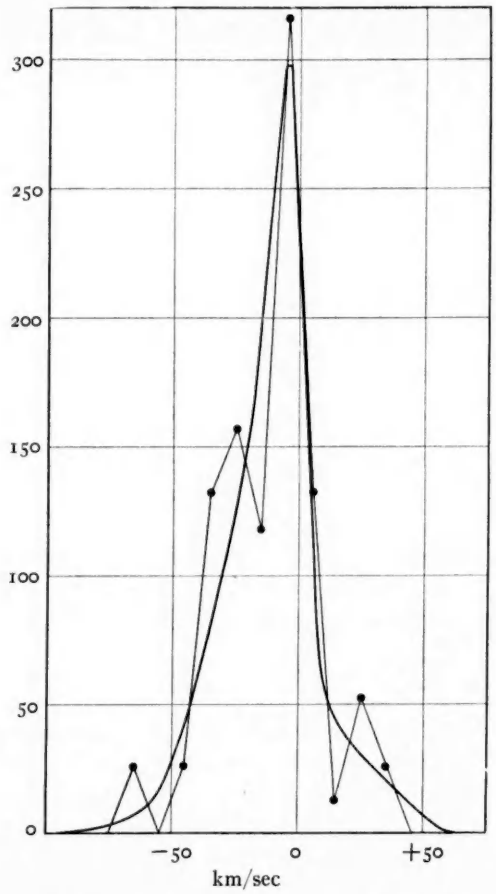

FIG. 2.—Distribution of y-components. Similar to Fig. 1

components. These data are shown in Figure 7 as four continuous curves, the distribution of spectroscopic absolute magnitudes being indicated by dots.

The least-squares solutions were based on normal places which were given weights proportional to the interval and inversely proportional to the mean values of the frequency itself, since it is ob-

vious that the admissible errors for the extreme ends of the observed distribution of reduced proper motions, where the actual frequency is very small, are much smaller than for those intervals for which the frequency is great. The intervals used were in general 2 mag.; and, by making several solutions, corrections to the assumed absolute-magnitude curve could be determined for intervals of half a magnitude.

The solutions were so arranged that corrections could be applied to those parts of the absolute-magnitude curve which were difficult to determine. These corrections were so adjusted that the frequency itself could not become negative anywhere.

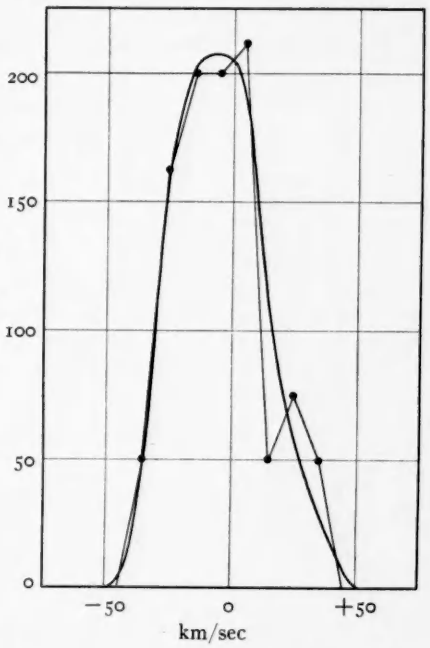

FIG. 3.—Distribution of z-components. Similar to Fig. 1.

In comparing the radial-velocity and proper-motion distributions along the three axes, we notice the large dispersion for the x-components, owing to the fact that the x-axis is approximately identical with the axis of maximum-velocity dispersion. We also note the asymmetry in the distribution of the y-components and recall that the y-axis was made identical with the axis of asymmetry in stellar motions. The asymmetry is very clearly marked in both the radial-velocity components (y_1) and the reduced proper-motion components (y_2). It is noticeable even for stars of moderate speed and does not suddenly set in at a velocity relative to the sun of around 60 or 70 km/sec as is often assumed when the high-velocity stars are considered as a group having motions different from the majority of stars in our neighborhood.[9]

[9] Cf. *Mt. W. Contr.*, No. 332, *Ap. J.*, **65**, 238, 1927.

The supergiants are not numerous enough to be studied by the method here described. There are only fifteen stars within the chosen intervals of spectral type and apparent magnitude having spectro-

TABLE III

FREQUENCIES OF REDUCED PROPER-MOTION COMPONENTS IN THREE EQUATORIAL ZONES

x y z	$F_e(x_2)dx_2$		$F_e(y_2)dy_2$		$F_e(z_2)dz_2$	
	O	C	O	C	O	C
−200	0	1	0	0	0	0
190	0	1	0	0	0	0
180	0	1	6	1	0	0
170	0	2	0	1	0	0
160	7	2	0	1	0	0
150	0	3	0	2	5	0
140	7	4	0	2	0	1
130	18	6	0	3	0	1
120	11	8	6	4	0	2
110	0	11	18	5	0	3
100	7	14	12	8	0	4
90	14	18	12	12	0	6
80	18	24	26	18	8	8
70	25	35	44	25	11	11
60	43	54	47	39	25	20
50	74	79	79	59	33	47
40	82	104	99	84	34	88
30	128	120	111	118	112	124
20	121	125	164	172	140	147
− 10	131	114	169	189	212	155
0	96	90	114	119	168	136
+ 10	42	63	46	47	92	95
20	28	42	12	28	70	59
30	42	28	23	21	25	38
40	50	18	6	15	31	24
50	14	11	6	10	17	12
60	14	7	0	6	11	6
70	0	4	0	3	0	3
80	0	2	0	2	6	3
90	7	2	0	1	0	2
100	0	1	0	1	0	2
110	0	1	0	1	0	1
120	14	1	0	1	0	1
130	0	1	0	1	0	1
140	0	1	0	1	0	0
150	7	0	0	0	0	0
+160						
No. of stars	141		171		179	

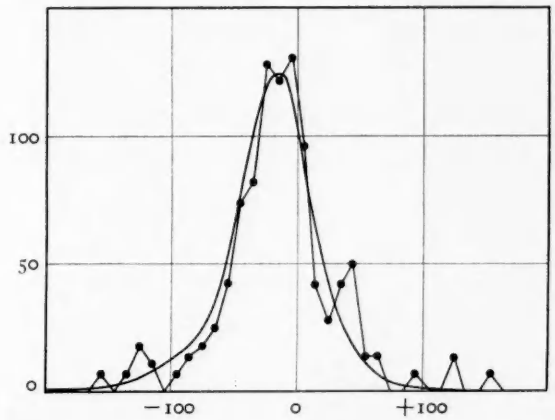

FIG. 4.—Distribution of reduced proper motions projected on the x-axis, for stars in the equatorial zones of the x-axis. Points indicate observed frequencies; continuous curves are computed from the distribution of radial-velocity components and from the combined solution for the absolute-magnitude distribution. Spectral types G8 to K2. Spectroscopic absolute magnitudes -0.5 to $+3.8$. Apparent magnitudes ≤ 5.8.

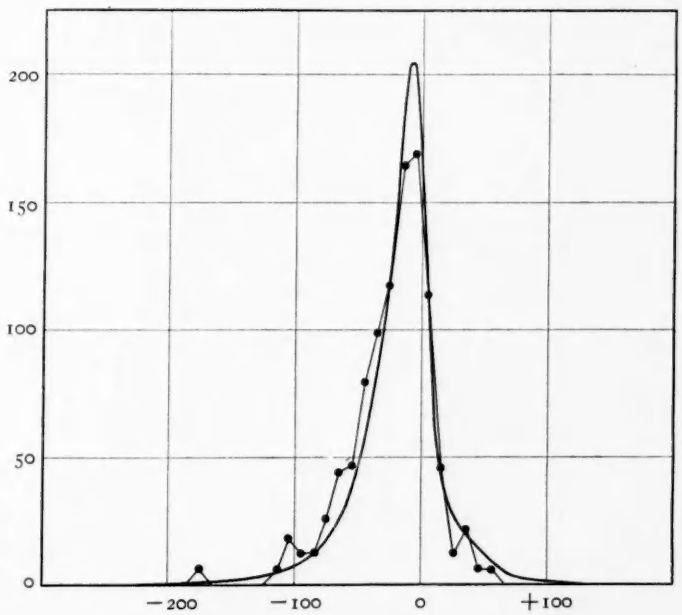

FIG. 5.—Distribution of y-components. Similar to Fig. 4

scopic absolute magnitudes brighter than -0.5, the brightest being -2.9. Since these stars are, on the average, much more distant than the other stars studied, corrections for galactic rotation were applied. Dr. R. E. Wilson, of the Department of Meridian Astrometry of the Carnegie Institution of Washington, very kindly furnished the writer

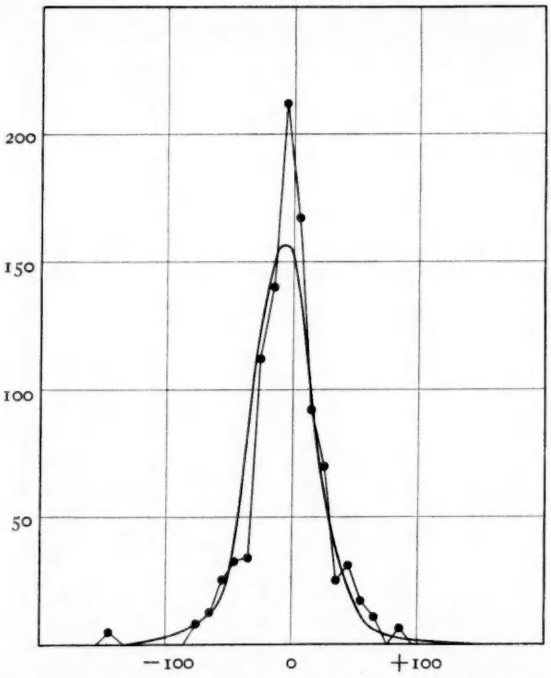

FIG. 6.—Distribution of z-components. Similar to Fig. 4

with the revised proper motions for these stars. After consultation with Dr. J. A. Pearce, of the Dominion Astrophysical Observatory, the following corrections were applied to the precession:

$$\Delta\mu_\alpha = +0^s.00007 - 0^s.00027 \sin\alpha \tan\delta\,,$$

$$\Delta\mu_\delta = -0''.0041 \cos\alpha\,.$$

These small corrections have, however, only a very small effect on the results.

A general study has been made of methods by which the mean absolute magnitude and the dispersion within a group of stars may

be determined from the proper motions. The theory will be published in a separate paper. Here it will be sufficient to say that the computation for the fifteen supergiants in question gave a mean absolute magnitude of -2.73 and a dispersion of ± 1.0 mag.

TABLE IV

DISTRIBUTION OF ABSOLUTE MAGNITUDES DETERMINED FROM RADIAL VELOCITIES AND PROPER MOTIONS PROJECTED ON THREE DIFFERENT AXES, AND FROM SPECTRAL CRITERIA

(Spectral Range G8 to K2, $m \leqq 5.8$, $M_{sp} -0.5$ to $+4$)

M	x	y	z	x, y, z	Spectrum
−2.0	4	0	7	2	0
1.8	20	0	26	6	0
1.6	25	0	32	8	0
1.4	18	1	30	9	0
1.2	10	3	27	9	0
1.0	8	4	20	6	0
0.8	6	5	18	5	0
0.6	3	6	16	5	3
0.4	0	8	12	6	9
−0.2	0	12	12	16	30
0.0	29	50	30	46	68
+0.2	124	148	104	149	188
0.4	218	213	222	220	275
0.6	197	215	200	201	242
0.8	82	100	77	95	123
1.0	25	37	24	34	13
1.2	2	12	2	10	8
1.4	1	8	0	2	3
1.6	14	14	5	9	2
1.8	30	28	15	22	5
2.0	40	36	26	30	13
2.2	45	37	31	35	16
2.4	40	33	31	32	2
2.6	30	21	24	23	0
2.8	19	9	9	13	0
3.0	9	0	0	6	0
3.2	1	0	0	1	0
3.4	0	0	0	0	0
3.6	0	0	0	0	0
3.8	0	0	0	0	0
+4.0					
No. of stars used.....	203	209	219	313	313

According to the spectroscopic data, the dwarf stars are separated from the "subgiants" by a clear gap of 1.4 mag. The brightest dwarf is of absolute magnitude 4.0; and the faintest, 6.5. Slight changes

would be introduced by using the trigonometric parallaxes; but as far as the distribution of absolute magnitudes is concerned, no systematic deviations remain.

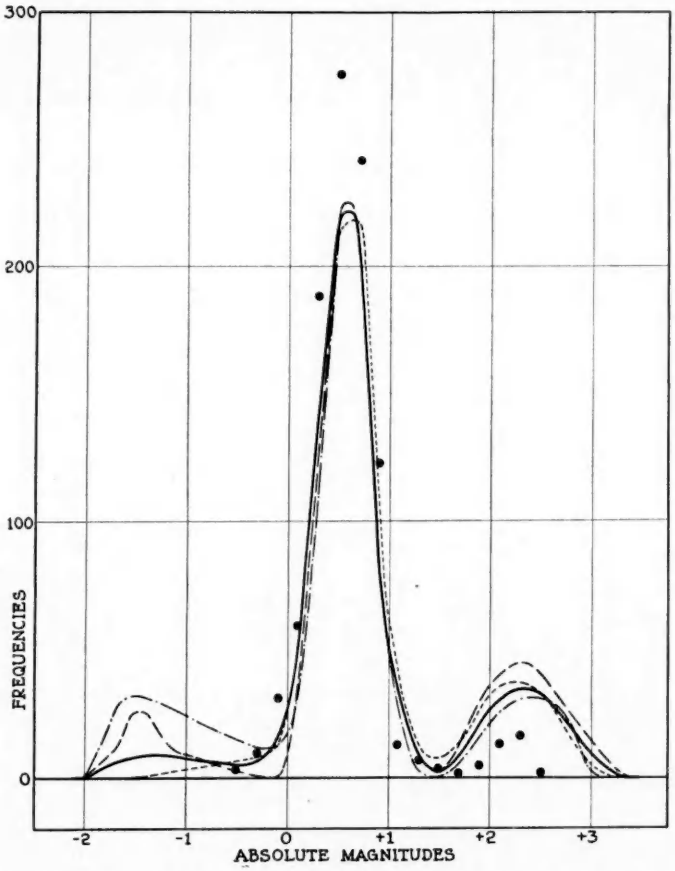

FIG. 7.—Distribution of the absolute magnitudes for stars of spectral types G8 to K2, spectroscopic absolute magnitudes -0.5 to $+3.8$, and apparent magnitudes ≤ 5.8. The long-dash curve is derived from the x-components of radial velocities and proper motions, the short-dash curve from the y-components, and the dash-dot curve from the z-components. The continuous curve represents the absolute-magnitude distribution given by the combined solution. The dots indicate the distribution of spectroscopic absolute magnitudes for the same stars.

Including the supergiants and the dwarfs, we obtain the final distribution of absolute magnitudes for stars of spectral types G8 to K2 and of apparent magnitudes brighter than or equal to 5.8, which is

given in Table V and shown graphically in Figure 8. The distribution of spectroscopic absolute magnitudes for exactly the same stars is also shown (dots). The computed distribution indicates more supergiants and more subgiants than the spectroscopic data. Comparison with the distribution-curve in Figure 5 of *Mount Wilson Contribution* No. 418[10] shows a good agreement; but the number of

TABLE V

DISTRIBUTION OF ABSOLUTE MAGNITUDES DETERMINED FROM MOTIONS AND FROM SPECTRA

(Spectral Range G8 to K2, $m \leqq 5.8$)

M	Motions	Spectra	M	Motions	Spectra	M	Motions	Spectra
−4.8	1	0	−0.8	6	9	+3.2	1	0
4.6	1	0	0.6	5	6	3.4	0	0
4.4	1	0	0.4	6	9	3.6	0	0
4.2	1	0	−0.2	15	28	3.8	0	1
4.0	2	0	0.0	42	63	4.0		
3.8	2	0	+0.2	137	174		965	1
3.6	3	0	0.4	203	253	4.2	.....	0
3.4	3	0	0.6	186	222	4.4	.....	3
3.2	3	0	0.8	87	113	4.6	.....	6
3.0	4	4	1.0	31	12	4.8	.....	0
2.8	4	2	1.2	9	7	5.0	.....	0
2.6	3	0	1.4	2	3	5.2	.....	3
2.4	3	3	1.6	8	2	5.4	.....	3
2.2	3	3	1.8	20	4	5.6	.....	3
2.0	4	2	2.0	28	12	5.8	.....	9
1.8	8	3	2.2	32	15	6.0	.....	3
1.6	9	7	2.4	29	1	6.2	.....	0
1.4	9	6	2.6	21	0	6.4	.....	3
1.2	9	0	2.8	12	0	6.6	.....	0
1.0	6	2	3.0	6	0	+6.8		
−0.8			+3.2					1000

stars brighter than −1.0 has been reduced from 14 to 7 per cent, the dip separating the normal giants from the subgiants is a little more marked than before, and the number of subgiants is somewhat increased.

The objection raised against my previous work may well be made to the present study, namely, that I have tried to determine details of a distribution function which cannot be derived from the observed data. It is true that we can get nearly as good a representation of the observed frequencies by smoothing out the dips on either side of the

[10] *Ap. J.*, **73**, 40, 1931.

group of normal giants and thus forming a general group of giant K stars with a larger dispersion, as was done by Gratton.[3] In a popular article Gyllenberg[11] has reported the same thing. For a certain group

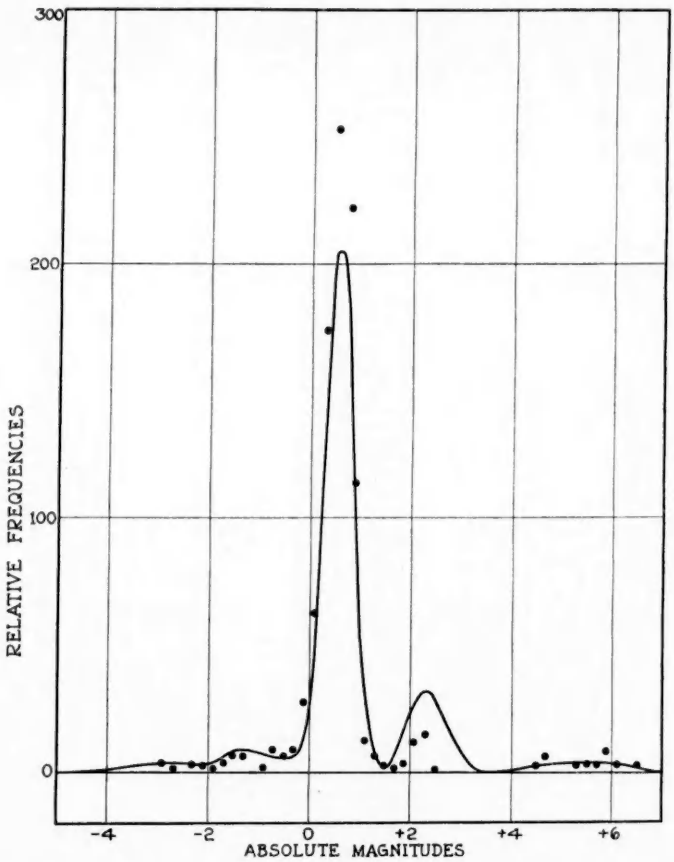

FIG. 8.—Distribution of absolute magnitudes for stars of spectral types G8 to K_2 and of apparent magnitudes ≤ 5.8. The continuous curve indicates the combined solution shown in Fig. 7 after the supergiants and the dwarfs have been included. The dots represent the spectroscopic absolute magnitudes for the same stars.

of stars he has even found an error-curve for the absolute-magnitude distribution which gives slightly smaller residuals than my distribution-curve. This is not surprising since Gyllenberg seemingly

[11] *Populär Astronomisk Tidskrift*, **17**, 31, Stockholm, 1936.

does not apply any weights to the differences between observed and computed frequencies of reduced proper motions, and in such a determination the constants of the error-curve are mainly determined from those parts of the frequency-curves for which the frequency is a maximum. The deviations for the other parts of the observed distribution have then very little effect; and, since they are by nature small, they cannot influence the sum of the squares very much. I think it is very important to give the deviations for the smaller frequencies very high weight, since these observed data have a very high accuracy.

Öpik *et al.*[2] argue that it is useless even to try to determine the shape of the luminosity distribution and prefer to express it as a few discrete frequencies, from which, by arbitrary smoothing, we can get some idea of the actual distribution. For many statistical studies this method is sufficient. We are dealing, however, with a problem which has an astrophysical importance. We want to know, for instance, if the sub-giants have a different constitution from the normal giants, a dip in the frequency function between the corresponding luminosity groups perhaps indicating that the groups are physically distinct and that stars of intermediate luminosities are infrequent and perhaps unstable. We should hence not neglect any possibility of determining the finer details of the luminosity distribution, which we have reason to believe is actually continuous. A good test of the computed luminosity distribution is the agreement between the results from the velocity distributions projected on three mutually perpendicular axes. For the highest luminosities the results are necessarily uncertain, but all three curves in Figure 7 show the dip at $M = +1.5$. As pointed out in the introduction, waves on top of the true distribution will be introduced by small errors, and it might be thought that the dips on each side at the principal maximum are due to the fact that we are too close to this maximum. But the corrections deduced in the separate solution are often of different signs for the same M, and it is difficult to see how they can all accidentally give a minimum at $M = +1.5$.

After my previous study had called attention to the possible existence of a group of subgiants, Mr. Adams studied the spectra of a number of stars which may fall within this group. Sufficient spec-

tral peculiarities were found, or rather such combinations of line intensities, as to make the existence of a group of subgiants among the G and K stars highly probable on the basis of spectral criteria alone. The bright star η Cephei is an excellent illustration of a member of this group. The search for possible subgiants, though extensive, was not carried through completely; and we should expect that several stars originally classified as normal giants would have appeared as subgiants had the later criteria been applied to all the material. It is thus to be expected that the spectroscopic criteria used should give too small a proportion of subgiants, as this computation seems to indicate.

The fact that the studies of the v- and τ-components of the proper motions of both the K and G stars in my previous article, and of the velocity components on three mutually perpendicular axes for the K stars in the present analysis, all show a group of subgiants separated from the normal giants strengthens the conviction that this group is really detached from the normal giants. We should then expect that the normal K giants have a very small dispersion in absolute magnitude, as the present study also indicates. The supergiants, which cover a large range in absolute magnitude, must then also form a separate group, since they can by no means be regarded as the asymptotic branch of an error-curve. Whether they are separated from the normal giants by a frequency minimum or not is still an open question.

CARNEGIE INSTITUTION OF WASHINGTON
MOUNT WILSON OBSERVATORY
June 1936

INTENSITIES OF BLENDED ABSORPTION LINES*

A. D. THACKERAY[1]

ABSTRACT

Intensities of nine solar multiplets, including fourteen *lines lying in the wings of the* H *and* K *lines*, have been measured from plates taken with the 75-foot spectrograph of the 150-foot tower telescope.

Exposures were taken at the *center* of the disk, at the *limb*, and over a *sun-spot*.

The lines, measured relative to the blending wing, show a *progressive weakening as the blending increases*. The intensities are roughly proportional to the intensity within the neighboring calcium wing.

The *central intensities* of the blended lines remain practically *constant irrespective of the blending*. *Rowland intensities* are shown to depend primarily on the intensity of the *core of the line*.

Eddington's theory of the formation of absorption lines depending on the two parameters η and ϵ is developed for the case of *two blended lines*. A similar weakening is found which agrees with that observed, especially when a correction is applied to allow for the fact that blended lines are formed in higher layers of the atmosphere where η is larger.

Severely blended lines, particularly *Fe* 3969, show an *excess weakening* which is partially accounted for by introducing the factor ϵ, involving *collisions or electron captures*. The remainder may be due to *interlocking*. It is found that the blending of *Fe* 3969 with the H line has little effect on the number of atoms in the upper state, i.e., on the intensities of other related lines, except in the *higher chromospheric layers*.

1. Problems of intensities of stellar absorption lines may be attacked by two general methods. Given a normal star, the intensity of a line usually remains constant; and, in order to study the effect of changed conditions, two alternatives are available: (1) comparison of the same line produced in different stars under different conditions of temperature and pressure, and (2) comparison of different lines produced under similar conditions in the same star. The first method is used in problems of maxima and for deriving ionization temperatures by the Adams-Russell[2] method; the second is applied in the measurement of spectroscopic absolute magnitudes and has also been used for the measurement of ionization temperatures through the comparison of neutral and enhanced lines.[3] As a result of the analysis of spectra and the increased knowledge of transition

* *Contributions from the Mount Wilson Observatory, Carnegie Institution of Washington*, No. 555.

[1] Fellow on the Commonwealth Fund.

[2] *Mt. Wilson Contr.*, No. 359; *Ap. J.*, **68**, 9, 1928.

[3] Woolley, *M.N.*, **93**, 691, 1933.

probabilities within multiplets, the second method has further been applied extensively in recent years to problems of the "curve of growth"[4]—the functional relationship between the intensity of a line and the "number of atoms above the photosphere."

The present investigation deals with the production of an absorption line within the wing of a strong neighboring line,[5] a problem which includes some features of both the foregoing methods: we measure the intensities of both blended and unblended lines belonging to the same multiplet, and from these latter derive the intensity that the blended line would have if it were unblended. This method provides a check on current theories of the formation of absorption lines. According to Milne,[6] absorption lines are formed in atmospheric layers intermediate between a state of local thermodynamic equilibrium, where the number of atoms in a given state is determined by collisions and follows a Boltzmann distribution, and a higher layer in a prevailing state of "monochromatic radiative equilibrium," where the number of atoms in a given state is determined by the radiation in the frequencies having a direct connection with that state. If a line falls near the core of another stronger line, it is clear that in regions where monochromatic radiative equilibrium prevails the number of atoms in the upper state will be abnormally dependent on transitions from other states (involving unblended lines). In nearly all theoretical treatments of absorption lines the presence of other lines connected with the same upper or lower state is neglected; hence the study of blended lines may serve to determine the validity of this procedure.

In the notation adopted here, the suffixes 1 and 2 are used to denote parameters of the stronger and weaker lines, respectively. The equivalent width of an absorption line is defined in the usual way, as the width of continuous spectrum inclosing the same amount of energy as the absorption line. In speaking of the equivalent width W of a blended line, the wing of the strong line 1 is always treated

[4] Minnaert, *Observatory*, **57**, 331, 1934.

[5] The problem of lines blended with hydrogen wings in stellar spectra has been considered by Unsöld, Struve, and Elvey, *Zs. f. Ap.*, **1**, 234, 1930, and recently by Swings and Struve, *Ap. J.*, **83**, 238, 1936.

[6] *Hand. d. Astrophysik*, **3**, Part I, 159, 1930.

as the continuous background for line 2. It simplifies the treatment both observationally and theoretically, if the intensity of the strong "blending" line is practically the same on both sides of the blended line.

W' refers to the width that a blended line would have if it were unblended (primed letters are similarly used for other parameters).

r is the ratio of intensity of radiation at a point within the contour of a line to that of the continuous region outside.

For a blended line:

r_2 is the ratio of intensity within line 2 to that outside both lines.

r_{21} is the ratio of intensity within line 2 to that in the wing of line 1 just outside. The parameters η and ϵ, used extensively, have the same significance as in Eddington's treatment of the formation of absorption lines.

2. Three conditions are essential for satisfactory observations:

(1) In order that the blended line 2 may be strong enough for reliable measurement and at the same time enough weaker than the blending line 1, the latter must be exceptionally strong.

(2) In order to estimate W', the blended line must belong to a multiplet with known relative intensities.

(3) The other multiplet lines must lie outside the blending line and should have widths both larger and smaller than W'.

3. For solar work, condition (1) restricts the observer to the H and K lines of Ca^+; and by good fortune two *Fe* multiplets satisfying perfectly the other conditions happen to lie partly within the wings of H and K. The well-known lines λλ 3920, 3922, 3927, and 3930 belonging to the $a^5D - z^5D^o$ multiplet form an excellent sequence running down the violet wing of K; and *Fe* 3969.27 ($a^3F - y^3F^o$) is only 0.79 A from the center of the H line, at a point where the radiation is reduced to one-sixth that of the continuous spectrum outside. Both these multiplets have recently been measured in absorption in the laboratory by R. B. and A. S. King.[7] The resulting f values were found to agree better than the theoretical intensities with the solar measures given below, a fact which assisted in obtaining a better estimate of W'. The lines λλ 3920–3930 are

[7] *Mt. Wilson Contr.*, No. 528; *Ap. J.*, **82**, 377, 1935.

all of medium intensity for the range within the multiplet; and although the stronger lines are situated in the region λλ 3850–3890, where other lines are very plentiful and the difficulties of drawing in the continuous background very great, it is again fortunate that the best lines for measurement are λ 3895 and λ 3899, which in the laboratory have much the same intensities as the lines λλ 3920–3930. Although λ 3969 is nearly the weakest in its multiplet, λλ 4005, 4132, and 4143 are all of nearly the same intensity. Thus the lines λλ 3920–3930 and λ 3969 provide five good measures of W'/W corresponding to varying degrees of blending (the intensity in the blending wing varies from 90 per cent of the continuous background for λ 3920 to 16 per cent for λ 3969). In addition, seven further multiplets containing ten blended lines allow other but less reliable measures.

THE OBSERVATIONS

4. Solar spectrograms of this region were made in the first and second orders of the 75-foot spectrograph of the 150-foot tower telescope at Mount Wilson. Eastman 33 and 40 plates were used and brush-developed in X-ray developer. The Michelson grating used, 70×135 mm with 15,800 lines per inch, gives a dispersion of 0.71 A per mm in the first order. The slit width was 0.15 mm. Plates were calibrated for photometric work with exposures on the sky some 6′ of arc from the limb, through a raster, designed by S. B. Nicholson, consisting of a plate with a series of apertures ranging from about 0.2 to 5 mm. This raster, which was essentially a step slit replacing the ordinary spectrograph slit, was given an oscillatory motion during exposures in order to wash out the absorption lines which were perceptible through the narrower apertures. It was so designed that the presence of absorption lines would not upset the calibration, except for a slight intermittency effect; but in practice, regions as free as possible from such lines were chosen. The calibration of such a raster is simple and independent of wave-length, since, of course, the intensity of light is proportional to the aperture. To minimize scattered light, violet filters were placed in front of the slit for the solar exposures.

Calibration exposures were of the order of 60 to 10 seconds, those on the solar disk about 3 seconds in the first order and 20 in

UNIV. OF MICH.

PLATE XVII

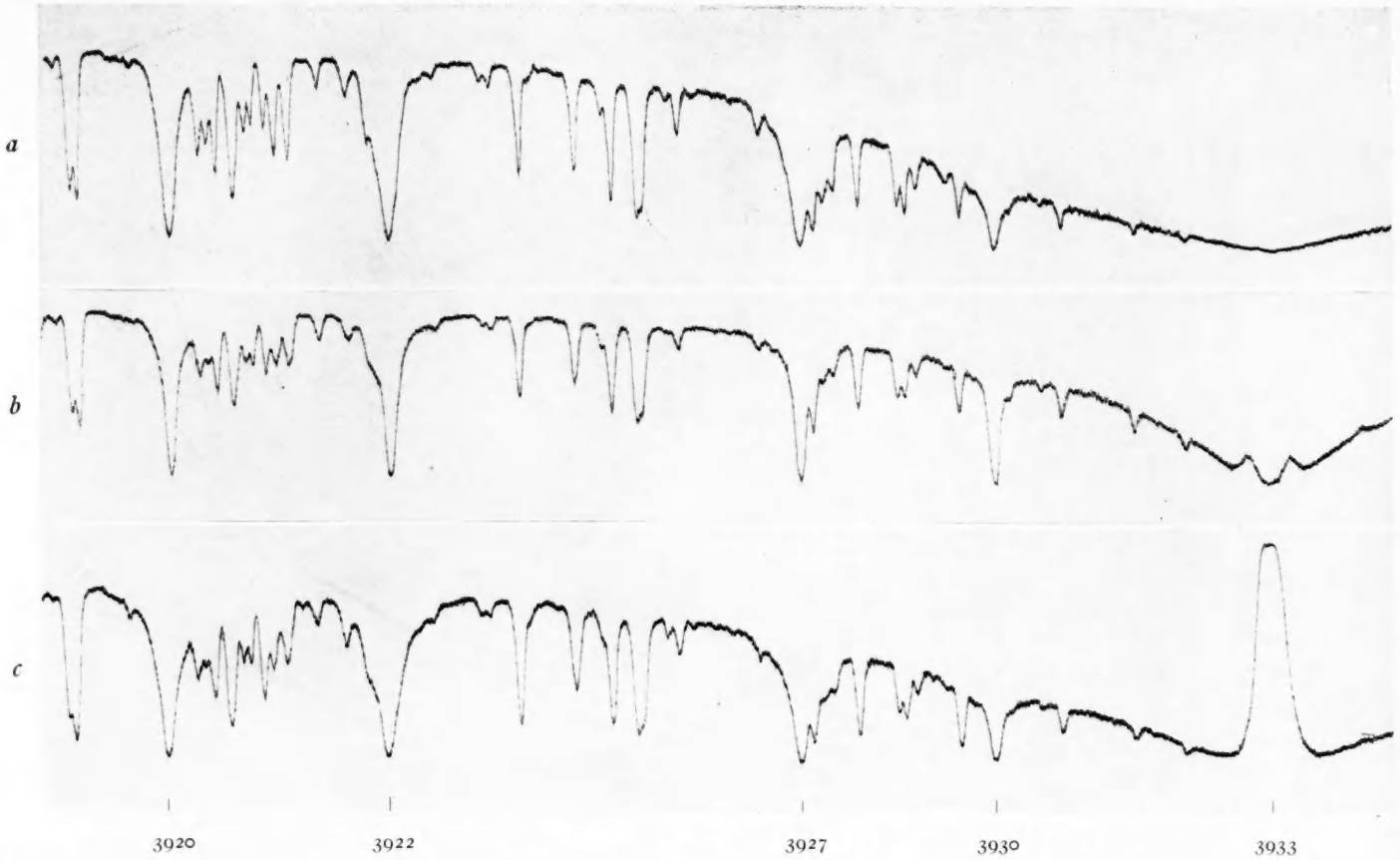

MICROPHOTOMETER TRACINGS (FROM THE SAME PLATE) OF THE VIOLET WING OF THE K LINE OF Ca^+ 3933

a, center; *b*, limb; and *c*, spot. Note that in spite of blending with the wing of K, the central intensities of the lines *Fe* 3920, 3922, 3927, 3930 remain practically constant.

the second. In the earlier exposures a step wedge was used in front of the slit as a check calibration on the raster; but as no systematic difference was noted, this procedure was dropped.

The plates were run through the photoelectric microphotometer constructed by Dunham, set for a magnification of 10 or 20; and the tracings were reduced in the normal manner. Some of the plates were also run through the Koch-Goos photometer of the California Institute of Technology, and satisfactory agreement between the two results was found.

A tracing of the region λλ 3920–3933 is shown in Plate XVII. It will be noted that the lines λ 3922 and λ 3927 are both badly blended on one wing, the other being comparatively clean. In such cases the lines were assumed to be symmetrical. For a few of the worst cases of blended lines it was assumed that the area of the contour below 70 per cent of the background, which was especially measured, bore the same ratio to the total area as for other unblended lines.

5. Table I summarizes the results of measures of nine solar multiplets containing fifteen blended lines. The first column gives the multiplet designation and the wave-lengths; the second, the number of plates, on most of which two exposures of different density were measured. The third column gives the equivalent width, W, in milliangstroms, of the lines at the center of the disk. In order to compare these results with the laboratory f values, they must be transformed into relative[8] numbers of active atoms, Nf, by means of the appropriate curve of growth. Allen[9] has published a valuable table giving $\log Nf$ as a function of W for various wave-lengths and atomic masses, and his computations for *Fe* at 4000 A have been used. The fourth column gives $\log (N_z f)$, which, following Allen's notation, is the value of $\log Nf$ increased by a small correction for differences in excitation potential within the multiplet. (The correction is $0.9 \times$ E.P. in volts.) The adjoining columns give similar quantities derived from measures at the solar limb (10″ inside)and from the sun-spot spectrum. The exposures on the limb were made

[8] Since we are concerned throughout with relative intensities and since the lines of a multiplet follow the same distribution of Nf with height, the absolute value of Nf and the optical depth to which it refers are both immaterial.

[9] *Mem. Commonwealth Solar Obs., Canberra,* No. 5, Part I, 27, 1934.

remain practically constant.

TABLE I

MEASURES OF SOLAR MULTIPLETS

MULTIPLET AND λ	n	CENTER			LIMB			SPOT			log f or log I
		W	log $(N_z f)$	log $(N_z f)'$	W	log $(N_z f)$	log $(N_z f)'$	W	log $(N_z f)$	log $(N_z f)'$	
Fe $a^5D - z^5D^\circ$											
3824.45	3	750:	4.88:	.....	460:	4.46:	.....	.....	.....	.....	0.94
3856.38	5	650:	4.81:	.....	440:	4.47:	.....	685:	4.85:	.....	1.04
3859.92	5	1470:	5.26:	.....	835:	4.98:	.....	1360:	5.40:	.....	1.54
3878.58	3	580:	4.73:	.....	390:	4.39:	.....	580:	4.74:	.....	0.94
3886.29	3	950:	5.14:	.....	660:	4.82:	.....	1140:	5.29:	.....	1.20
3895.67	5	337	4.29	.....	314	4.22	.....	418	4.47	.....	0.72
3899.72	6	425	4.47	.....	373	4.35	.....	497	4.60	.....	0.85
3906.49	6	198	3.75	.....	197	3.75	.....	251	4.00	.....	0.28
3920.27	5	301	4.20	4.25	291	4.17	4.18	395	4.43	4.41	0.68
3922.92	5	358	4.30	4.36	324	4.19	4.26	426	4.44	4.51	0.76
3927.93	5	285	4.14	4.47	257	4.03	4.35	295	4.16	4.61	0.85
3930.31	5	166	3.56	4.53	159	3.50	4.39	152	3.46	4.66	0.89
Fe $a^3F - y^3F^\circ$											
3969.27	4	040	1.37	4.58	53	1.72	4.47	48	1.59	4.76	0.18
4005.25	1	390:	4.37:	.....	290:	4.11:	.....	523	4.63	.....	0.08
4045.82	2	1240	5.32	.....	1010	5.14	.....	1600	5.54	.....	0.74
4063.60	3	847	5.06	.....	730	4.93	.....	1010	5.20	.....	0.65
4071.75	3	730	4.98	.....	660	4.88	.....	890	5.15	.....	0.59
4132.07	3	392	4.43	.....	349	4.33	.....	.....	.....	.....	0.04
4143.88	3	500	4.59	.....	461	4.52	.....	.....	.....	.....	0.15
Cr $a^5D - z^5D^\circ$											
3886.80	1	33:	1.24:	1.95:	27:	1.08:	1.91:	39	1.39	2.45	*0.56*
3908.76	6	79	2.47	.....	89	2.69	.....	117	3.08	.....	*0.92*
3916.24	5	52	1.71	.....	52	1.71	.....	70	2.21	.....	*0.38*
3921.05	5	95:	2.78:	.....	73:	2.23:	.....	126:	3.17:	.....	*1.26*
3928.65	5	37	1.34	2.12	41	1.44	2.03	57	1.86	2.59	*0.68*
3941.50	5	51	1.72	1.95	45	1.57	1.91	63	2.06	2.45	*0.56*
Fe $a^5F - y^5D^\circ$											
3820.43	2	1590	6.30	.....	1100	5.98	.....	.....	.....	.....	2.49
3825.89	3	1230	6.12	.....	725	5.66	.....	.....	.....	.....	2.34
3834.23	3	990:	5.98:	.....	645	5.61	.....	.....	.....	.....	2.18
3840.45	2	660:	5.66:	.....	424	5.27	.....	.....	.....	.....	1.94
3849.98	1	460:	5.37:	.....	380	5.20	.....	.....	.....	.....	1.71
3865.53	3	342	5.11	.....	279	4.92	.....	343	5.11	.....	1.62
3872.51	3	510:	5.43:	.....	360:	5.13:	.....	.....	.....	.....	1.61
3878.03	3	560:	5.49:	.....	380:	5.15:	.....	.....	.....	.....	1.62
3887.06	3	430	5.21	.....	320	4.94	.....	422	5.21	.....	1.43
3898.01	4	208:	4.61:	.....	191:	4.53:	.....	.....	.....	.....	0.72
3917.18	5	126	4.03*	.....	141	4.17*	.....	176	4.42*	.....	0.62
3940.89	5	84	3.40	3.60:	83	3.38	3.80:	100	3.70	4.00:	0.20
Fe $z^5D^\circ - f^5D$											
3909.67	6	76	2.39	.....	68	2.19	.....	96	2.82	.....	*0.62*
3931.13	5	23	0.93	2.45:	18	0.72	2.25:	24	0.95	2.88:	*0.68*
3965.52	4	29	1.11	2.33:	31	1.15	2.13:	33	1.20	2.76:	*0.56*
Ti $a^3F - y^3F^\circ$											
3924.53	5	64	2.06*	.....	61	1.96*	.....	80	2.47*	.....	*0.54*
3929.88	5	30	1.15	2.15:	32	1.16	1.97:	55	1.76	2.62:	*0.54*
3948.68	5	100:	2.84:	.....	90:	2.67:	.....	110:	2.96:	.....	*1.28*
3956.34	4	100:	2.86:	.....	87:	2.62:	.....	126:	3.17:	.....	*1.45*
3958.22	4	87	2.66	.....	76	2.36	.....	110	3.01	.....	*1.61*
Cr $a^5G - z^5H^\circ$											
3963.69	4	55	1.76*	.....	46	1.53*	.....	.....	.....	.....	*2.00*
3969.76	2	10	0.35	2.11:	10	0.34	1.80:	.....	.....	.....	*1.91*
3984.34	1	53	1.61	.....	48	1.59	.....	.....	.....	.....	*1.81*
3991.12	1	71	2.21	.....	55	1.76	.....	.....	.....	.....	*1.61*
Ti+ $a^2G - z^2G^\circ$											
3900.54	6	165	3.47	.....	144	3.31	.....	188:	3.61:	.....	*1.94*
3913.47	6	120	3.07	.....	112	2.98	.....	113	3.00	.....	*1.84*
3932.02	4	010:	0.41	1.63:	013:	0.51	1.52:	010:	0.36	1.63:	*0.30*

TABLE I—*Continued*

Multiplet and λ	n	Center			Limb			Spot			log f or log I
		W	log $(N_z f)$	log $(N_z f)'$	W	log $(N_z f)$	log $(N_z f)'$	W	log $(N_z f)$	log $(N_z f)'$	
Fe $a^3F-y^3D^o$											
3815.85	3	1063	5.18	.....	662	4.77	.....	.....	.....	.....	3.72
3827.83	3	833	5.04	.....	448	4.49	.....	.....	.....	.....	3.67
3841.06	2	595	4.79	.....	381	4.41	.....	.....	.....	.....	3.56
3888.52	3	480:	4.61:	.....	302:	4.19:	.....	.....	.....	.....	3.08
3902.95	5	485	4.57	.....	393	4.36	.....	.....	.....	.....	3.25
3966.07	4	057	1.94	3.74:	060	2.02	3.37:	.....	.....	.....	*(2.36)*

on the same plates as those for the center; for the spot measures, four plates of the large spot (Mount Wilson No. 4685) taken on November 28 and 29, 1935, were used. In the final column appear the laboratory values of log f; when these are not available, the theoretical intensities log I are used and distinguished by italics.

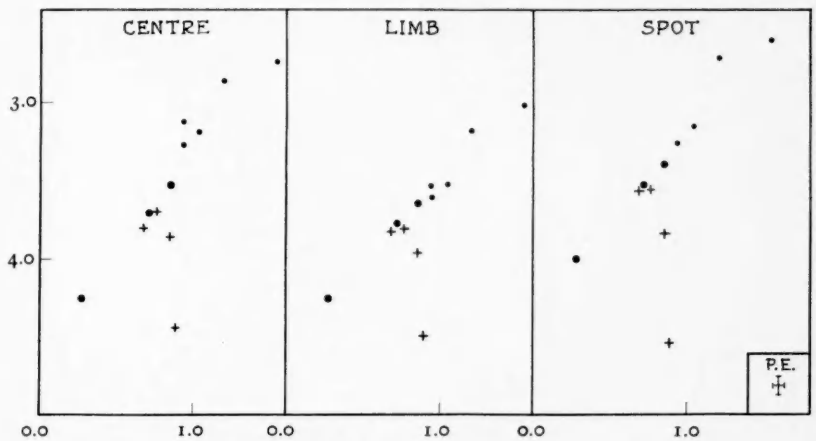

FIG. 1.—Relation between solar intensities (log $N_z f$, ordinates) and laboratory intensities (log f, abscissae) for the multiplet *Fe* $a^5D - z^5D^o$. Crosses represent the four blended lines λλ 3920, 3922, 3927, and 3930.

The fifth, eighth, and eleventh columns of Table I give the values of log $(N_z f)'$, i.e., the values of log $(N_z f)$ that the blended line would have if unblended, interpolated from the unblended lines and the expected intensities log f or log I. How closely these values can be interpolated may be seen from Figures 1 and 2, where the plots of solar and laboratory intensities for *Fe* $a^5D-z^5D^o$ and *Fe* $a^3F-y^3F^o$

show a satisfactorily linear correlation. In the other multiplets the fit is not so good, partly, no doubt, owing to deviations from the theoretical intensities. In some cases extrapolation was necessary; in others (marked with an asterisk), slightly blended lines were given

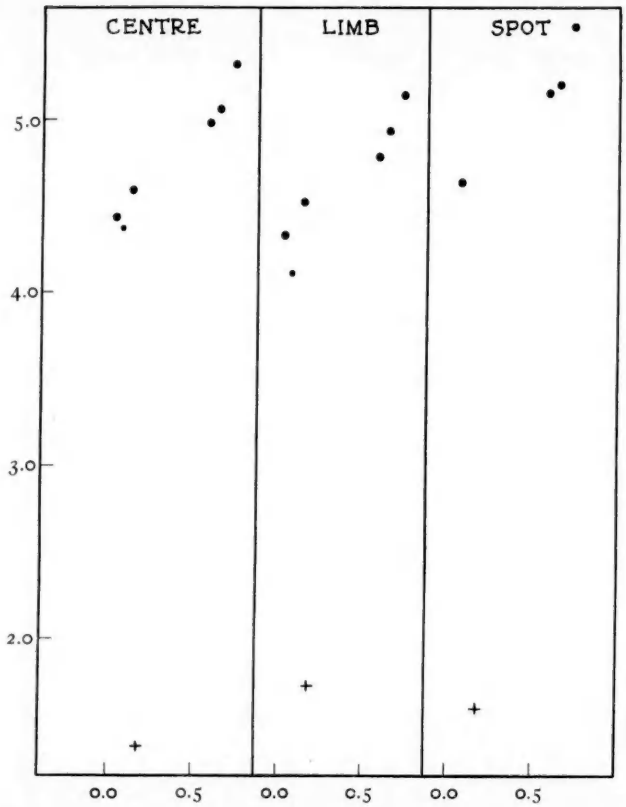

FIG. 2.—Relation between solar intensities (log $N_z f$, ordinates) and laboratory intensities (log f, abscissae) for the multiplet *Fe* $a^3F - y^3F^\circ$. The cross represents the blended line λ 3969.

a small correction in order to derive a value of log $(N_z f)'$ for one more severely blended. Even so, the error in log $(N_z f)'$ should not exceed 0.2 in the logarithm. Measures of small weight are marked with a colon. Only one line (*Cr* 3886.80) blended with lines other than H and K has been used; the blending lines in this case are *Fe* 3886.29, 3887.06.

The internal agreement between the separate measures of the lines in the $a^5D - z^5D^o$ multiplet indicates a mean probable error of 7 per cent.

6. Available for comparison with the present measures are the observations of Mulders[10] on the $a^5D - z^5D^o$ multiplet, and those of Woolley[11] and Allen[9] on $a^3F - y^3F^o$. The values of W are collected in Table II. Mulders found his measures in other parts of the spectrum to be systematically higher than those of Woolley by a factor of the order of 1.3. Since the same ratio appears here and since the

TABLE II

VALUES OF W BY DIFFERENT OBSERVERS

λ	Mulders	Allen	Woolley (×1.3)	Thackeray
3856	545	.....	.....	650
3859	1070	.....	.....	1470
3886	832	.....	.....	950
3899	426	.....	.....	425
3906	260	.....	.....	198
3920	281	.....	.....	301
3922	315	.....	.....	358
4045	.....	1160	1170	1240
4063	.....	860	910	847
4071	.....	732	740	730
4132	.....	418	420	392
4143	.....	511	510	500

general agreement with the present measures and with Allen's is good, Woolley's measures have been multiplied by this factor. We can be confident that the relative intensities have been observed with fair accuracy. The agreement between the present measures and those of Mulders is not so good; but this is not surprising, in view of the difficulties of measurement in this region of the spectrum.

7. The observed central intensities r_c for the same two multiplets are collected in Table III. A correction δr_c for resolving power has been computed (for slit width 0.15 mm) and applied to give the final central intensity r_c'. It will be seen that the central intensities of the blended lines are always higher than those of the other lines;

[10] *Zs. f. Ap.*, **10**, 297, 1935.

[11] *Ann. Solar Physics Obs. Cambridge*, **3**, Part II, 1933.

but, since they are referred to the wing of H or K, they must be multiplied by the appropriate r_1 in order to express them in terms of the continuous spectrum outside the calcium line. When thus reduced, the intensities are of the same order as those of the unblended lines, i.e., *the actual amount of light in the centers of the lines of a multiplet is practically constant, irrespective of whether they are blended or not.* The slight increase of central intensity in the weaker lines is to be expected on theoretical grounds from the influence of the damping constant.

TABLE III

CENTRAL INTENSITIES (CORRECTED FOR RESOLVING-POWER) EXPRESSED AS PERCENTAGE OF CONTINUOUS BACKGROUND

MULTIPLET AND λ	CENTER				LIMB				SPOT			
	r_c	δr_c	r'_c	$r_c r_1$	r_c	δr_c	r'_c	$r_c r_1$	r_c	δr_c	r'_c	$r_c r_1$
Fe $a^5D - z^5D^0$												
3824	10	1.5	8.5	....	17	2.5	14.5	....	....	....	....	....
3856	10	2	8	....	19	2.5	16.5	....	22	1.5	20.5	....
3859	7	0.5	6.5	....	17	1.5	15.5	....	21	1	20	....
3878	9	2	7	....	19	3	16	....	21	2	19	....
3886	9	1	8	....	16	1.5	14.5	....	20	1	19	....
3895	12	3	9	....	21	3.5	17.5	....	22	2.5	19.5	....
3899	13	2.5	10.5	....	20	3	17	....	22	2	20	....
3906	18	6	12	....	21	6	15	....	22	4.5	17.5	....
3920	18	3.5	14.5	13.	23	3.5	19.5	17.5	24	2.5	21.5	19.5
3922	18	2.5	15.5	12.5	23	3	20	17	26	2	24	19
3927	24	2	22	11.5	25	3	22	14.5	35	2	33	18
3930	36	2.5	33.5	11	34	3.5	30.5	15.5	52	3	49	18
Fe $a^3F - y^3F^0$												
3969	61	3	58	9.5	54	3	51	11	....	....	....	....
4005	14	3	11	....	20:	4	16:	....	....	....	....	....
4045	8	1	7	....	14:	1	13:	....	....	....	....	....
4063	10	1.5	8.5	....	16:	1.5	14.5	....	....	....	....	....
4071	10	1.5	8.5	....	20:	2	18:	....	....	....	....	....
4132	16	3	13	....	20:	3.5	16.5:	....	....	....	....	....
4143	14	2	12	....	20:	2.5	17.5:	....	....	....	....	....

It is evident from Figures 1 and 2 that blended lines, when measured relative to the blending wing, are weakened, the weakening increasing as the line falls nearer the core. It should be mentioned in passing that, although the lines *Fe* 3927, 3930, and 3969 have much smaller measured widths than *Fe* 3899, all these lines have

the same Rowland intensity (10). The explanation of this is to be found in the fact that the central intensities are apparently unaffected by blending. When a densely exposed negative is examined

TABLE IV

WEAKENING OF BLENDED LINES

MULTIPLET AND λ	E.P. VOLTS	CENTER			LIMB			SPOT		
		Δ log N	r_1	[Δ log N]	Δ log N	r_1	[Δ log N]	Δ log N	r_1	[Δ log N]
Fe $a^5D-z^5D^o$										
3920.27	0	0.05	0.90	0.05	0.01	0.91	0.01	−0.02	0.90	−0.02
3922.92	0	0.06	.81	0.06	0.07	.86	0.07	+0.07	.80	+0.07
3927.93	0	0.33	.52	0.33	0.32	.66	0.32	0.45	.54	0.45
3930.31	0	0.97	.32	0.97	0.89	.50	0.89	1.20	.37	1.20
Fe $a^3F-y^3F^o$										
3969.27	1.5	3.21	.16	3.06	2.75	.29	2.62	3.17	.22	3.05
Cr $a^5D-z^5D^o$										
3886.80	1.0	0.71	.45	0.65	0.83	.58	0.77	1.06	.39	0.99
3928.65	1.0	0.78	.44	0.72	0.59	.60	0.53	0.73	.48	0.67
3941.50	1.0	0.23	.70	0.17	0.34	.76	0.28	0.39	.65	0.33
Fe $a^5F-y^5D^o$										
3940.89	1.0	0.20:	.66	0.14:	0.42:	.69	0.36:	0.30	.64	0.24:
Fe $z^5D^o-f^5D$										
3931.13	3.2	1.52:	.27	1.27:	1.53:	.43	1.31:	1.93:	.31	1.70:
3965.52	3.2	1.22:	.38	1.01:	0.98:	.55	0.78:	1.56:	.43	1.35:
Ti $a^3F-y^3F^o$										
3929.88	0	1.00:	.35	1.00:	0.81:	.52	0.81:	0.86:	.40	0.86:
Cr $a^5G-z^5H^o$										
3969.76	2.5	1.76:	.21	1.55:	1.46:	.36	1.28:	.....	....	.....
Ti^+ $a^2G-z^2G^o$										
3932.02	1.1	1.63:	.21	1.54:	1.52:	.35	1.44:	1.63:	0.26	1.55:
Fe $a^3F-y^3D^o$										
3966.07	1.6	1.80:	0.33	1.68:	1.35:	0.50	1.24:	.....	....	.....

visually, the four lines λλ 3920, 3922, 3927, and 3930 all appear about equally strong. Hence it is evident that *Rowland intensities depend primarily on the intensities of the line cores.*

8. We obtain a convenient measure of the weakening of a blended line by writing

$$\Delta \log N = \log (N_z f)' - \log (N_z f) .$$

In Figures 1 and 2, $\Delta \log N$ is the vertical displacement of the point corresponding to a blended line below the plot of the unblended lines.

The values of $\Delta \log N$ for fifteen blended lines are collected in Table IV. Values of r_1 are also given, that is, of the intensity within the blending wing in the immediate neighborhood of the line. A correction proportional to the excitation potential of the lower state has been applied to yield the final $[\Delta \log N]$. This correction allows for

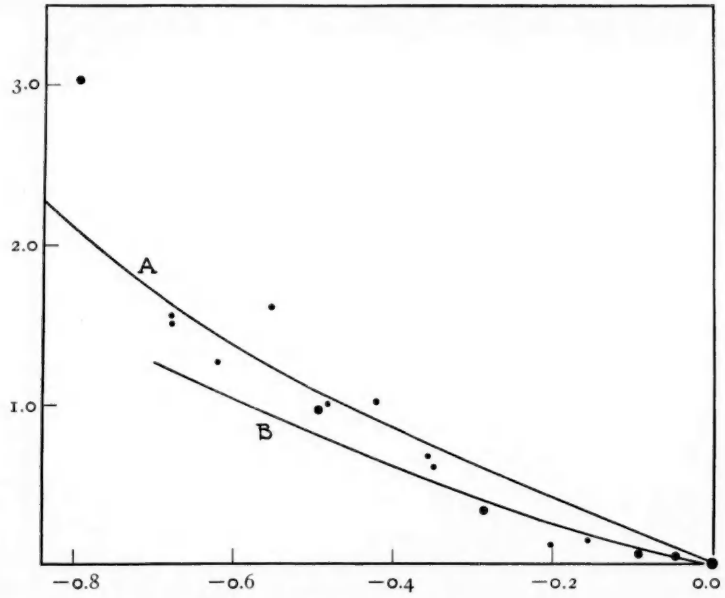

FIG. 3.—Progressive weakening of blended lines at the center of the disk. Ordinates, $[\Delta \log N]$; abscissae, $\log r_1$. Curves for $\epsilon = 0.005$; A, η independent of τ; B, η varies with τ.

the fact that the blended lines must originate in a somewhat higher layer where the reduced temperature diminishes the relative number of atoms in excited states. The method of estimating this correction is described in the following theoretical section.

Figures 3, 4, and 5 summarize the observational material, the weakening, $[\Delta \log N]$, being plotted against $\log r_1$, and represent the progressive weakening of blended lines as the core of the blending line is approached. On the same diagrams appear the curves of weakening to be expected from the theory as developed in the following section.

THEORETICAL INTENSITIES OF BLENDED LINES[12]

9. In the theoretical treatment of two blended lines we shall follow Eddington's[13] method of approach, using the same notation. The theory gives the intensity r within an absorption line as a func-

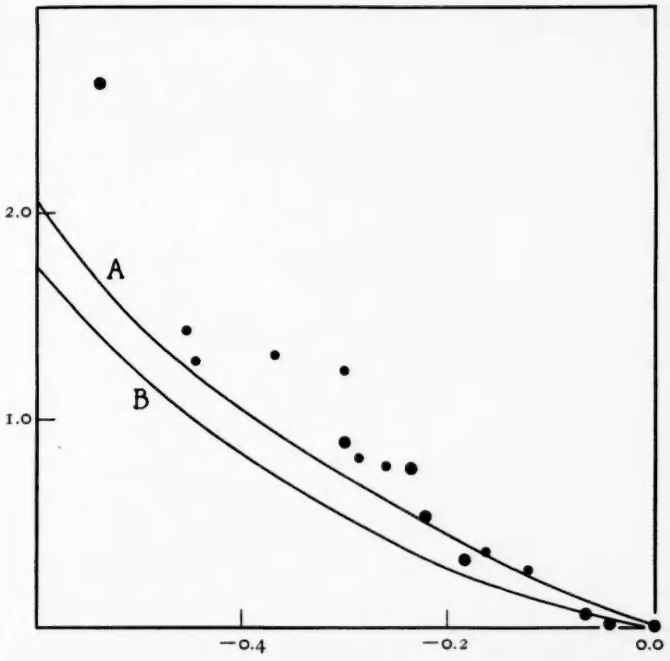

FIG. 4.—Progressive weakening of blended lines at the limb. $\epsilon = 0.030$

tion of η (the ratio of line to continuous absorption) and ϵ, the collision factor. In computations of contours it is necessary to know the

[12] The theory of two blended lines is dealt with in Swings and Struve's paper[5] which appeared while the present work was in course of preparation. Two cases are there considered: the line coefficient l_1 is (*a*) included in the continuous absorption coefficient k (§ 3), and (*b*) treated separately (§ 4). In the present discussion only case (*b*) is considered. The distinction lies in the fact that in case (*a*) a redistribution in frequency is postulated for the blending line l, while in (*b*) such redistribution is neglected. It is unfortunate that the theoretical weakening of the blended line is practically the same in both cases; otherwise this might prove a powerful method of solving the important problem of the existence of "atomic memory."

[13] *M.N.* **89**, 620, 1929.

variation of η with wave-length. In the wings it is legitimate to use the approximation

$$\eta \propto \frac{1}{(\lambda-\lambda_0)^2}; \qquad (1)$$

but near the center this law fails, as Doppler broadening becomes predominant. We shall first consider the simplest case, neglecting

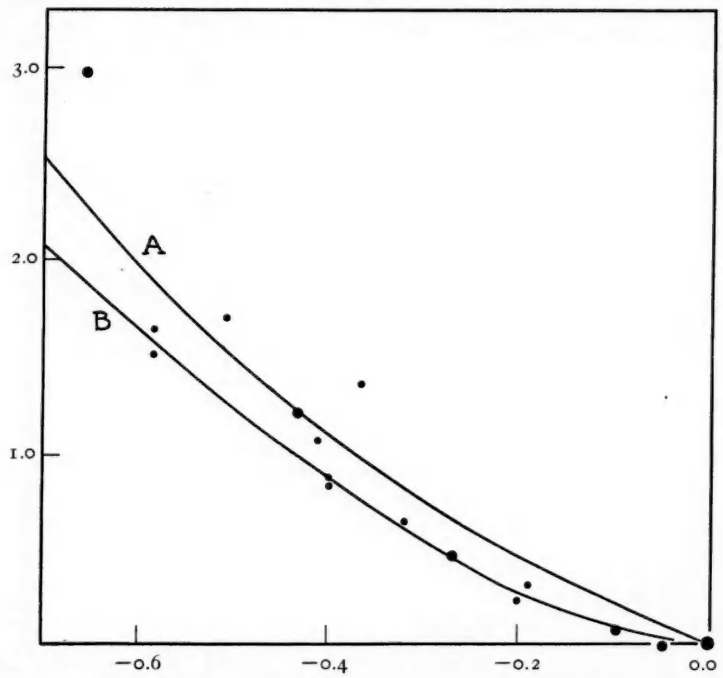

FIG. 5.—Progressive weakening of blended lines in the spot. $\epsilon=0.030$

(*a*) the collision factor ϵ, (*b*) Doppler broadening, and (*c*) variation of η with depth. In later sections the theory is developed to include all these factors.

Denote the two line coefficients of absorption by l_1, l_2, the former being taken independent of wave-length across the second line. The fundamental equation of transfer of radiation within the two lines now becomes

$$\cos\theta \frac{dJ'_\nu(\theta)}{\rho dr} = -(k+l_1+l_2)J'_\nu(\theta)+\{(1-\epsilon_1)l_1+(1-\epsilon_2)l_2\}J'_\nu + (\epsilon_1 l_1+\epsilon_2 l_2+k)J_T, \qquad (2)$$

whence

$$\frac{dH'_\nu}{d\tau}=(1+\epsilon_1\eta_1+\epsilon_2\eta_2)(J'_\nu-J_T)\ , \tag{3}$$

$$\frac{dJ'_\nu}{d\tau}=3(1+\eta_1+\eta_2)H'_\nu\ , \tag{4}$$

where

$$d\tau=-k\rho dr\ , \qquad \eta_1=l_1/k\ , \qquad \eta_2=l_1/k\ .$$

The standard case with η_1, ϵ_1, η_2, ϵ_2 all constant with respect to τ, and $J=J_T$, now becomes

$$\frac{H'_\nu}{H}=r_2=\frac{1+\frac{2}{3}q}{1+\eta_1+\eta_2+\frac{2}{3}q}=F(\eta_1,\epsilon_1,\eta_2,\epsilon_2)\ , \tag{5}$$

where

$$q^2=3(1+\eta_1+\eta_2)(1+\epsilon_1\eta_1+\epsilon_2\eta_2)\ ,$$

and r_2 represents the emergent radiation in the blended line referred to the *continuous background outside both lines*. The measured quantity r_{21} (referred to *the wing of the blending line*) is

$$r_{21}=\frac{r_2}{r_1}\ . \tag{6}$$

With the substitutions

$$\eta_1+\eta_2=\eta\ , \qquad \epsilon_1\eta_1+\epsilon_2\eta_2=\epsilon\eta\ ,$$

equation (5) becomes identical with Eddington's result. With collisions neglected, $\epsilon_1=\epsilon_2=0$, and we may write

$$r_2=F(\eta_1+\eta_2)\ , \qquad r_{21}=\frac{F(\eta_1+\eta_2)}{F(\eta_1)}\ .$$

For practical computation the procedure is as follows: for a particular η_1 [corresponding to a point $r_1=F(\eta_1)$ on the wing of the blending line] calculate $F(\eta_1+\eta_2)/F(\eta_1)$ for a series of values of η_2 such that r_{21} ranges between 0.95 and 0.10. Plot r_{21} against $\log\eta_2$ and compare the result with the similar curve for r_2 obtained by taking $\eta_1=0$, corresponding to the unblended line. Such curves have been

called by Allen[9] "*F*-curves." Examples are shown in Figure 6, where it will be seen that, as η_1 increases (i.e., as the blended line 2 falls nearer the core of the blending line 1), the curve for r_{21} is shifted along the η_2 axis; this corresponds to a weakening of the blended line. Moreover, the curves remain very nearly constant in shape, i.e., the

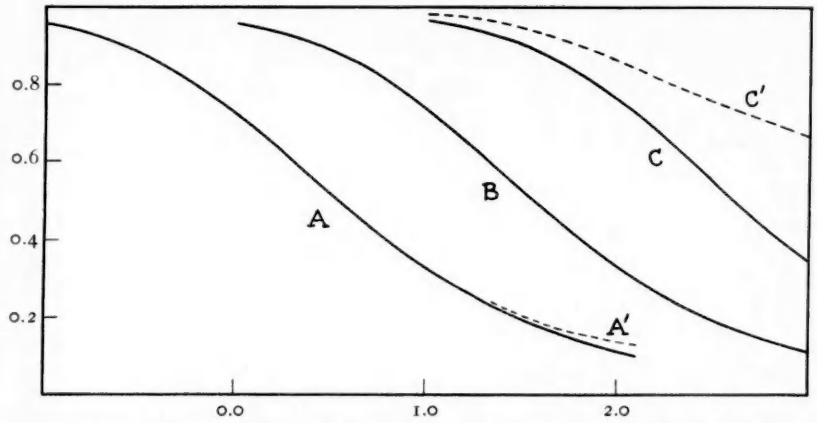

FIG. 6.—*F*-curves of blended lines. Ordinates, $r_{21} = F(\eta_1 + \eta_2)/F(\eta_1)$; abscissae, log η_2. Curve *A*, limiting case, $\eta_1 = 0$ (unblended line), $\eta_1 = 0$ (*A'*, $\epsilon = 0.005$). Curve *B*, $\eta_1 = 10$, $\epsilon = 0$; *C*, $\eta_1 = 128$, $\epsilon = 0$; *C'*, $\eta_1 = 128$, $\epsilon = 0.005$.

shift $\Delta \log \eta_2$ relative to the curve for $\eta_1 = 0$ is nearly the same for all values of r. It is therefore possible to write, with fair accuracy:[14]

$$r_{21} = \frac{F(\eta_1 + \eta_2)}{F(\eta_1)} = F(\alpha\eta_2) = F(\eta_2') \text{ , say,} \tag{7}$$

where, for a given η_1, α is a constant less than unity and independent of η_2.

The factor α is a direct measure of the amount the line has been weakened by blending, and may be called the "coefficient of weakening"; for a value $\eta_2' = \alpha\eta_2$ produces in the unblended line the same r as

[14] The accuracy of the approximation may be seen by an example of the shift of the *F*-curve when $\eta_1 = 10$, corresponding to $r_1 = 0.326$.

r_{21}	0.95	0.90	0.80	0.70	0.60	0.50	0.40	0.30	0.20
$\Delta \log \eta_2$	1.04	1.04	1.03	1.02	1.02	1.02	1.01	0.99	0.99

Mean, $\Delta \log \eta_2 = 1.02 = -\log \alpha$

η_2 does in the blended line, and hence, when Doppler broadening is negligible and equation (1) holds, the width at all points of the contour is reduced by the factor $\sqrt{a}$.

Actual computation shows that, correct within 3 per cent, $a = r_1^2$, whence, in terms of equivalent widths, we have the very simple result

$$W = r_1 W' . \tag{8}$$

That is, *in the absence of Doppler broadening and collision effects, the equivalent width of a line is diminished by blending in proportion to the intensity in the adjacent parts of the wing of the blending line.*

10. *Doppler broadening.*—Proceeding, now, to the case where Doppler broadening is present, we have

$$\eta_2 = Nf\phi(\Delta\lambda_2) ,$$

where ϕ includes coefficients for both natural and Doppler broadening[15] but does not contain Nf. For the blended line,

$$r_{21} = F\{aNf\phi(\Delta\lambda_2)\} ;$$

and for an unblended line,

$$r' = F\{N'f'\phi(\Delta\lambda')\} .$$

Comparing the same r, and with $Nf = N'f'$, we find

$$\phi(\Delta\lambda') = a\phi(\Delta\lambda_2) .$$

The ratio $\Delta\lambda'/\Delta\lambda_2$ is no longer a simple function of a, but the equivalent width of the blended line is

$$\left.\begin{aligned} W &= \int (1 - r_{21}) d\lambda , \\ &= \int [1 - F\{aNf\phi(\Delta\lambda_2)\}] d\lambda , \end{aligned}\right\} \tag{9}$$

which, as before, is exactly the same as the width of an unblended line produced by Nfa atoms.

In other words, Doppler broadening affects the contours of weak

[15] For the complete form of $\phi(\Delta\lambda)$ see Minnaert, *Zs. f. Ap.*, **2**, 168, 1931.

lines of the same width in the same way, irrespective of whether they are blended or not.

Our conclusion is therefore that, in transforming the observed widths W into $\log(Nf)$ by means of the curve of growth, we may treat the lines weakened by blending exactly as if they were normal lines and apply the correction for Doppler broadening appropriate to their width. This is what has been done in deriving the values of $\log(Nf)$ in Table I. As it happens, the lines λ 3927 and λ 3930 are still strong enough to be scarcely affected by Doppler broadening, but the effect on λ 3969 is considerable.

11. *Collisions.*—Now consider the effect of introducing into the computations the collision factors ϵ_1 and ϵ_2, which, like η_1 and η_2, are taken constant with respect to optical depth. The values to be used may be estimated from the observed central intensities of the blended and blending lines. At the center of the disk, the central intensities of both the H and K lines and the strong *Fe* lines are of the order $r_c = 0.075$, which corresponds to the collision factor $\epsilon = 0.005$; while at the limb and in the spot $r_c = 0.17$, $\epsilon = 0.030$.

We have

$$r_{21} = \frac{F(\eta_1, \epsilon_1, \eta_2, \epsilon_2)}{F(\eta_1, \epsilon_1)}, \tag{10}$$

and the new F-curves can be calculated as before for a given value of η_1. As we might expect, it is only for large values of η_1 and η_2 that the collision factors have any appreciable effect on the shapes of the F-curves; but with large η_1 (i.e., with intense blending) the complication arises that the factor $\log a$ measuring the shift of the curve varies with r. This means that the contours have to be plotted, with the aid of equation (1) expressing η as a function of λ, and the areas compared by planimeter measures.

Samples of the computations of r_2 and r_{21}, with various values of η_1 and ϵ_1, are shown in Table V, together with the ratio W/W' of the areas of the blended and unblended contours. The resulting $\Delta \log \eta_2$ $(= -\log a)$ as a function of r_1 is plotted in Figure 3 with $\epsilon = 0.005$ for comparison with the observations at the center of the disk. In Figures 4 and 5 appears the similar curve with $\epsilon = 0.030$ for comparison with the limb and spot observations.

12. *Variation of J and η with depth.*—In the foregoing treatment we have assumed

(1) $J=J_T=H(2+3\tau)$,

(2) η constant with respect to τ.

TABLE V

COMPUTED CONTOURS OF BLENDED AND UNBLENDED LINES

η_2	Unblended Line $\eta_1=0$	Blended Line $\eta_1=60$					
	$\epsilon_1=\epsilon_2=0$ $r_1=1.0$	$\epsilon_1=\epsilon_2=0$ $r_1=0.143$		$\epsilon_1=\epsilon_2=0.005$ $r_1=0.158$		$\epsilon_1=\epsilon_2=0.030$ $r_1=0.211$	
	r_2	r_2	r_{21}	r_2	r_{21}	r_2	r_{21}
∞	0.00	0.00	0.00	0.075	0.48	0.167	0.79
300	.07	.060	.42	.095	.60	.175	.83
100	.11	.089	.62	.115	.72	.185	.88
30	.20	.118	.82	.138	.87	.198	.94
10	.33	.133	.93	.151	.96	.205	.97
3	0.52	0.140	0.98	0.155	0.98	0.210	0.99
W/W'	1.00	0.133		0.090		0.034	

Eddington[13] has shown that the assumption $J=J_T$ holds true at one point of the solar spectrum and may be allowed for elsewhere by taking

$$J=a+b\tau,$$

where

$$\frac{b}{a}=\frac{3}{8}\frac{h\nu}{R\tau}.$$

He then finds

$$r=\frac{\frac{b}{a}+q}{\frac{b}{a}+\sqrt{3}}\,\frac{1+\frac{2}{3}\sqrt{3}}{1+\eta+\frac{2}{3}\sqrt{3}}=F(\eta).$$

The computations of $F(\eta_1+\eta_2)/F(\eta_1)$ for the modified function $F(\eta)$ may be made exactly as before but are somewhat heavier. The F-curves are again unchanged in shape, and the shift may be ob-

tained directly as a measure of the change in equivalent width. Three cases were computed with $b/a=2.25$, corresponding to $\lambda=4000$ A, for comparison with the standard case $J=J_T(b/a=1.5)$:

r_1	0.17	0.29	0.49
$\Delta \log \eta_1(b/a=1.5)$	1.59	1.10	0.63
$\Delta \log \eta_2(b/a=2.25)$	1.51	1.01	0.62

The differences are negligible.

13. The variation of η with τ may be partly allowed for by taking the approximation

$$\frac{1}{1+\eta}=\alpha+\beta\tau\ . \tag{11}$$

For this case Eddington[13] gives the solution

$$r=\frac{\alpha-\frac{\alpha}{3}(2+\beta)\frac{K_0'}{K_0}}{1-\frac{\alpha}{3}\,2\,\frac{K_0'}{K_0}}=\psi(\alpha,\beta)\ .$$

With two coefficients the solution is the same, except that we write

$$\frac{1}{1+\eta_1+\eta_2}=\alpha'+\beta'\tau\ ,$$

and

$$r_2=\psi(\alpha',\beta')\ ,\qquad r_{21}=\frac{\psi(\alpha',\beta')}{r_1}\ .$$

Woolley[16] has developed a method of calculating contours based on this solution which has been applied to three cases of blended lines for comparison with those for constant η:

r_1	0.20	0.35	0.50
$\Delta \log \eta_2$ (η const.)	1.45	0.94	0.61
$\Delta \log \eta_2$ (η var.).....	1.48	0.88	0.62

The variation of η apparently has little effect on the predicted weakening $\Delta \log \eta_2$. The result depends, however, on the depth used for the linear approximation (11). The preceding calculations are all for the same depth ($\tau=0.3$). Strictly, they should be made for smaller

[16] *M.N.*, **92**, 495, 1932; **93**, 691, 1933.

depths, since blended lines originate in the higher layers of the atmosphere. An attempt to allow for this circumstance follows:

14. We refer the whole of the blended and unblended lines to the "mean optical depths" $\bar{\tau}$ and $\bar{\tau}'$, respectively, and let $\bar{\eta}$ and $\bar{\eta}'$ denote the values of η corresponding to these depths. In an atmosphere with η independent of depth, a difference in η for blended and unblended lines could be entirely attributed to a change in $\lambda-\lambda_0$, i.e., to a change in line width. When η varies with depth we have to be careful to make the comparison at the same depth for both lines.

As before in equation (7), the same intensity r is produced in a blended line with $\eta=\eta_2$ at $\bar{\tau}$ as in an unblended line with $\eta=a\eta_2$ at $\bar{\tau}'$, or $\eta=(\bar{\eta}/\bar{\eta}')a\eta_2$ at $\bar{\tau}$. Hence, comparing η's at the same depth, we find $a\bar{\eta}/\bar{\eta}'$ for the coefficient of weakening. Now η increases with height owing to the decrease in the continuous absorption coefficient k; the rapid decrease in electron pressure brings the atoms into greater prominence relative to the electrons. Thus, although blending weakens a line, the weakening is less in an atmosphere in which η increases with height than in one in which η is constant.

The definition of the "mean optical depth" is necessarily rather arbitrary, but fortunately does not seriously affect the final results. For a line blended in the wing of H or K, we proceed as follows: Knowing the variation of η with τ for ionized calcium, we calculate the contour based on this variation by Woolley's adaptation of Eddington's solution. This gives r_1 as a function of η_0 (the value of η at $\tau=0.3$); then calculate the mean value $\bar{\eta}_1$, which would give the same r_1 as in an atmosphere with constant η. The depth at which the calculated variable η equals $\bar{\eta}_1$ is taken as the mean optical depth, $\bar{\tau}$, for a line lying at a point on the Ca^+ wing corresponding to r_1.

Calculations of the distribution of η with τ for Ca^+ and *Fe* yield the following results:

τ	0.6	0.5	0.4	0.3	0.2	0.1	0.08	0.05	0.02	0.01
Ca^+	91	93	95	100	110	138	150	181	276	384
Fe	82	86	91	100	112	130	146	168	233	305

Contours of Ca^+ and *Fe* based on this variation of η are given in Table VI, together with the mean value $\bar{\eta}$ which would yield the same r and the mean optical depth $\bar{\tau}$ as defined above. It is interest-

ing to note that the values of $\bar{\tau}$ found for the ionized line are all smaller than those for the neutral line.

The mean optical depth $\bar{\tau}'$ adopted for the unblended line is $\tau = 0.3$, which applies strictly only to the point $r = 0.72$; but any value between 0.6 and 0.2 would scarcely affect the results, since within these limits η does not vary greatly. In the sixth column of Table VI appears $\bar{\eta}_2/\eta_0$, the correction to be applied to the simple curve A of Figures 3, 4, and 5 for constant η. Since η increases as τ decreases, the curve B lies below curve A.

TABLE VI

η_0 VALUE OF η AT $\tau = 0.3$	Ca^+					Fe			
	r_1	η_1	$\bar{\eta}_1/\eta_0$	$\bar{\tau}$	$\bar{\eta}_2/\eta_0$	r_2	$\bar{\eta}_2$	$\bar{\eta}_2/\eta_0$	$\bar{\tau}$
10	0.20	30	3.0	0.016	2.80	0.25	18	1.8	0.04
3	.43	5.2	1.73	.056	1.68	.47	4.0	1.3	.09
1	.65	1.53	1.53	.075	1.50	.72	1.0	1.0	.30
0.3	0.86	0.38	1.27	0.130	1.23	0.90	0.25	0.8	0.58

15. *Subordinate lines.*—The calculated variation of η with τ applies only to resonance lines. Since the proportion of atoms in excited states diminishes with height, we should expect blended subordinate lines to show more weakening than resonance lines. In order to render all lines comparable *inter se*, we apply a correction for excitation potential. The radiation temperature T as a function of depth is[17]

$$T = T_e(\tfrac{1}{2} + \tfrac{3}{4}\tau)^{1/4} ,$$

from which the temperatures $\overline{T}$ and $\overline{T}'$ corresponding to the depths $\bar{\tau}$ and $\bar{\tau}'$ for blended and unblended lines are calculated. The required correction is then

$$\delta(\log N) = 5040E\left(\frac{1}{\overline{T}} - \frac{1}{\overline{T}'}\right) ,$$

[17] The temperature gradient given by this well-known equation is considerably greater than that indicated by H. H. Plaskett (*M.N.*, **96**, 422, 1936) as obtaining in the uppermost layers. This means that the corrections have probably been overestimated here, but they are not large enough to affect the main conclusions.

and is thus proportional to the excitation potential E. For $E = 1$ volt its values are:

r_1	0.20	0.43	0.65	0.86	1.0
$\bar{\tau}$	0.016	0.056	0.075	0.125	0.3
$\delta(\log N)$	0.087	0.068	0.060	0.046	0.0

Such a correction has been added to the observed $\Delta \log N$ for all subordinate lines given in Table IV to yield the final $[\Delta \log N]$. It is this latter quantity which is plotted in Figures 3, 4, and 5 and compared with the theoretical weakening.

COMPARISON OF THEORY AND OBSERVATION

16. For the simplest case of blended lines, i.e., with η independent of τ and Doppler broadening and collisions neglected, we have found that the intensity of a blended line is reduced in proportion to the intensity within the blending line (equation [8]). Such a weakening[18] has been observed in stellar absorption lines by Unsöld, Struve, and Elvey,[5] and by Swings and Struve.[5] The results of the latter authors are particularly interesting since the deviations from the simple law of weakening for certain *O* II lines are much larger than those found in solar lines, and, further, deviations in the opposite sense are found for stellar *Ca* II blended with $H\epsilon$. Swings and Struve suggest stratification as a possible explanation, and indeed their observations may be explained qualitatively in terms of a variable η by considering some of the theoretical developments given in preceding sections. The increase of η with height for resonance lines is more rapid for *Ca* II than for *Fe* I and would lead to less weakening, such as is found for *Ca* II blended with $H\epsilon$; while high excitation, leading to a decrease of η with τ, results in greater weakening. It may well be that the marked weakening of the *O* II lines lying in the wings of $H\gamma$, where the absorption is only 10 per cent, is due to the fact that these lines have the very high E.P. of 22.9 volts. For instance, with

[18] One conclusion from the existence of this weakening is that the simple Beer law of exponential absorption does not hold in stellar atmospheres, for, if it did, we should expect the blending wing to reduce the intensity of the blended line in the same ratio throughout, leaving the equivalent width unaffected. This is what is assumed in studies of all spectra whose light has reached the photographic plate through the terrestrial atmosphere and through the optical parts of the spectrograph.

a temperature of 18,000° C. the weakening from this effect for $r=0.86$ (i.e., 14 per cent H absorption), calculated by the method of § 15, is found to be

$$\delta (\log N)=0.35 ,$$

while the weakening expected from equation (8) is

$$\Delta \log \eta=0.14 .$$

The correction is of the right order to account for the deviations from the simple theory. Since the E.P. effect appears to be considerably larger than the simple blending effect for these high excitation lines and since the former cannot be estimated with great accuracy, a detailed comparison of theory and observation would be unprofitable.

Returning to consideration of Figures 3, 4, and 5, we notice that the simple law of weakening (equation [8]) would be represented by a straight line touching the curve A at the origin. The introduction of a collision factor, which produces the curvature in A, leads to better agreement with observation for the strongly blended lines. The observed points tend to lie below the curve A for the less blended lines. This systematic discrepancy appears to be real and receives adequate explanation in the fact that the blended lines arise in a higher atmospheric layer (where η is larger) than unblended lines. The corresponding correction, which has been derived by an admittedly crude method, increases the discrepancy between the observed and theoretical weakening of the strongly blended line, *Fe* 3969. It would require an increase of 100 per cent in the observed width of this line to bring it into agreement with the theoretical curve A of Figure 3; the corresponding departure from the curve B is of the order of 175 per cent. There appear to be two ways of explaining this excess weakening.

17. The numerical values of the collision factor ϵ have been derived from the observed central intensities and have been taken constant throughout the atmosphere. Actually we should expect collisions to be more frequent in the lower layers of greater pressure. Thus, if the assumed values apply to the centers of the lines arising at great heights, we should apply a larger value in the wings arising

in lower layers. However, we meet a difficulty here: the central intensities suggest values of ϵ in the spot and limb lines, both of which are formed at lower pressures than the lines at the center. B. Strömgren[19] in a recent paper suggests that electron captures are partly responsible for the central intensities and derives equations formally identical with Eddington's, except that his ϵ has a somewhat different definition and might possibly be larger for the spot and limb, in spite of the reduced pressures. The fact that the present observations indicate, in agreement with theory, that lines of the same multiplet have the same central intensities whether they are blended or not, suggests that we may interpret these intensities as arising from some such factor ϵ, whether they are due to collisions or to electron captures. If ϵ increases with depth, we can explain the excess weakening of lines at the center of the disk; but then we should have to assume a smaller ϵ in the spot and limb, which would increase the discrepancy in these cases. If, as in Figures 3, 4, and 5, we take ϵ larger for the lower pressures obtaining in spot and limb, we are left in all cases with an excess weakening which is largest for the center lines. Thus, however ϵ varies with depth, the observed weakening of *Fe* 3969 cannot be simultaneously accounted for at center, limb, and spot.

18. The second possible explanation of the behavior of severely blended lines involves the effect of interlocking in the upper layers of the atmosphere. Eddington has stressed the fact that his equations are strictly applicable only to atoms capable of two states. At great heights, where lines are already well formed, the absence of central line frequencies will reduce the numbers of atoms reaching a given upper state, especially for strong lines. The emission from the upper state depends only on the number of atoms in that state and on constant transition probabilities. This would result in cyclic transitions involving a lack of thermodynamic equilibrium, weak lines being strengthened relative to strong lines. This process, put forward by Woolley[20] to explain anomalous multiplet intensities, has been suggested by Cherrington[21] as an explanation of the behavior of the *Mg* b lines at the limb where interlocking effects appear to be in-

[19] *Zs. f. Ap.*, **10**, 237, 1935. [20] *Mt. Wilson Contr.*, No. 413; *Ap. J.*, **72**, 256, 1931.
[21] *Lick Obs. Bull.*, **17**, 161 (No. 477), 1935.

creased. This is in accordance with results obtained by the writer,[22] from which it appears that interlocking increases with height in the atmosphere and is especially marked in sun-spots. A glance at Figure 1 shows that the weak lines of the multiplet *Fe* $a^5D - z^5D^o$ are strengthened relative to the strong lines in both the spot and the limb. The gradients of the multiplet are actually 1.30, 1.06, and 1.09 at center, limb, and spot, respectively; there seems to be no obvious reason why the gradients should always be greater than unity.

Interlocking effects, if present, should be particularly marked in blended lines, since here the number of atoms reaching the upper state is diminished by deficiency of incident radiation to a far greater extent than for an unblended line. Since the line *Fe* 3969 must be affected by interlocking more than any of the other blended lines, we shall examine it in some detail.

19. Consider all the lower energy-levels in the *Fe* spectrum connected with the upper state ($y^3F_3^o$) of λ 3969 by strong lines. We neglect the broadening of the lower states, but consider the upper state B as broadened into a set of substates $B(\Delta\nu)$ with a mean energy value B_0. Atoms reach the substate B_0 by absorbing the central frequencies of the corresponding lines. Since the central intensities of lines in the same multiplet appear to be the same, irrespective of blending, the relative numbers of atoms reaching the upper state B_0 by absorbing the central frequencies will be constant, whatever blending occurs, and interlocking will be negligible. Interlocking, if appreciable, *must occur most strongly in the wings of a blended line.*

Now consider a point on the wing of *Fe* 3969 corresponding to a certain frequency difference $\Delta\nu$, where the intensity is nearly the same as in the neighboring calcium wing (we shall take $\Delta\lambda = 0.15$ A), and compare corresponding points in the other lines connected with the same upper state. Table VII lists all the stronger lines in the observable solar spectrum with $y^3F_3^o$ as the upper state. The last column gives approximate values of the intensity $I(\Delta\nu)$ within the lines at the same frequency difference. For the lines in the red the corresponding $\Delta\lambda$ increases to 0.36 A, which brings one outside the lines altogether. The number of atoms reaching the upper substate $B(\Delta\nu)$ is proportional to the sum $\Sigma f I(\Delta\nu)$. The relative f values of the lines λλ 3969, 4063, and 4132 are known from King's measures;

[22] *M. N.*, **94**, 99, 1933.

the others are estimated very roughly from intensities in the solar spectrum (the error involved will not affect the present argument).

With the H line present, the number of atoms reaching the upper state will be proportional to about 20.7; if absent, the corresponding number would be 25.7. If, therefore, the number of atoms in the substate $B(\Delta\nu)$ depends only on absorption of radiation by atoms in lower states (i.e., if monochromatic radiative equilibrium is predominant), the effect of the blending with H is to reduce the number of atoms in the substate by about 20 per cent. Owing to the constant central intensities, the number of atoms reaching the mean state B_0 will be unaffected by blending. These transitions will control most

TABLE VII

SOLAR LINES WITH $y^3F_3^o$ AS UPPER STATE

λ	Lower State	Rowland Intensity	Equivalent Width	Relative Nf (Lab.)	$I(\Delta\nu)$	
					H Present	H Absent
3969.27	a^3F_4	10	0.05	15	0.16	(0.50)
4063.61	a^3F_3	20	.86	45	0.24	.....
4132.07	a^3F_2	10	.40	11	0.50	.....
6137.71	b^3F_3	7	.15	(1.5)	1.0	.....
6200.33	b^3F_2	6	0.07	(0.5)	1.0	.....
6592.93	a^3G_4	7	.....	(1)	1.0	.....

of the atoms in the upper state. Hence we can conclude that the total number of atoms in the state $y^3F_3^o$ will be diminished by considerably less than 20 per cent owing to the blending of *Fe* 3969 with the H line. Further, the reduction will be still smaller at lower depths in the atmosphere, where the H line is only partially formed.

20. Any reduction in the number of atoms in the state $y^3F_3^o$ should be observable in two ways:

a) Absorption lines having $y^3F_3^o$ as lower state should be weakened.

b) Chromospheric emission lines having $y^3F_3^o$ as upper state should be weakened.

The four strongest lines of class (*a*) in the solar spectrum are *Fe* 5565.71, 5706.01 ($y^3F^o-f^3D$) and 5806.73, 5914.12 ($y^3F^o-e^3G$). Examination of Allen's material shows no anomalies, in either total or central intensity, for any of these lines. This suggests that these

lines, which are of medium intensity (Rowland numbers 3–5) and of high E.P. (4.5 volts), are formed in layers where the blending of λ 3969 has little effect on the number of atoms in the state $y^3F^o_3$, i.e., local thermodynamic equilibrium still prevails.

21. Turning to the chromospheric lines of class (*b*), we find some evidence of a diminution in numbers of atoms in the state $y^3F^o_3$ which increases with height. In Table VIII we quote Menzel's[23] in-

TABLE VIII

I.Q.	λ	Level 1	2	3	4	5	*f* (Lab.)
		$a^3F-y^3F^o$					
4–3	3969	.....	.....	.....	.....	.....	15
3–2	4005	19	16	12	2.3	.....	12
4–4	4045	54	53	58	23	7.3	55
3–3	4063	.....	46	41	15	4.6	45
2–2	4071	59	42	41	15	4.5	39
2–3	4132	30	22	16	4.0	.....	11
3–4	4143	30	25	18	7.7	2.7	14
		$a^5D-z^5D^o$					
0–1	3920	10	8.2	6.9	.....	.....	48
3–4	3922	12	8.9	7.2	2.4	.....	58
1–2	3927	10	11	10	3.5	.....	70
2–3	3930	8.9	11	12	4.2	.....	78

tensities in the flash spectrum at different levels for both the $a^3F-y^3F^o$ multiplet and the lines λλ 3920–3930.

On comparing the line λ 4063 ($a^3F_3-y^3F^o_3$) with its neighbors, λ 4045 and λ 4071, a weakening is noticeable in levels 3–5. The same is true of λ 4132 ($a^3F_2-y^3F^o_3$) when compared with λ 4143. This suggests that monochromatic radiative equilibrium prevails in Menzel's flash levels 3–5. The lines λλ 3920–3930 display the curious behavior of having quite different intensity gradients, the blended lines λ 3927 and λ 3930 both growing relatively stronger with in-

[23] *Lick Obs. Pub.*, **17**, 172, 170, 1931.

creasing height. Here it seems reasonable to suppose that the emission lines are actually absorbed by the outlying Ca^+ vapors, and most strongly in the lower layers of higher density. Further photometric data on the gradients of these lines would be very valuable.

22. Although there is no evidence of interlocking in the absorption lines having $y^3F_3^0$ as lower state, we need not reject interlocking as a possible explanation of the excessive weakening observed in the blended line *Fe* 3969. We have found that the effect of blending with the H line is to diminish the number of atoms in the upper state $y^3F_3^0$ by less than 20 per cent. This means that the emission of *Fe* 3969 will be reduced by this amount; but the absorption of λ 3969 will be reduced in proportion to the intensity within the calcium wing, i.e., by a factor of 6 in the wings, diminishing to unity at the line center. Thus there will be a tendency toward emission of λ 3969.27, especially in the wings, which will increase with height. This might be the explanation of the emission which appears at λ 3969.40[24] at the limb; but, if so, there is no apparent reason why there should not be a similar emission on the violet edge of λ 3969.

23. To sum up, Eddington's theory of absorption lines based on the two parameters η and ϵ, the lines being treated as though arising from two isolated states, suffices to explain the observed intensities of blended solar absorption lines except in cases of severe blending ($r_1 < 0.3$). Interlocking may be the cause of the excess weakening of these lines, but it does not appreciably affect other lines connected with the same states except when observed in emission in the upper chromospheric layers.

The writer wishes to express his sincerest thanks to Director W. S. Adams and the Commonwealth Fund of New York for the privilege of working at the Mount Wilson Observatory; to Dr. Seth B. Nicholson for much helpful advice in connection with the use of the 75-foot spectrograph; and to Dr. Rudolf Minkowski and Professor H.N. Russell for the enjoyment of stimulating discussions of the results.

CARNEGIE INSTITUTION OF WASHINGTON
MOUNT WILSON OBSERVATORY
August 1936

[24] Evershed, *M.N.*, **87**, 350, 1927; **89**, 566, 1929.

THE THEORETICAL INTERPRETATION OF EQUIVALENT BREADTHS OF ABSORPTION LINES

DONALD H. MENZEL

ABSTRACT

Formulae relating the theoretical strength of a line to its equivalent breadth, W, are developed. Allen's empirical discovery, that W/λ rather than W must be employed when lines of various spectral regions are to be related to one another, is explained theoretically.

By means of the formulae referred to above, a theoretical curve of growth is constructed for *Fe* I at a temperature of 5740°. The agreement with Allen's empirical curve is surprisingly close when we consider the elementary character of the assumptions and the approximations used in obtaining the equations.

The effect of a variable opacity on the lines of neutral and ionized elements is examined. It is shown that lines of both neutral and ionized atoms should be strongest at the frequency of maximum spectral intensity. Toward the violet or the red the lines of neutral elements should decrease in intensity more rapidly than those of the ionized elements.

The intensity of a stellar absorption line is undoubtedly an index to the number of atoms above the photosphere that are active in producing the line. Owing partly to observational difficulties (low dispersion, imperfect resolution, scattered light, etc.) and partly to the lack of satisfactory theoretical formulae, the study of line profiles has lagged. At present the study of "equivalent widths" appears to be more promising. The purpose of the present paper is to develop the theory of "equivalent widths," with special emphasis on the problem of related atomic lines, as in a transition array, where the lines fall in different spectral regions. We are to determine the relation between the equivalent width, W, and the various factors that contribute to the intensity of a given line. Let $r(\nu)$ be the ratio of the intensity at any frequency, ν, within the line profile to the intensity outside the line. Then $\Delta\nu$, the effective width in frequency units (i.e., the width of a line of rectangular profile, zero central intensity, and area equal to that of the actual line), is given by

$$\Delta\nu = \int_0^\infty [1 - r(\nu)]d\nu \,. \tag{1}$$

In the absence of any satisfactory formula for $r(\nu)$, we shall adopt one of the more elementary solutions, based on the assumption that the photosphere is a definite radiating surface, surmounted by an atmosphere, transparent in all wave-lengths except those bordering on the absorption line. If the atmosphere is purely absorbing,

$$r(\nu) = e^{-N a_\nu}, \tag{2}$$

where N is the number of "active" atoms above the photosphere and a_ν is the atomic absorption coefficient. If the atmosphere is supposed to be purely scattering, and if further we make the Schuster-Schwarzschild approximation, we arrive at the well-known expression

$$r(\nu) = \frac{1}{1+N a_\nu}. \tag{3}$$

Eddington, Milne, Pannekoek, and others have given still different formulae. For our purposes, however, where we wish merely to determine the functional nature with respect to frequency of the relation between W and $N a_\nu$, we may conveniently employ (3) and write

$$\Delta\nu = \int_0^\infty \frac{N a_\nu}{1+N a_\nu}\, d\nu. \tag{4}$$

a_ν is given by[1]

$$a_\nu = \frac{\pi e^2}{mc} f \left[\frac{1}{\sqrt{\pi}} \frac{c}{v\nu_0} e^{-(\nu-\nu_0)^2 c^2/\nu_0^2 v^2} + \frac{\Gamma}{4\pi^2} \frac{1}{(\nu-\nu_0)^2} \right], \tag{5}$$

where f is the oscillator strength, v the root-mean-square kinetic velocity of the atoms, ν_0 the frequency of the line center, and Γ the damping constant, defined as the sum of the reciprocal mean lifetimes of the upper and lower states involved in the atomic transition. The first term of (5) gives the broadening due to Doppler effect and is to be employed near the center of the line. The second term, which applies only for very strong lines, arises from damping by radiation or collision.

[1] Cf. Menzel, Pub. Lick Obs., **17**, 230 ff., 1931.

Combine (4) and (5) and integrate. We distinguish three cases:
I. When $Na_{\nu_0} < 1$, we easily find

$$\Delta\nu = N\frac{\pi\epsilon^2}{mc} f\left(1 - \frac{X_0}{\sqrt{2}} + \frac{X_0^2}{\sqrt{3}} \cdots\right), \tag{6}$$

where

$$X_0 = N\frac{\pi\epsilon^2}{mc} f \frac{1}{\sqrt{\pi}} \frac{c}{v\nu_0}. \tag{7}$$

But

$$\lambda_0 = \frac{c}{\nu_0} \tag{8}$$

and

$$\Delta\lambda = W = \frac{c}{\nu_0^2}\Delta\nu, \tag{9}$$

where W is the equivalent width in units of wave-length. Hence

$$\frac{W}{\lambda} = \sqrt{\pi}\frac{v}{c} X_0\left(1 - \frac{X_0}{\sqrt{2}} + \frac{X_0^2}{\sqrt{3}} - \cdots\right) \sim \sqrt{\pi}\frac{v}{c} X_0, \tag{10}$$

when $X_0 \ll 1$. The general integral for the Doppler case becomes

$$\Delta\nu = 2v\frac{\nu_0}{c}\int_0^\infty \left(\frac{1}{1 + \frac{e^{p^2}}{X_0}}\right) dp, \tag{11}$$

where

$$p = \frac{c}{v}\left(\frac{\nu - \nu_0}{\nu_0}\right).$$

II. When $lnX_0 \gg 1$, the following asymptotic expansion holds:

$$\Delta\nu = 2\frac{v\nu_0}{c}(lnX_0)^{1/2}\left[1 - \frac{\pi^2}{24}\frac{1}{(lnX_0)^2} - \frac{7\pi^4}{384}\frac{1}{(lnX_0)^4} \cdots\right], \tag{12}$$

whence

$$\frac{W}{\lambda} = 2\frac{v}{c}(lnX_0)^{1/2}[1 - \cdots]. \tag{13}$$

III. For intermediate values of X_0 the following semi-empirical formula, derived by Mr. James G. Baker (see paper following *Ap. J.*, **84**, 474, 1936) and checked by numerical integration, may be employed:

$$\log \frac{W}{\lambda} = \log X_0 \frac{v}{c}\sqrt{\pi} - \tfrac{1}{2}\log(1+X_0) - \frac{\tfrac{1}{2}\log 4\sqrt{\pi}\,\frac{v}{c}\,\frac{\nu}{\Gamma}}{1+15e^{-2\log X_0}}. \qquad (14)$$

When X_0 is very large, the second term of (5) comes into account and we have

$$\Delta\nu = \int_0^\infty \frac{1}{1+\left(\frac{\sqrt{\pi}\,v\nu_0}{c} X_0 \frac{\Gamma}{4\pi^2}\frac{1}{(\nu-\nu_0)^2}\right)^{-1}} d\nu = \frac{\pi^{1/4}}{2}\left[X_0\Gamma\frac{v\nu_0}{c}\right]^{1/2}, \qquad (15)$$

$$\frac{W}{\lambda} = \frac{\pi^{1/4}}{2}\left(\frac{v}{c}\right)^{1/2}\left(X_0\frac{\Gamma}{\nu_0}\right)^{1/2}. \qquad (16)$$

If, now, we make the assumption that Γ/ν_0 is a constant for the related group of lines, we may write

$$\frac{W}{\lambda} = F(X_0), \qquad (17)$$

where F is some function. From the character of the astronomical problem it appears that the true equation, based on an accurate expression for $r(\nu)$ instead of on (3), will also be of the foregoing form. The distinctive feature of (17), which appears not to have been previously noted, is the occurrence of W/λ, instead of W on the left-hand side of the equation. The usual procedure of finding the relationship between W and X_0 is to plot the observed equivalent widths against the theoretical strengths for the lines of a given multiplet and then to combine the curves by superposition. This method may still be used to obtain the mean curve for lines in any given wave-length region. But when curves for different regions are superposed, it is clear that the W's must be divided by the mean λ for the respective intervals in order to make the curves parallel. Strictly speaking, one should treat $W/\lambda v$, in order to reduce to the same scale the curves for elements of different atomic weight.

It is significant that Allen,[2] in an analysis of equivalent widths by this method, actually found it necessary to plot W/λ rather than W, in order to relate the curves for different spectral regions. In Figure 1 the solid line represents the curve of growth predicted by the foregoing equations. The transition cases were checked by numerical integration. The velocity chosen was that of iron atoms at a temperature of 5740°. A value of $\Gamma/\nu_0 = 1.52 \times 10^{-6}$ was chosen to give the best possible fit for the right-hand portion of Allen's curve. The

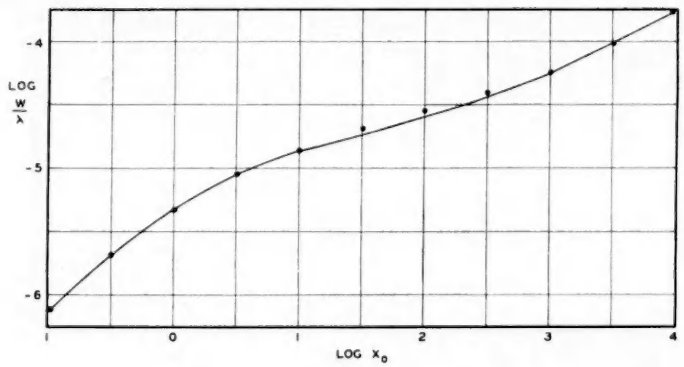

FIG. 1

damping constant is about ten times the classical value. The dots are observed points taken from Allen's empirical curve, which has been independently checked at this Observatory. The agreement is more surprising than convincing in view of the elementary character of the assumptions and of the approximations used in obtaining the equations. Table I, computed by Mr. Baker, illustrates the agreement.

We now proceed to investigate X_0 as a function of ν. We suppose the atmosphere to be isothermal. In this case, the number of "active" atoms—i.e., the number of atoms in the lower of the two atomic levels involved in the transition—is given by the Boltzmann formula:

$$N = N_a \frac{\bar{\omega}_{j'}}{b(T)} e^{-\chi_{j'}/kT} , \tag{18}$$

[2] *Mem. Commonwealth Solar Obs.*, **5**, Part I, 21, 1934.

where N_a is the total number of atoms of the given element in the particular stage of ionization considered, $\bar{\omega}_{j'}$ the statistical weight of the level, $\chi_{j'}$ the excitation potential, and $b(T)$ the partition function,

$$b(T)=\sum_i \bar{\omega}_i e^{-\chi_i/kT} . \tag{19}$$

Let s be the theoretical strength of a line in a given multiplet expressed on some arbitrary scale and Σs the sum of the strengths for all the lines of the multiplet. Let S be the theoretical strength of the

TABLE I

Log X_0	Allen's log W/λ	Computed log W/λ	Diff. (O−C)
−1.0	−6.15	−6.133	−0.02
−0.5	5.70	5.696	.00
0.0	5.34	5.323	− .02
0.5	5.06	5.057	.00
1.0	4.87	4.880	+ .01
1.5	4.69	4.748	+ .06
2.0	4.56	4.614	+ .05
2.5	4.41	4.449	+ .04
3.0	4.25	4.247	.00
3.5	4.02	4.012	− .01
4.0	−3.78	−3.766	−0.01

multiplet, measured in units of σ^2, the square of the first order electric moment between the two electronic configurations. σ^2 is constant for all the multiplets of a given transition array. Then $A(j,j')$, the Einstein probability of spontaneous transition, is[3]

$$A(j,j')=\frac{1}{\bar{\omega}_j}\frac{64\pi^4\nu^3\sigma^2}{3hc^3}S\frac{s}{\Sigma s} . \tag{20}$$

The physical dimensions of σ are $a\epsilon$, where a is a length of the order of an atomic radius and ϵ is the electronic charge. Hence, setting a equal to the radius of the first Bohr orbit, we may write

$$\sigma^2=\phi a^2\epsilon^2=\phi\frac{h^4}{16\pi^4m^2\epsilon^2} , \tag{21}$$

[3] Condon and Shortley, *The Theory of Atomic Spectra*, p. 98, 1935.

where ϕ is a dimensionless constant, characteristic for the transition array. A is related to f by the well-known formula

$$f=\frac{\tilde{\omega}_j}{\tilde{\omega}_{j'}}\frac{mc^3}{8\pi^2\epsilon^2\nu^2}A(j,j'), \tag{22}$$

whence, by equations (7), (18), (20), (21), and (22),

$$X_0=\frac{N_a}{b(T)}e^{-\chi_{j'}/kT}\frac{1}{3\sqrt{\pi}R}\frac{\pi\epsilon^2}{mc}\phi\frac{c}{v}S\frac{s}{\Sigma s}, \tag{23}$$

where R is the Rydberg constant,

$$R=\frac{2\pi^2\epsilon^4 m}{h^3}=3.290\times 10^{15}\ \text{sec}^{-1}. \tag{24}$$

$$\frac{\pi\epsilon^2}{mc}=2.639\times 10^{-2}\ \text{cm}^2\ \text{sec}^{-1};\qquad v=\sqrt{\frac{2kT}{m_1\mu}}=1.289\times 10^4\sqrt{\frac{T}{\mu}}\ \text{cm sec}^{-1}, \tag{25}$$

where μ is the atomic weight. Numerically,

$$X_0=3.510\times 10^{-12}\frac{N_a}{b(T)}e^{-\chi_{j'}/kT}\sqrt{\frac{\mu}{T}}\phi S\frac{s}{\Sigma s}. \tag{26}$$

X_0 proves to be independent of ν, except for possible change in N_a with λ.

Physically, the effect of a photosphere is produced by general opacity, which may be different from one spectral region to another. Milne has shown, however, that the actual intensity of a line will be approximately the same as that produced in a fictitious transparent atmosphere backed by a radiating surface, if we take N_a equal to the number of atoms in the real atmosphere down to optical depth $\tau=\frac{1}{3}$. Menzel and Pekeris[4] have shown theoretically that

$$d\tau_\nu=2.02\times 10^{40}\frac{P^2}{\nu^3T^{5/2}}(e^{h\nu/kT}-1)dh, \tag{27}$$

approximately, where P is the electron pressure (in dynes) and dh an element of the vertical co-ordinate.

[4] *M.N.*, **96**, No. 1, eq. (2.26), 1935.

For a homogeneous atmosphere, H, the depth of the effective photosphere, can be evaluated directly by setting

$$\tau_\nu = \tfrac{1}{3} = 2.02 \times 10^{40} \frac{P^2}{\nu^3 T^{5/2}} (e^{h\nu/kT} - 1) H . \tag{28}$$

Thus we may reduce N_a, the number of atoms observed at any frequency ν, to N_a', the number at some standard frequency (corresponding to, say λ 5000) by

$$N_a = N_a' \frac{(e^{h\nu'/kT} - 1)}{(e^{h\nu/kT} - 1)} \frac{\nu^3}{\nu'^3} \sim N_a' e^{-h(\nu - \nu')/kT} \frac{\lambda'^3}{\lambda^3} . \tag{29}$$

In this case

$$X_0 = 3.510 \times 10^{-12} \frac{N_a'}{b(T)} e^{h\nu'/kT} \frac{\lambda'^3}{\lambda^3} e^{-\chi_j/kT} \sqrt{\frac{\bar{\mu}}{T}} \phi S \frac{s}{\Sigma s} , \tag{30}$$

since

$$\chi_j = \chi_{j'} + h\nu . \tag{31}$$

For an atmosphere of mean atomic weight $\bar{\mu}$, in gravitational equilibrium under the action of effective gravity, g,

$$\tau_\nu = \tfrac{1}{3} \sim \frac{1.34 \times 10^{24}}{\bar{\mu} m_1 g} \frac{P^2}{T^{3/2}} \frac{(e^{h\nu/kT} - 1)}{\nu^3} , \tag{32}$$

where P now refers to the pressure at the base of the atmosphere. This equation. for given T and ν, suffices to determine P. The variable opacity will affect the lines of neutral and ionized elements differently. Milne's[5] approximation is sufficient to show the nature of the effect. Let N_1 and N_0 be the respective numbers of ionized and neutral atoms per cm^2 column down to the level where the electron pressure is P. Let

$$N = N_1 + N_0 .$$

Then

$$N_1 = N \frac{2K}{P + 2K} \quad \text{and} \quad N_0 = N \frac{P}{P + 2K} . \tag{33}$$

$$K = \frac{(2\pi m)^{3/2} (kT)^{5/2}}{h^3} e^{-\chi_0/kT} \frac{2b_1(T)}{b_0(T)} , \tag{34}$$

[5] *Ibid.*, **89**, 17, 1928.

where χ_0 is the ionization potential and $b(T)$ a partition function, as indicated by the subscript.

As before, let primes indicate the values of the respective quantities determined for some standard wave-length region. Then

$$\frac{P}{P'}=\left(\frac{\lambda}{\lambda'}\right)^{3/2} e^{h(\nu-\nu')/2kT} . \tag{35}$$

The ratio N/N' varies as the ratio of the total pressures. The metals of the solar atmosphere are almost completely ionized, even to fairly low depths. If the relative proportion of metals to hydrogen is constant, the ratio of the total pressure to electron pressure is also constant, and we may write

$$\frac{N}{N'}\sim\frac{P}{P'} , \tag{36}$$

whence

$$N_1=N_1'\frac{P'+2K}{P+2K}\frac{P}{P'} \qquad \text{and} \qquad N_0=N_0'\frac{P'+2K}{P+2K}\left(\frac{P}{P'}\right)^2 . \tag{37}$$

For the metallic atoms of the solar atmosphere we may usually neglect P or P' as compared with $2K$. When this is done, the value of X_0 for neutral lines reduces to that for the uniform case, equation (26). For ionized atoms,

$$X_0=3.510\times 10^{-12}\frac{N_1'}{b(T)}\, e^{-\chi_i'/kT}\left(\frac{\lambda'}{\lambda}\right)^{3/2} e^{h(\nu-\nu')/2kT}\sqrt{\frac{\mu}{T}}\,\phi S\,\frac{s}{\Sigma s} . \tag{38}$$

The difference between equations (26) and (38) is of interest. The minimum of opacity occurs at the frequency of maximum spectral intensity. Lines of both neutral and ionized atoms should be strongest in this region. Toward the violet or red the lines of neutral elements should decrease in intensity more rapidly than those of the ionized. Neutral atoms of high ionization potential should behave like ionized atoms.

With the exception of ϕ, all the factors of these equations are known. Values of S have been given by Goldberg.[6] For convenience

[6] *Ap. J.*, **82**, 1, 1935.

in tabulation, these strengths were divided by some arbitrarily chosen factor. The constant factors necessary to reduce the strengths as published to an absolute scale have been tabulated.[7] The evaluation of ϕ is a wave-mechanical problem, which has been solved in certain elementary cases. In general, for a transition $n, l \to n', l\text{-}1$,

$$\phi = \frac{1}{4l^2 - 1}\left[\int_0^\infty rR(n, l)R(n', l-1)dr\right]^2, \tag{39}$$

where $R(n, l)$ and $R(n', l\text{-}1)$ are the normalized radial eigenfunctions of the jumping electron, expressed in atomic units.

The value of Γ for the various levels of a transition array is a matter of interest. Precise evaluation of the quantum-mechanical damping constant for complex atoms involves the accurate computation of the radial quantum integral (39), and hence of radial wave functions. Meanwhile, the nature of the general approach to the problem may be demonstrated. We shall consider first the mean lifetimes of the upper electronic levels of a transition array in which the jumping electron is not equivalent to any others in either the initial or the final configurations. Then

$$\frac{1}{T_j} = \sum_{j'} A_{j,\,j'} = \sum_{j'} \frac{1}{\bar{\omega}_j} \frac{4}{3} \frac{h^3}{m^2\epsilon^2} \left(\frac{\nu}{c}\right)^3 \phi S \frac{s}{\Sigma s}, \tag{40}$$

by (20) and (21). The summation refers to the totality of allowed transitions from the level j to the lower levels of the transition array. The quantity $S(s/\Sigma S)$ is just the strength of the line $j - j'$ in units of σ^2. The occurrence of ν^3 in the summation (40) presents a certain amount of difficulty, which may be circumvented by adopting a mean value of the frequency for all the lines of the entire transition array. By the sum rule,[8]

$$\sum_{j'} S \frac{s}{\Sigma s} = (2j+1)(l)(2l-1), \tag{41}$$

[7] Goldberg, *Ap. J.*, in press, **84**, 11, 1936.

[8] Shortley, *Phys. Rev.*, **47**, 295, 1935.

where l is the upper value of the orbital angular momentum of the jumping electron. Hence

$$\frac{1}{T_j} \sim \frac{4}{3} \frac{h^3}{m^2\epsilon^2} \frac{\bar{\nu}^3}{c^3} \frac{l}{(2l+1)} \left[\int_0^\infty rR(n, l)R(n', l-1)dr \right]^2 \tag{42}$$

is independent of j, S, or L; i.e., constant for any level of the array. The classical damping factor

$$\frac{1}{\tau} = \frac{8\pi^2\epsilon^2\nu^2}{3mc^3} . \tag{43}$$

Hence the ratio of quantum-mechanical to classical damping is

$$\frac{\tau}{T} \sim \frac{\bar{\nu}}{R} \frac{l}{2l+1} \left[\int_0^\infty rR(n, l)R(n, l-1)dr \right]^2 \tag{44}$$

by (24), for the case of $n = n'$. The damping factor should be summed over all transition arrays that involve either the upper or the lower of the atomic levels. It is likely, however, that the array containing $n = n'$ will predominate.

The approximation of adopting a mean value for ν^3 is not particularly serious, since damping is likely to be important for only the strongest lines of the strongest multiplets of the array, and these multiplets, having greatest weight, will predominate in the sum. It should be noted, further, that the assumption of constant Γ/ν, for equation (16), is essentially equivalent, by (44), to adopting a damping factor that is directly proportional to the classical expression for all spectral regions.

When the jumping electron is equivalent to others in one of the two configurations, the problem becomes more complicated, since the J-file sum rule[9] does not apply, except in the rare cases where the electrons are equivalent in the upper of the two configurations. Numerical values of Γ may be obtained when desired for specific cases. The damping factor is usually larger for the equivalent case, since all the strengths contain, as a factor, the number of equivalent electrons.

[9] Condon and Shortley, *op. cit.*, p. 279.

The treatment of the problem in the present paper ignores the possible deviations that frequently occur from the theoretical sum-rule intensities, but the general approach to the problem will not be greatly different if finite, instead of zero, strengths are assigned to intersystem combinations. It is probable that accurate astrophysical determinations of W, analyzed by the foregoing principles, will yield experimental values of the strengths that may be employed for other purposes. An analysis of Allen's data by the foregoing formulae is now in progress at Harvard Observatory.

In conclusion I wish to express my appreciation to Mr. Leo Goldberg, who kindly placed at my disposal various data relating to the problem of absolute multiplet strengths, and made many valuable suggestions during the progress of the investigation, and to Mr. James G. Baker for valuable assistance in deriving equation (14) and in preparing Table I.

HARVARD OBSERVATORY
CAMBRIDGE, MASSACHUSETTS
June 1936

NOTES

NOTE ON EQUIVALENT BREADTHS OF ABSORPTION LINES

J. G. BAKER

ABSTRACT

A formula has been derived for the curve of growth of a stellar absorption line. The results, shown in graphical form, agree satisfactorily with equivalent breadths computed by numerical integration from the line-absorption coefficient.

The curve of growth of an absorption line is a complicated function of a number of variables. Menzel[1] has shown that W/λ rather than W, the equivalent width, should be used as a measure of absorption-line intensity. For very strong lines, or for very weak lines, the theoretical expression for W/λ is simple. For lines of intermediate intensity the integral cannot be evaluated in finite form. Accordingly, numerical methods of integration have been employed. The results can be represented by a semi-empirical formula that is applicable over a wide range of variables.

The absorption coefficient, as derived from quantum mechanics for an assembly of atoms with thermal motion, may be written as follows (in Menzel's notation)[2]:

$$a_\nu = D \int_{-\infty}^{+\infty} \frac{e^{-\hat{\omega}^2} d\hat{\omega}}{\frac{1}{q^2} + (p+\hat{\omega})^2} . \tag{1}$$

When (1) is inserted in equation (4) of Menzel's paper, we find

$$\frac{W}{\lambda} = 2 \frac{v}{c} \int_0^{+\infty} \frac{1}{1 + \dfrac{\pi q}{X_0 \displaystyle\int_{-\infty}^{+\infty} \dfrac{e^{-\hat{\omega}^2} d\hat{\omega}}{\frac{1}{q^2} + (p+\hat{\omega})^2}}} \, dp . \tag{2}$$

[1] *Ap. J.*, this issue.

[2] *Pub. Lick Obs.*, **17**, 230, 1931.

The asymptotic expressions for the straight-line portions of the curve of growth are given by Menzel, but in the regions of transition the values must be obtained by connecting the known portions with a smooth curve. Equation (2) is integrable by numerical integration, provided the value of q is known:

$$q=4\pi\frac{v\nu}{c\Gamma}\,. \tag{3}$$

The numerical value of v/c, which corresponds to the Doppler motion of iron atoms at a temperature of 5740°, was obtained by fitting

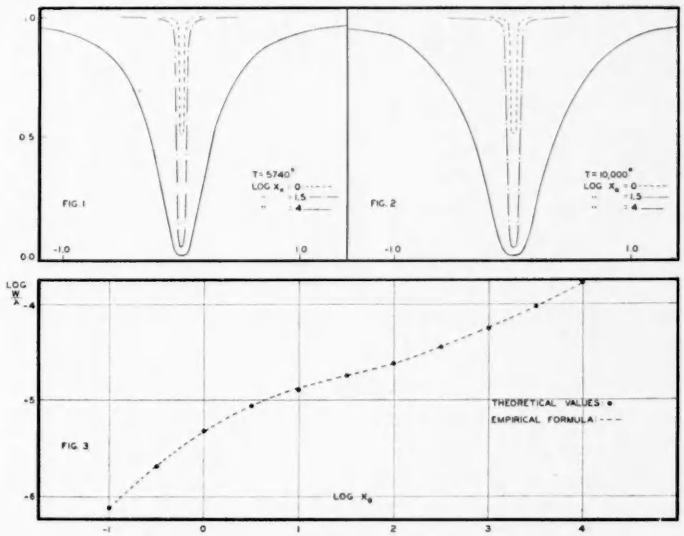

equation (10) of Menzel's paper to the lower part of the curve of growth. Similarly, the numerical value of Γ/ν was obtained by fittng equation (16) of Menzel's paper to the upper part of the curve of growth. The adopted value of q was 36.04.

Equation (1) was integrated by combined series and numerical integration in order to obtain the exact values of the areas involved for a large number of values of p. The plotted values of the integrand of equation (2) gave the theoretical profiles of lines formed in a purely scattering atmosphere. Several such profiles are shown in Figures 1 and 2. The areas under the profiles were found by numeri-

cal methods. The results are given in Table I of Menzel's paper, and, when plotted, give the complete curve of growth.

In the case of relatively few atoms contributing to the line, one would expect to find an approximately linear relation between the amount of absorption and the number of particles. In the wings the thermal motion has no appreciable effect. Accordingly, for very strong lines the expression for the equivalent width may be obtained, without resorting to integration over all velocities. Thus

$$\frac{W}{\lambda} = 2\int_0^\infty \frac{\frac{v}{c}X_0}{\pi + X_0 q\sqrt{\pi + p^2}}\,dp \tag{4}$$

$$= \frac{v}{c}\sqrt{\pi}\,X_0\left(1+4\sqrt{\pi}\frac{v}{c}\frac{\nu}{\Gamma}X_0\right)^{-1/2} \tag{5}$$

or

$$\log\frac{W}{\lambda} = \log X_0\frac{v}{c}\sqrt{\pi} - \tfrac{1}{2}\log\left(1+4\sqrt{\pi}\frac{v}{c}\frac{\nu}{\Gamma}X_0\right). \tag{6}$$

When X_0 is small, this equation agrees with Menzel's equation (10); when X_0 is large, the formula goes over into Menzel's equation (16). With the help of this formula it was found possible to represent the curve of growth quite satisfactorily by the following empirical formula:

$$\log\frac{W}{\lambda} = \log X_0\frac{v}{c}\sqrt{\pi} - \tfrac{1}{2}\log(1+X_0) - \frac{\frac{1}{2}\log 4\sqrt{\pi}\,\frac{v}{c}\frac{\nu}{\Gamma}}{1+15e^{-2\log X_0}}. \tag{7}$$

The logarithmic terms are all expressed to the base 10. The exponential term is used for convenience when $\log X_0$ is employed as the variable. Figure 3 shows the plot of this equation for the values of v/c and Γ/ν adopted above. The numerically computed values are entered as points to illustrate the agreement. Equation (7) should hold rather closely for all reasonable values of q.

HARVARD OBSERVATORY
CAMBRIDGE, MASS.
June 1936

CONSTANCY OF WAVE-LENGTH OF A SPECTRAL LINE

GUY C. OMER, JR., AND JAMES L. LAWSON

ABSTRACT

The line λ 4358 of mercury was observed with a Fabry and Perot etalon from June 24 to August 27, 1935. The wave length of this line was found to be constant to within 2 parts in 1,000,000.

The question of the constancy of the velocity of light raised by De Bray[1] and by Pease and Pearson[2] brings up the supplementary question of the constancy of the wave-length of light. The most direct experimental approach to this problem is through a study of the constancy of wave-length of a spectral line. R. J. Kennedy[3] carried on an excellent series of observations of this type, using a Michelson interferometer to set up his interference pattern. There might be some objection to his method, however, because his interfering beams were at right angles to each other and it is conceivable that some extraneous influence might affect the two paths disproportionately.

This objection cannot be made to the Fabry and Perot etalon, since the interfering beams travel in identical paths. Moreover, the interference pattern of the etalon is considerably sharper than that of the interferometer. The authors observed the line λ 4358 of mercury, using a Fabry and Perot etalon. A Hilger etalon with a 9-mm spacer of fused quartz was hermetically sealed into a brass chamber with end windows. This chamber was maintained at a relatively constant temperature by means of a heater winding and a mercury thermostat. A thermometer mounted on the brass chamber was used to check this temperature, which was never observed to deviate more than a few hundredths of a degree from the mean. No direct checks were made on the pressure within the chamber, but continuous records were taken of the barometric pressure within the room.

A continuous photographic system of recording was used. By

[1] Letters to the Editor, *Nature*, **120**, 602, 1927; **133**, 948, 1934.

[2] A. A. Michelson, F. G. Pease, and F. Pearson, *Ap. J.*, **82**, 26, 1935.

[3] R. J. Kennedy and E. M. Thorndike, *Phys. Rev.*, **42**, 400, 1932.

means of slits all of the interference pattern except a narrow vertical slice through the center was occluded. This slice was photographed upon 16-mm motion-picture film, which was moving perpendicularly to the direction of the slice. The developed negative showed, therefore, a series of lines which would be strictly parallel if the wave-length remained constant. The time scale used was such that a deviation of but a few seconds in duration could be observed. A change in wave-length of 1 part in 41,250 would have produced a complete fringe shift in this apparatus. Because the pattern was sufficiently sharp that a twelfth of a fringe shift would be noticed, any change in wave-length greater than 2 parts in 1,000,000 could be detected.

A series of records was taken from March 27 to April 7, 1935. These records show slight variations in wave-length, but as these variations were found to correlate exactly with the corresponding barometric records, they were ascribed to small air leaks in the chamber. Accordingly, the chamber was dismantled, cleaned, and resealed and a new series of records taken from June 24 to August 27, 1935. No variations in wave-length can be found in this set of records. If it is assumed that the frequency of a spectral line remains constant, the short-period fluctuations in velocity reported by Pease and Pearson should have produced a wave-length change of 70 parts in 1,000,000. Likewise, the long-period variations postulated by De Bray should have caused a shift of 10 parts in 1,000,000 during this period.

The authors wish to thank Dr. C. V. Kent for his aid in this experiment.

BLAKE PHYSICAL LABORATORIES
UNIVERSITY OF KANSAS
June 1936

A NEW BINARY OF LARGE PARALLAX

The well-known M dwarf 17 Lyrae C ($19^h03^m.6$, $+32°21'$) has recently been found to be a close double star in the 40-inch telescope:

1936.80 80°.1 0″.32 $\Delta m = 0^M.4$ 40,950× seeing 3+

The star had been examined previously with the 36-inch telescope of the Lick Observatory, but no duplicity was noted at that time:

1934.63 single 36, 1040× seeing 4

The separation at that date was probably less than 0".2 or 0".15. The parallax of the system is 0".123 ± ".006, the proper motion 1".66 in 49°. The present separation is less than 3 astronomical units,

TABLE I

Name	m_{AB}	Δm	1000 π	Abs. Mag.
Ross 165	12.4	0.9	116±11	½(A+B)=13.6
Krüger 60	9.64	1.58	258± 4	B =13.5
Capella Hh	10.20	3.5±	73± 3	*h =13.1±
o_2 Eridani BC	9.48	1.7	202± 3	C =12.9
17 Lyrae C	11.16	0.4	123± 6	½(A+B)=12.4
ADS 433, 440	10.21	1.9	103± 7	B =12.3
Furuhj. 54	10.03	1.9	97± 8	*B =12.0
Krüger 60	9.64	1.58	258± 4	A =11.9
+45°2505	9.43	0.4	144± 7	½(A+B)=11.0
−8°4352 AB	9.20	0.1	148± 4	½(A+B)=10.8
μ Herc BC	9.82	0.1	109± 6	½(A+B)=10.8
ADS 433, 440	10.21	1.9	103± 7	A =10.4
+68°278 BC	10.83	0.0	54± 9	½(A+B)=10.2
Furuhj. 54	10.03	1.9	97± 8	A =10.1
ι U Maj. BC	10.19	0.0	67±12	½(A+B)=10.1

* The colors and spectra of these two stars are unknown.

and the period may be of the order of five years. The apparent magnitude of the pair is 11.16 on the international photovisual system, as determined from measures made at Leiden. The two components are accordingly 11.73 and 12.1, and the absolute visual magnitudes are 12 2 and 12 6. In view of the large parallax, and the small Δm, the system will in time afford a new absolute mass determination.

The field star (C') nearest to 17 Lyrae C is optical:

1934.63 61°.8 20".05 C' = 15.3 36,540 seeing 4
1936.80 65.0 16.67 C' = 15.0 40,350 seeing 2+

For comparison with the new pair the close M dwarf[1] binaries of large parallax, fainter than absolute magnitude 10.0, are collected

[1] The white dwarfs Sirius B and o_2 Eridani B, and also Procyon B, are omitted here since they do not obey the mass-luminosity relation, and differ in nature from the M dwarfs.

in Table I. These binaries are useful, or will be so in the near future, in giving absolute mass determinations. They are arranged in order of increasing luminosity. About half of them were found double in the writer's survey with the 36- and 40-inch telescopes. The photometric data are based on measures or estimates by the writer; the values in column 2 are on the international photovisual scale.

For Krüger 60, ADS 433, 440, and Furuhjelm 54, the components are entered separately, since the mass ratio may be determined for these pairs. For the other binaries the average mass may be obtained, which may be related to the average absolute magnitude of the components.

G. P. KUIPER

YERKES OBSERVATORY
October 28, 1936

ERRATUM

On page 241 of the October issue of this *Journal*, in the first two lines of the text (following the abstract): *for* the Rumford Fund of the National Academy of Sciences *read* the Rumford Fund of the American Academy of Arts and Sciences.

THE EDITORS